Uncovering the Functional Effects of Multifaceted Cholesterol-Kir2 Interactions via Molecular Modeling

BY

Nicolas Barbera

B.S., Johns Hopkins University, 2013

M.S.E., Johns Hopkins University, 2014

THESIS

Submitted as partial fulfillment of the requirements

for the degree of Doctor of Philosophy in Chemical Engineering

in the Graduate College of the

University of Illinois at Chicago, 2020

Chicago, Illinois

Defense Committee:

Belinda Akpa, Advisor, Department of Molecular Biomedical Sciences, NCSU

Irena Levitan, Advisor, Pulmonary, Critical Care, Sleep and Allergy

Lewis Wedgewood, Chair, Chemical Engineering

Vivek Sharma, Chemical Engineering

Al George, Feinberg School of Medicine

This thesis is dedicated to my parents, Joanne and Anthony Barbera, for their love and support throughout my life. (And for finally giving me that pudding)

ACKNOWLEDGEMENTS

I would like to express my deepest appreciation to my advisors, Drs. Belinda Akpa and Irena Levitan, for their supervision and support during my PhD and for creating such a positive research experience. I also wish to thank my Committee members, Drs. Lewis Wedgewood, Vivek Sharma, and Al George for their guidance and input. The help and encouragement of my friends, coworkers, and colleagues is likewise greatly appreciated. In particular, Dr. Manuela Ayee for her help in teaching me MD simulations.

I would also like to extend my deepest gratitude to my parents, Joanne and Anthony Barbera for their constant love and support, and to Harry and Beverly Scrudato and the rest of my family.

And finally, thank you to Annie Helmer for her love and patience throughout the process.

NB

CONTRIBUTION OF AUTHORS

Chapters 2 and 3 in this dissertation each contain work that was previously published. Material from chapter 2 was published in *Barbera, Nicolas A., Baruch Minke, and Irena Levitan. "Comparative docking analysis of cholesterol analogs to ion channels to discriminate between stereospecific binding vs. stereospecific response." Channels 13.1 (2019): 136-146*. In that publication: Nicolas Barbera, Baruch Minke, and Irena Levitan wrote the manuscript and designed the research, while Nicolas Barbera performed the research and analyzed the data.

Material from chapter 3 was published in *Barbera, N., M. A. Ayee, et al. (2018). "Molecular Dynamics Simulations of Kir2.2 Interactions with an Ensemble of Cholesterol Molecules." Biophysical journal 115(7): 1264-1280.* In that publication: Nicolas Barbera, Irena Levitan, and Belinda Akpa wrote the manuscript and designed the research; Nicolas Barbera performed the research; Nicolas Barbera, Manuela A. Ayee, and Belinda Akpa contributed analytic tools; Nicolas Barbera and Belinda Akpa analyzed the data.

TABLE OF CONTENTS

LIST OF TABLES

LIST OF FIGURES

LIST OF ABBREVIATIONS

BK Channel - Large conductance calcium-activated potassium channel

CG – Coarse grained

CRAC - Cholesterol recognition/interaction amino acid consensus

$GABA_A$ - Gamma-aminobutyric acid A receptor

IQR – Inter-quartile range

Kir – Inwardly rectifying potassium channel

MD – Molecular Dynamics

PIP2 – phosphatidylinositol 4,5-bisphosphate

POPC – 1-palmitoyl-2-oleoyl-sn-glycero-3-phosphocholine

TRPV1 – Transient receptor potential cation channel subfamily V member 1

VRAC – Voltage regulated anionic current

SUMMARY

As a major component of mammalian lipid membranes, cholesterol is an important regulator of membrane biophysical phenomena, including regulating membrane fluidity, thickness, and lipid domain compartmentalization. Likewise, the cholesterol-mediated regulation of membrane proteins – particularly ion channels – represents an important mechanism for controlling their function. This thesis focuses on utilizing computational techniques to understand the regulation of inwardly rectifying potassium channels by cholesterol. Inwardly rectifying potassium (Kir) channels form a family of transmembrane proteins that help regulate resting membrane potential, selectively allowing the influx or efflux of K+. They are found in a wide variety of cells including endothelial cells, epithelial cells, cardiac myocytes, and neurons, and play a key role in regulating the action potential duration in electrically excitable cells and in maintaining the resting membrane potential. With respect to Kir channels, cholesterol has been shown to suppress their function in both model liposome systems and in mammalian cells, primarily through direct and specific interactions with the channel. However, although it is well established that cholesterol regulates the activity of Kir channels, the specific mechanisms through which cholesterol binding mediates channel function remain unclear.

In this dissertation, I utilized three sucessive approaches to answer this question of cholesterol regulation. First, I performed molecular docking of cholesterol and its chiral isomers to five different ion channels, including Kir2.2 and its bacterial homologue, KirBac1.1. Second, I performed coarse-grained molecular dynamics simulations of Kir2.2 in a lipid bilayer with different levels of cholesterol and developed an analytical technique based on network theory to characterize the interactions of Kir2.2 and cholesterol in a

dynamic membrane environment. Finally, to examine the specific structural consequences of cholesterol binding, I developed a second network theory-based approach to understand the effects of cholesterol on the intra-protein dynamics of Kir2.2 in the same coarse-grained simulation systems.

Overall, I found that interactions between cholesterol and Kir2.2 are multifaceted and complex. Multiple cholesterol molecules interact with the channel simultaneously, with these interactions occurring on a range of different timescales. Furthermore, interaction sites on the channel are promiscuous: cholesterol and its chiral isomers ent-cholesterol and epicholesterol interact with sites on the channel with similar favorability, and cholesterol was found to be highly flexible within its binding site during the coarse-grained simulations. Lastly, I found that these cholesterol binding events mediate the interactions of functionally important domains of the channel, with an increase in membrane cholesterol causing these domains to “de-couple” from one another. These de-coupling events were found to be governed by specific residue-residue interactions, which could be correlated to cholesterol binding.

1. INTRODUCTION

Proteins play a critical role in the function of cells, actively contributing to a wide array of functions including biochemical signaling, enzyme catalysis, cell structure maintenance, regulation of DNA translation and transcription, and environmental homeostasis (Bruce, Alexander et al. 2002). The biological functions of proteins are in part realized through interactions with specific ligands, such as small molecules, lipids and lipid membranes, nucleic acids, peptides, and ions. These interactions are facilitated by molecular recognition, which is the process through which two or more molecules interact with one another in a complimentary manner to form macromolecular complexes. Molecular recognition occurs through non-covalent bonding such as hydrogen bonding, hydrophobic forces, Van der Waals forces, and/or electrostatic interactions. Understanding the process of molecular recognition and the broader question of protein-ligand interactions represents a significant portion of research at the cellular level, particularly with respect to the fields of pharmacology and drug design.

1.1. Lipid-Membrane Protein Interactions

An important class of protein-ligand interaction is the interactions of membrane-embedded proteins with their surrounding lipid environment. These lipid-comprised biological membranes play a critical role in the organization of cells, acting to delineate distinct biological compartments and acting as diffusion barriers within a cell and between a cell and its surroundings. Likewise, these lipid membranes are often very compositionally complex, containing hundreds of different lipid types such as phospholipids, sphingolipids, fatty acids, and cholesterol. In addition to a complex composition, lipid membranes are

embedded with a large array of membrane proteins, which allow for selective diffusion and active transport across these membranes. This selectivity moves nutrients and waste, helps establish electrochemical gradients via ion concentrations, and can help alter the pH of distinct biological compartments (Sackmann 1995). Indeed, it is estimated from genomics analyses that 25% of proteins are membrane proteins (Wallin and Heijne 1998).

My studies have focused on ion channels, specifically potassium channels. Ion channels are a major class of membrane proteins which span the cell membrane and allow for the passage of ions from one side of the membrane to the other. These channels are selective, meaning that different classes of ion channel only allow for the passage of certain ions through them. Functionally, ion channels play critical roles in regulating resting membrane potential, controlling neuronal excitability, and cell volume regulation (Purves, Cabeza et al. 2008). Generally speaking, ion channels are oligomeric proteins with three structural features: 1) a ion conducting pore, which is an aqueous pathway containing a narrow filter that confers ion selectivity, 2) gates, which open and close the conducting pore, and 3) sensors, which detect outside stimuli such as chemical signals or changes in electrical potential (Minor).

1.2. Membrane Structure

Our views of cell membranes and protein-lipid interactions have changed markedly over the past decades, beginning with the early fluid mosaic model. This model envisioned the lipid bilayer as a relatively homogeneous, 2D fluid-like solvent in which amphiphilic proteins were embedded (Singer and Nicolson 1972). This has evolved into the modern view of the cell membrane, which conceptualizes proteins and lipids as being heterogeneously

distributed throughout the membrane and organized into dynamic domain structures enriched with sphingolipids, cholesterol, and select membrane proteins.

Compartmentalization is a ubiquitous theme in biology, and this includes in cell membranes. As amphiphilic molecules, lipids preferentially interact with one another over water, creating impermeable barriers that delineate compartments within a cell. Furthermore, lipids are a diverse group of molecules with different head groups, tail lengths, saturation levels, and structure (Gerl, Sampaio et al. 2012). As a result, there are hundreds of different lipids in cell membranes, and this variety can lead to lateral heterogeneity, particularly at small length- or time-scales. Likewise, as a consequence of their individual geometric features and physiochemical properties, select lipids will also preferentially interact with one another (Almeida 2009). With respect to biological membranes, an important example of this phenomenon is the interaction between sterols, saturated lipids, and sphingolipids (**Fig 1-1**). Sterols interact more favorably with saturated lipids over unsaturated lipids and through these preferential interactions can induce the formation of tightly packed membrane domains, which have lipid and protein compositions distinct from the surrounding membranes (Levental, Levental et al. 2020). Numerous studies have explored the existence and functional significance of these ordered membrane domains, frequently termed “lipid rafts”. Although still an unsettled topic, these rafts are thought to play a role in regulating a number of different ion channels (Dart 2010).

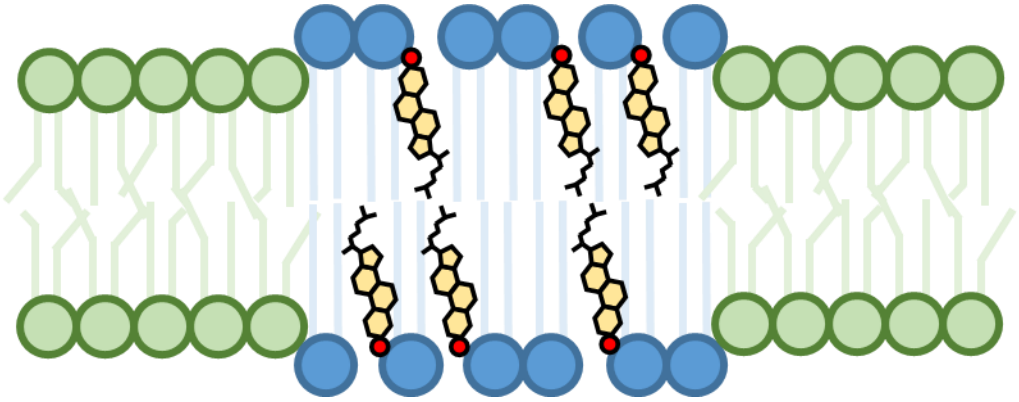

Figure 1-1. Illustration of a lipid domain. Cholesterol (yellow) is interacting preferentially with saturated phospholipids (blue) over unsaturated phospholipids (green). This preferential interaction forms a region of the membrane with a lipid composition that is distinct from its surroundings.

1.3. Cholesterol in the Lipid Membrane

Cholesterol (3β-hydroxy-5-cholestene) is a major lipid component of the cell membrane of eukaryotic cells and comprises 10 to 45 mol% of the membrane with respect to other lipids (Yeagle 1985). Owing to its unique structure relative to membrane phospholipids, cholesterol plays an important role in altering the physical properties of the membrane, including increasing lipid order, decreasing biological membrane fluidity, and increasing bilayer thickness and stiffness (Yeagle 1985; Needham and Nunn 1990; Yeagle 1991). Furthermore, as described above, cholesterol induces the formation of lipid domains, which are cholesterol-enriched regions with saturated phospholipids and sphingolipids. Structurally, cholesterol consists of an asymmetric, rigid planar tetracyclic ring with a small β3 hydroxyl head group at C3, a pair of methyl group on one side, and an isooctyl chain attached to C17 (**Fig. 1-2A**). These methyl groups create a "rough" β-face of the molecule

opposite to its smooth α-face. The asymmetric orientation of the methyl and hydroxyl groups on the cholesterol molecule also point to an important feature governing its regulatory properties: its chirality. Chirality is an essential feature of many organic molecules, arising from the specific three-dimensional orientation of their constituent atoms and the tendency of carbon molecules to form tetrahedral-shaped bonds. With respect to molecular symmetry, it means that depending on the structure or identity of various moieties bond to a given carbon atom, even very simple molecules with identical chemical formulas can adopt structurally distinct geometries, called stereoisomers. This "molecular handedness" means that stereo-isomers cannot be superimposed on one another and that functionally, stereoisomers represent separate molecules with distinct chemical and physical properties. Cholesterol has eight distinct stereocenters, which are located at C3, C8, C9, C10, C13, C14, C17, and C20. The two most commonly used chiral isomers in experiments are the synthetic analogs ent-cholesterol (enantiomeric cholesterol) and epicholesterol (3α-hydroxy-5-cholestene). Ent-cholesterol is the mirror image of cholesterol, and is characterized by the opposite arrangement of each of its eight stereocenters with respect to cholesterol (**Fig. 1-2C**). In contrast, epicholesterol has an almost identical structure to cholesterol. Here, the difference is in the placement of its hydroxyl group at the 3α position rather than the 3β position of C3 (**Fig. 1-2B**). The differences between the orientation of the stereocenters of epi-cholesterol and ent-cholesterol to cholesterol yields major differences not only in the 3-dimensional structures of these analogues but their position within the bilayer as well. Consequently, this alters their respective effects on membrane properties.

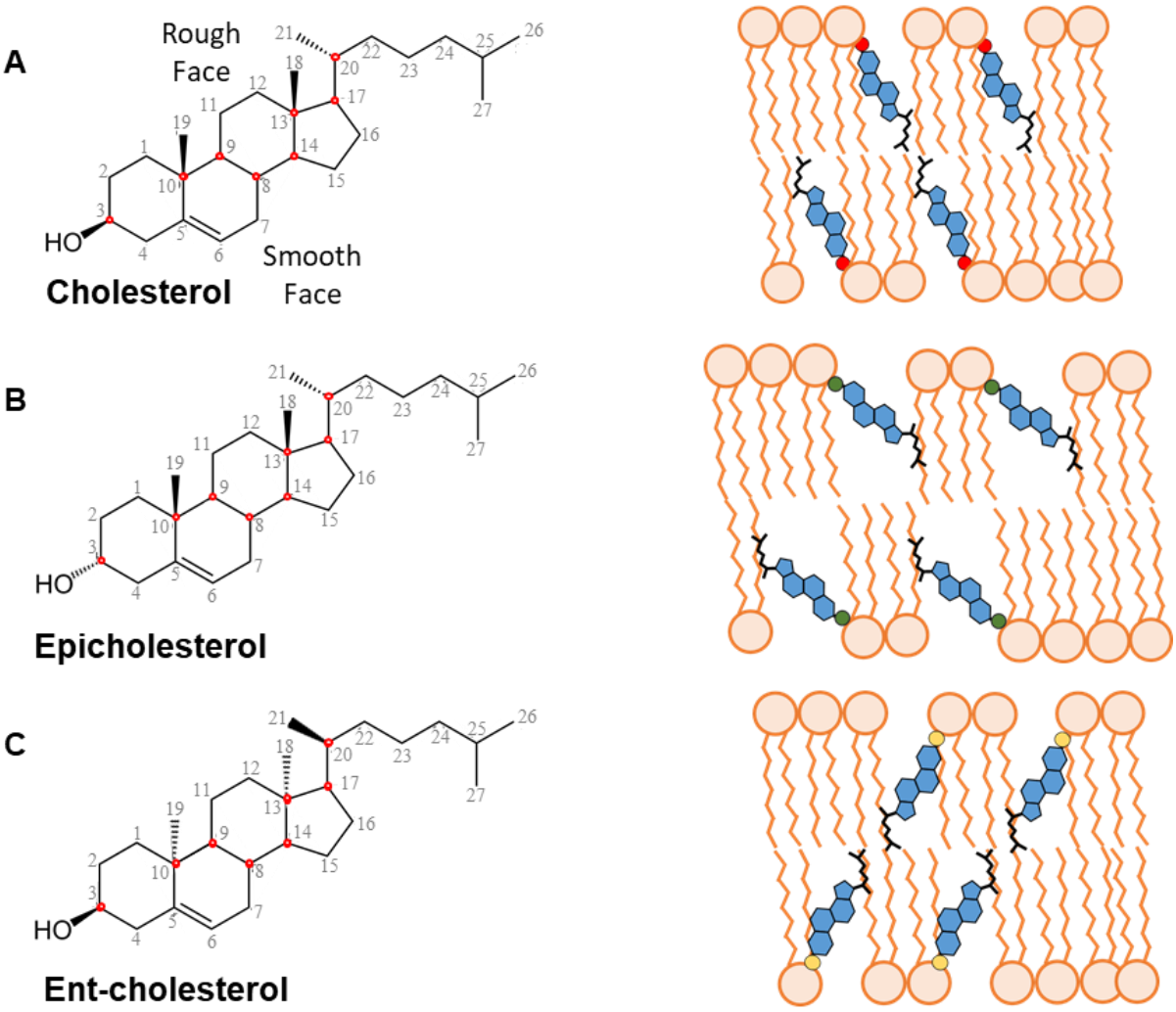

Figure 1-2. Cholesterol and its Chiral Isomers. ***A****) The molecular structure of cholesterol, with its chiral centers highlighted in red (left). Cholesterol in the membrane environment (right).* ***B****) The molecular structure of epicholesterol, with its chiral centers highlighted in red (left). Epicholesterol in the membrane environment (right).* ***C****) The molecular structure of ent-colesterol, with its chiral centers highlighted in red (left). Ent-cholesterol in the membrane environment (right).*

1.3.1. Cholesterol Regulation of Membrane Proteins

Cholesterol plays an important role in regulating the function of a number of membrane proteins, including two major classes: ion channels and G-protein coupled receptors (GPCRs) (Yeagle 1985; Yeagle 1991; Rosenhouse-Dantsker, Mehta et al. 2012; Chattopadhyay 2014; Levitan, Singh et al. 2014; Gimpl 2016). For many ion channels, the effect of increased membrane cholesterol is functional inhibition, either through a decrease in open probability or the number of active channels in the membrane. This was shown to be the case for multiple K^+ channels, including inwardly rectifying K^+ channels (Romanenko, Rothblat et al. 2002; Romanenko, Fang et al. 2004) , voltage-gated K^+ channels (Hajdú, Varga et al. 2003; Abi-Char, Maguy et al. 2007), and Ca^{2+}-sensitive K^+ channels (Crowley, Treistman et al. 2003; Bukiya, Singh et al. 2011). Likewise, cholesterol was shown to functionally inhibit volume-regulated anion channels (Romanenko, Rothblat et al. 2004) and voltage-gated Na^+ and Ca^{2+} channels (Lundbæk, Birn et al. 2004). Conversely, cholesterol was also shown to help activate ion channels and stabilize them in the open state, as in the case of nicotinic acetylcholine receptors (Barrantes 2007; Fantini and Barrantes 2013) (Baenziger, Hénault et al. 2015). For some families of ion channels, cholesterol was also shown to have both positive and negative effects such as with TRP channels (Picazo-Juarez, Romero-Suarez et al. 2011), y-aminobutyric acid receptors ($GABA_AR$) (Sooksawate and Simmonds 2001), and across sub-families of Kir channels (Romanenko, Rothblat et al. 2002; Romanenko, Fang et al. 2004; Hibino and Kurachi 2007; Rosenhouse-Dantsker, Leal-Pinto et al. 2010).

Similarly to ion channels, cholesterol has been shown to modulate various aspects of GPCR function, including oligomeric organization (Ganguly, Clayton et al. 2011), stability (Saxena and Chattopadhyay 2012; Zocher, Zhang et al. 2012), and ligand binding activity

(Harikumar, Puri et al. 2005). As with ion channels, the effects of cholesterol vary across the different receptors. In the case of rhodopsin, it was shown that increasing membrane cholesterol inhibits its activation in its signal cascade (Albert and Boesze-Battaglia 2005). In β2 adrenergic receptors, cholesterol was also shown to have an inhibitory effect, as cholesterol depletion enhanced adrenergic signaling in cardiac myocytes (Paila, Jindal et al. 2011). In contrast, cholesterol was found to be necessary for a number of different GPCRs. Removal of membrane cholesterol reduced the response of μ-opiod receptors to its agonist, while having no effect on δ-opiod receptors (Levitt, Clark et al. 2009). Likewise, it was found that for serotonin 1A receptors, cholesterol is necessary for ligand binding and G-protein coupling (Pucadyil and Chattopadhyay 2004).

1.3.2. Principles of Cholesterol Regulation

As such a major component of lipid membranes, with widespread effects on the function of many membrane proteins, uncovering the mechanisms underlying the functional effects of cholesterol on ion channels is a central question. In general there are three principles describing cholesterol regulation: 1) cholesterol acts on proteins indirectly, via its alteration of membrane properties, 2) cholesterol facilitates the formation of lipid domains which localize protein signaling complexes, and 3) cholesterol regulates proteins directly, via specific interactions with binding sites (**Fig 1-3**).

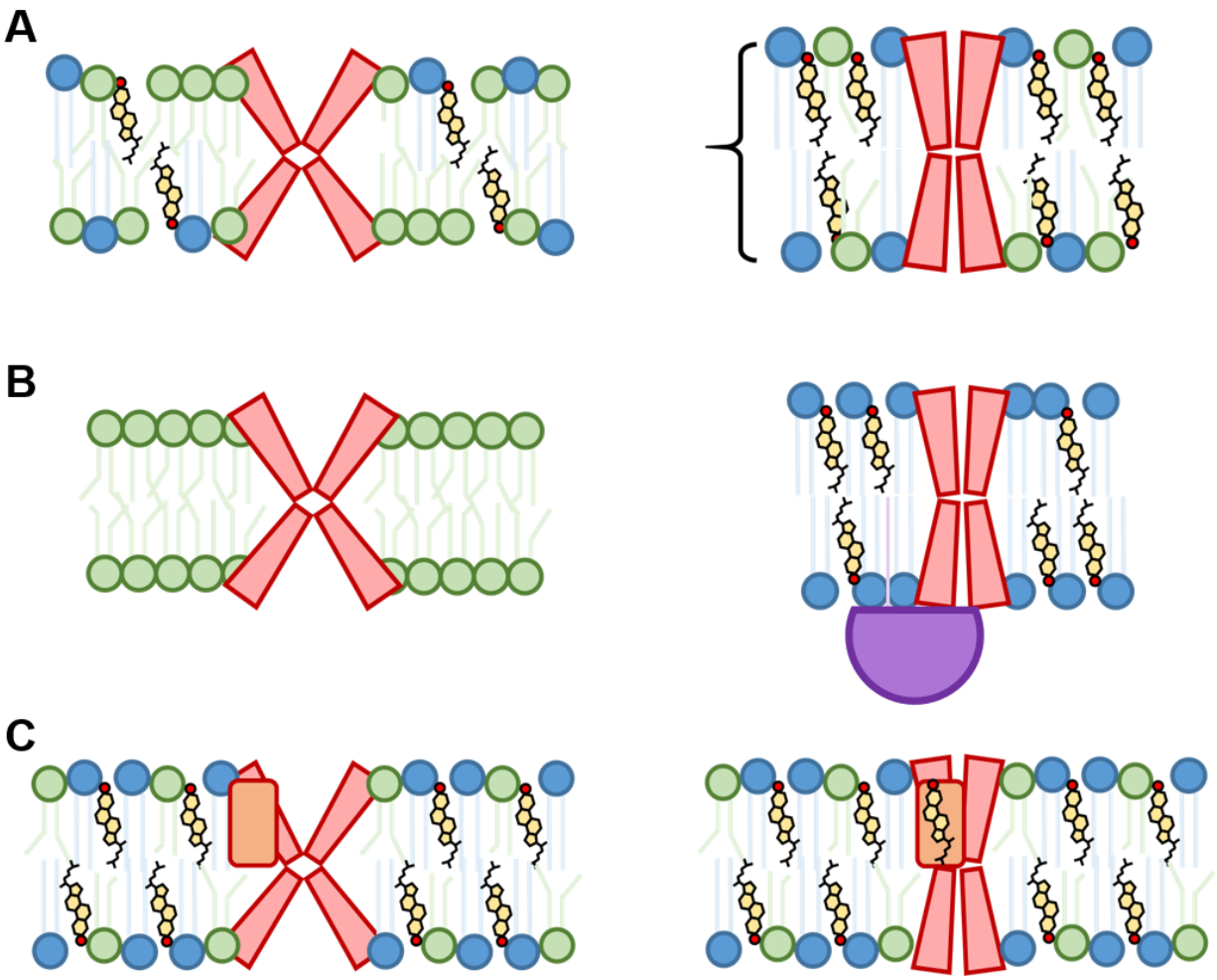

Figure 1-3. The 3 principles of cholesterol-mediated regulation of membrane proteins. Saturated lipids are draw in blue, unsaturated lipids are drawn in green, and cholesterol is drawn in yellow. Images show a cartoon representation of a membrane protein in two conformational states. ***A****) Cholesterol acts on proteins indirectly, via its alteration of membrane properties and creating hydrophobic mismatch which helps stabilize the protein in a different conformation.* ***B****) Cholesterol facilitates the formation of lipid domains which localize protein signaling complexes that alter protein function.* ***C****) Cholesterol regulates proteins directly, via specific interactions with binding sites that alter protein function.*

In the case of indirect regulation, cholesterol mediates the function of membrane proteins by altering the stiffness, curvature, or thickness of the lipid environment surrounding the membrane protein. For ion channels, the energetics and kinetics of channel gating are directly related to the surrounding lipid environment. Conformational changes related to gating can cause local disturbances in the surrounding bilayer, meaning that the overall energetic cost of a channel transition will include not only the intrinsic channel activation energy, but the energy associated with membrane deformation as well (Andersen and Koeppe 2007). As a result, these cholesterol mediated alterations to the membrane lipid environment can cause effects like hydrophobic mismatch between the protein and the lipid environment and help to stabilize or de-stabilize a conformational state by changing the energetic cost of gating. For example gramicidin A, a cation-selective channel, is a mini protein formed by the trans-bilayer association between two monomers and is highly sensitive to lipid bilayer thickness (Mobashery, Nielsen et al. 1997; Lundbæk, Collingwood et al. 2010). When bilayer thickness is altered, gramicidin A responds by distorting the local membrane environment to compensate, incurring an energetic cost that affects the equilibrium between associated and disassociated monomers and altering channel function. Similarly, it was shown that VRAC is sensitive to sterol-induced membrane properties, irrespective of whether this change was through cholesterol or a chiral isomer (Romanenko, Rothblat et al. 2004).

Cholesterol can also indirectly influence the activity of ion channels via its tendency to form lipid domains. In addition to endogenous lipids, there are a number of different signaling proteins and complexes which can modulate the function of ion channels. Many of these have been shown to accumulate in specific lipid domains, including a number of G-

protein coupled receptors, various classes of G protein, nitric oxide synthase, protein kinase C, and tyrosine kinases (Dart 2010). By facilitating the formation of lipid domains that attract these signaling proteins and complexes, cholesterol can act as an indirect regulator of ion channel activity, co-localizing ion channels with their respective inhibitors/enhancers. This phenomenon is exemplified in caveolae, which are small invaginated membrane structures characterized by their enriched cholesterol and sphingolipid composition, along with the small (21–25 kD) cholesterol-binding protein "caveolin" (Murata, Peränen et al. 1995). These caveolae have been shown to be important regulators of cardiac ion channel function, as a number of different channels including Kv1.5, Nav1.5, and Cav1.2 have been shown to localize into these rafts (Martens, Sakamoto et al. 2001; Yarbrough, Lu et al. 2002; O'Connell, Martens et al. 2004) .

Besides indirectly affecting ion channel activity, cholesterol can also directly modulate channels by acting as a specific ligand, binding to a functional binding pocket and allosterically or orthosterically stabilizing the protein in a particular conformation or activity state. In the case of direct regulation, an important consideration is whether cholesterol interacts with annular or non-annular site on the channel. This definition of "annular" or "non-annular" reflects the location of cholesterol molecules relative to the bulk lipid environment and the channel. Here, "annular" refers to those sterols which preferentially bind to or interact with the surface of membrane proteins. Due to the fluid nature of lipid membranes and the ability of its constituents to laterally diffuse, these sterols can interact with the protein with different residence times and on different areas on the protein surface. These residence times are mediated by the physical properties of the lipids, including polar head-group interactions and hydrophobic matching with transmembrane regions of the

protein. Short residence times represent rapid exchanges with surrounding bulk lipid, while longer residence times can point to functionally relevant interaction sites. When these residence times are reduced, the ring of lipids and sterols closest to the protein can form a shell or annulus. Indeed this annular shell can be detected with experimental methods such as EPR (Marsh and Horváth 1998; Marsh and Páli 2004).

In contrast to these, sterols that have even lower exchange rates in more secluded regions of the protein can form "non-annular" interactions. While the more readily accessible annular lipid sites have been thought to form the basis of direct cholesterol regulation, it has been increasingly shown that non-annular interactions often constitute lipid binding sites, and can play a functional role in the regulation of membrane proteins (Lee 2003; Muller, Jiang et al. 2019).

Discriminating between the different mechanisms of cholesterol regulation remains a difficult challenge. Cholesterol is an integral constituent of the membrane and it can exist at a relatively high concentration, interacting with many different membrane components. Likewise, the experimental tools available to discriminate between the two mechanisms are still limited. One approach that has been used successfully has been through experiments with chiral isomers. By judiciously choosing isomers of cholesterol that have similar effects on the membrane environment, it is possible to partially de-convolute the indirect, membrane effects of cholesterol from its direct, binding effects. Previous experiments using ent-cholesterol and epicholesterol have been successful in identifying direct interactions between cholesterol and Kir channels, BK channels, and TRPV1 (Romanenko, Rothblat et al. 2002; Singh, Rosenhouse-Dantsker et al. 2009; Bukiya, Belani et al. 2011; D'Avanzo, Hyrc et al. 2011; Picazo-Juarez, Romero-Suarez et al. 2011).

1.4. Experimental Methods to Study Cholesterol-Ion Channel Interactions

As the importance of cholesterol and the lipid environment in the regulation of ion channels and membrane proteins has become better understood, there has been great interest in better characterizing this process in detail. Consequently, an array of different experimental techniques have been developed to interrogate sterol-protein interactions generally, and sterol-ion channel interactions specifically. Often, these functional techniques investigate protein activity or protein turnover properties in different model membrane systems, such as nanodiscs, liposomes, or lipid monolayers. In other experiments, particularly those involving some sort of functional assay, measurements are taken *in vivo* with cell systems.

1.4.1. Electrophysiology

The primary experimental method for measuring the function of ion channels is electrophysiology. Generally speaking, electrophysiology is the recording of currents from cells or tissues. With respect to studying the effects of cholesterol on ion channel function, intracellular recording techniques are especially effective because they can provide information on the biophysical properties of ion channels as well as cellular membrane properties such as membrane potential and membrane resistance. In order to obtain this level of detail, direct electrical access to the interior of cells is needed. This is achieved through two general techniques: sharp microelectrode studies and patch clamp studies.

In the first technique, measurements are taken by inserting the tip of a microelectrode into a cell. This was the approach first used by Hodgkin and Huxley in their fundamental work on understanding action potential generation in neurons (Hodgkin and

Huxley 1952). While their initial work involved inserting a fine wire into squid axons, most current experiments following this methodology instead use a fine-tipped (<1 μm diameter) glass electrode with resistances of tens to hundreds of MΩ. In these experiments, the micropipets are usually filled with a saturating concentration of KCL, along with a cholorided silver wire. This silver wire connects the pipet to an amplifier and signal processing circuit, which allows for voltage drop across the membrane and conductance across the membrane to be recorded. Owing to the nature of the technique, experiments involving sharp microelectrodes are performed on larger cells, such as oocytes. However while this technique is still used, for many applications it has been replaced by the second technique: patch clamp.

Unlike the first technique, which uses an electrode to puncture the cell, in patch clamp experiments a blunt glass electrode adheres to the membrane and uses suction to form a high resistance (GΩ) seal. This allows for measuring currents in whole cells or patches of cell membrane. Because the electrode is adhered to the cell membrane, there are four different configurations that can be utilized in patch clamp experiments: cell-attached, whole-cell, inside-out, and outside-out. An example of these configurations can be seen in **Figure 1-4.** The cell-attached configuration is achieved once a seal is formed between the pipet and the membrane. This can be changed to a whole cell configuration by rupturing the membrane beneath the electrode while maintaining the seal, allowing for direct contact between the electrode medium and the cytoplasm. In both of these cases, the cell is otherwise intact and measurements can be taken with respect to the whole cell. In contrast, inside-out and outside-out patching involve rupturing the membrane and taking a single patch containing ion channels. In inside out patch clamp, the membrane patch is take such that the

cytoplasmic surface of the membrane is exposed to the bathing solution. In outside out patch, the extracellular surface is instead exposed to the bathing solution. With respect to studying cholesterol-channel interactions, the patch clamp technique provides a way to directly assess the effects of increasing or decreasing membrane cholesterol, and has been used extensively for that purpose (Romanenko, Rothblat et al. 2004; Bukiya, Belani et al. 2011; Picazo-Juarez, Romero-Suarez et al. 2011; Rosenhouse-Dantsker, Noskov et al. 2013). Indeed, these techniques are very flexible for studying the biophysics of ion channels, and are the "gold standard" approach.

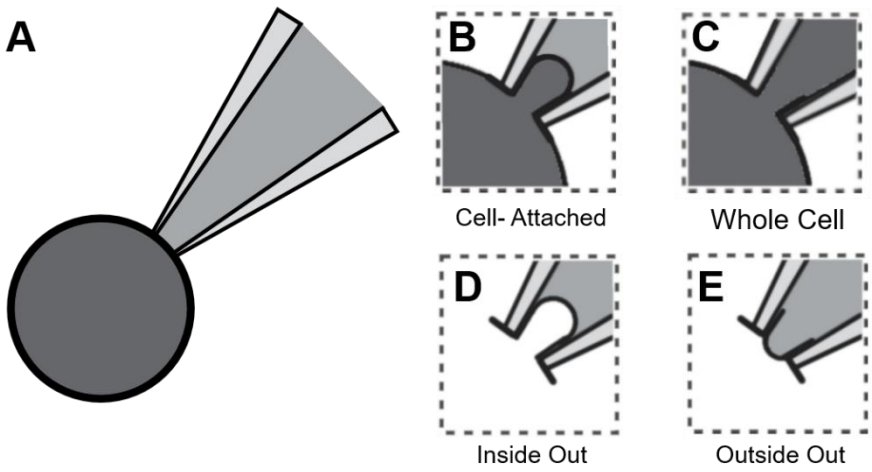

Figure 1-4. Schematic of Different Types of Patch Clamp. A) A schematic of a blunt electrode adhered to a cell. B) An electrode in the cell-attached configuration. Ni this configuration, ion channel activity can be recorded within the membrane patch isolated in the microelectrode tip. C) Disrupting the membrane patch within the pipette without disrupting the seal converts it to a whole-cell configuration, allowing direct contact between the cytoplasm and pipet solution. D) If instead, the pipet is pulled away abruptly and a patch is successfully pulled away from the cell, an inside-out patch is formed. Here, the cytoplasmic side of the membrane is exposed to the bathing solution. E) In contrast, if a whole cell configuration is achieved before the pipet is successfully removed, an outside-out patch is formed. In this configuration, the extracellular side of the membrane is exposed to the bathing solution.

In both patch clamp experiments and sharp microelectrode experiments, ion channel activity can be studied using either a voltage clamp or a current clamp technique**.** In the first case, the voltage across the membrane is held at a constant, predetermined level by applying a current that is equal and opposite to the sum of all membrane currents. Conversely, in the second case, a constant current is maintained across the membrane, allowing for the measurement of changes in membrane potential.

1.4.2. Modulating Cholesterol Concentration

One of the most common ways to control the amount of membrane cholesterol present is through methyl-β-cyclodextrin (MβCD), a cyclic oligosaccharide consisting of a macrocyclic ring of glucose subunits joined by α-1,4 glycosidic bonds (Zidovetzki and Levitan 2007). These oligosaccharides have a hydrophobic cavity which can hold cholesterol, and incubating cells with MβCD can effectively sequester cholesterol from cell membranes. Likewise, incubating cells with MβCD that has been pre-loaded with cholesterol can increase cell membrane composition. The benefit of this approach is that chiral isomers of cholesterol can also be loaded via MβCD, meaning chiral isomer studies can be performed in identical conditions. The combination of MβCD and patch clamp experiments have been used to show the effects of cholesterol on a number of different ion channels, including Kir channels (Rosenhouse-Dantsker, Noskov et al. 2013), VRAC (Romanenko, Rothblat et al. 2004), TRPV channels (Picazo-Juarez, Romero-Suarez et al. 2011), and BK channels (Bukiya, Belani et al. 2011).

1.4.3. Förster Resonance Energy Transfer (FRET)

FRET experiments provide a powerful biophysical tool to determine the spatial proximity between elements in membranes and proteins, specifically fluorophores. The basic concept of FRET involves a donor and an acceptor fluorophore. These are chosen such that the emission spectrum of the donor has substantial overlap with the excitation spectrum of the acceptor. In this way, spatial proximity between the fluorophores can indirectly be measured via fluorescence (Piston and Kremers 2007; Chakraborty and Chattopadhyay 2015). In the context of sterol-protein interactions, FRET can be used to interrogate the direct interactions between cholesterol and its target protein, or the indirect effects of cholesterol on protein function. For example Antollini and Barrantes (1998) measured the FRET efficiencies from the tryptophan residues on the nAChR to the fatty-acid derivative, 6-lauroyl-2-dimethylaminonaphthalene (laurdan), under different cholesterol conditions (Antollini and Barrantes 1998). In another study, which used the fluorescent sterol cholestatrienol as the FRET acceptor from tryptophan residues in rhodopsin, it was shown that the protein exhibited greater affinity for cholesterol than for ergosterol, likely through competition for a common binding site in the protein (Albert, Young et al. 1996). These examples also highlight a limitation of FRET. As a relatively small molecule with important structural effects on surrounding the surrounding lipid membrane environment, it is difficult to create a cholesterol-analog fluorophore that acts in a similar manner to cholesterol. Consequently, FRET studies with cholesterol either measure effects indirectly, via other fluorophores, or through cholesterol analogs.

Another approach to FRET focuses instead on fluorophores within the target protein, indirectly measuring the effect of lipids and sterols on the conformational ensemble of the

protein. In the case of ion channels, this has been used to study the effects of PIP2 on bacterial potassium channels (Wang, Vafabakhsh et al. 2016).

1.4.4. X-ray and Electron Crystallography

At the atomic structural level, the major experimental techniques are x-ray crystallography and electron crystallography. In the last several decades, high resolution crystal structures of channel-lipid complexes have be used to characterize specific lipid binding sites. X-ray crystallography structures are obtained by extracting ion channels from their lipid bilayers via solubilization with detergents. Because of the use of these detergents, annular lipid or lipids that might otherwise be associated with the protein structure are often lost in the experimental process. However despite this limitation, more tightly bound, non-annular lipids have been co-crystallized with their protein targets for several different types of proteins, including ion channels and GPCRs, and have provided important insight into lipid binding, particularly for cholesterol binding sites (Wacker, Fenalti et al. 2010; Wacker, Wang et al. 2013) (Segala, Guo et al. 2016).

Electron crystallization has also provided important structural insights. Here, rather than solubilizing with detergent, a purified protein is reconstituted in a lipid bilayer to form a periodic array, or 2D crystal. Because lipids surrounding the protein are imaged in the periodic array, this technique allows for visualizing proteins in a more native-like lipid environment and provides insight into some of the interactions of annular lipids with the crystallized protein. Even in the absence of co-crystallized lipids, the atomistic protein structures obtained from crystallography have been crucial for use in computational methods, particularly when multiple conformational states are resolved.

1.5. Computational Methods to Study Cholesterol-Protein Interactions

In spite of the insight gained from the array of experimental approaches employed and described above, there are huge questions left unanswered about cholesterol-protein interactions, particularly at the molecular level where viewing the atomic details remains challenging. Although techniques like x-ray crystallography and cryo-EM provide detailed structural information about proteins at the molecular level, they lack dynamic information. Furthermore, it is difficult to co-crystallize transmembrane proteins with more than a handful of annular lipids, depriving them of an important context. NMR experiments in contrast provide dynamic information about the protein, but only for small protein peptide systems. Other experimental approaches sacrifice resolution for scope. Fluorescence techniques are limited to supra-atomic resolution, and functional assays, while excellent at discerning the regulatory impacts of specific lipid interactions, often cannot provide detail on the underlying mechanisms. To remedy these deficiencies, there are a number of different computational approaches that have been developed to elucidate the molecular details of protein-lipid interactions. Two of the most commonly used computational techniques to explore ligand binding are molecular docking and molecular dynamics simulations.

1.5.1. Molecular Docking

Molecular docking is a computational method which attempts to predict the orientation of ligand molecules within their respective binding pockets on a target protein. The overall aim of this approach is to simulate the process of molecular recognition and find a binding conformation that minimizes the free energy of the protein-ligand complex (Chaudhary and Mishra 2016; de Ruyck, Brysbaert et al. 2016). Overall, the experimental methodology for molecular docking consists of two parts: 1) the search algorithm and 2) the

scoring function. The search algorithm determines how the program explores the conformational space of the ligand within its target binding site. There are a number of different algorithms that can be employed, including genetic algorithms, systematic searches, fragment-based searches, and Monte Carlo methods (Rarey, Kramer et al. 1997; Chaudhary and Mishra 2016). Regardless of the chosen algorithm, the end goal is the same: a list of conformations for the ligand on its target receptor. Once this list is generated, the individual conformations are ranked according to the scoring function. The scoring function is used to predict the binding affinity of a given ligand conformation to identify the best results. These scoring functions can be generated from empirical data or molecular mechanics, and they take into account four different classes of interactions between a ligand and receptor: 1) electrostatic interactions (dipole-dipole, charge-dipole, and charge-charge), 2) Van der Waals forces, 3) hydrogen bonding and hydrophobic interactions, and 4) steric interactions. An example of a molecular docking result is shown in **Figure 1-5**.

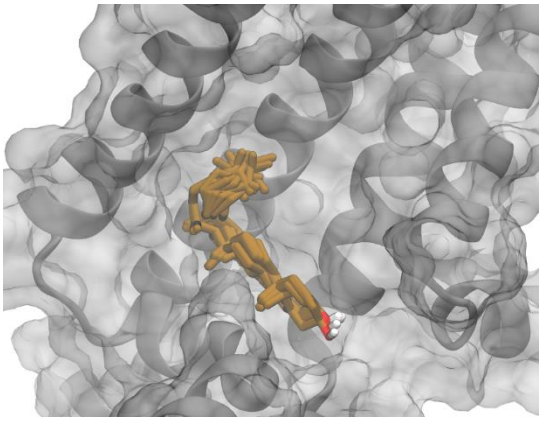

Figure 1-5. Example of a molecular docking result. The predicted poses of the target ligand are shown in brown. The protein is shown in a ribbon view, overlaid with its molecular surface.

An important technical consideration for molecular docking is the resolution of the target protein structure. A low resolution crystal structure which incorrectly identifies tertiary structure of the protein can lead to incorrectly shaped or oriented binding sites and increase the chances of generating false-positive results. As crystallography techniques continue to improve in resolution however, this is becoming less of an issue. A significant limitation for molecular docking studies is that docking analyses typically use a static protein structure while utilizing molecular force fields or turnkey methods for predicting favorable binding poses and binding energetics, which by nature are an approximation (Morris, Huey et al. 2009; Chaudhary and Mishra 2016). This use of static structures is a major limitation, as proteins in their native environment can have flexibility in their secondary and tertiary structures. Specifically, for binding events, amino acids in a binding pocket can rotate and shift position to accommodate different ligands (Arkin, Randal et al. 2003), something which is not taken into account in a static-structure docking study. Likewise inter-subunit binding sites, wherein a lipid or cholesterol molecule inserts itself and shifts the surrounding structure, would be difficult to detect via docking to a static structure. In addition to rigid protein receptors, another potential limitation in molecular docking techniques is the flexibility of the target ligand. Because molecular docking algorithms explore the conformational space of the target ligand, highly flexible molecules with many rotational degrees of freedom are difficult if not impossible to dock accurately. In the context of protein-ligand binding, this severely limits applicability to lipids, as the fatty-acid tails of these lipids are highly flexible and would be computationally intractable. Nevertheless, success has been achieved by docking more rigid molecules, such as cholesterol, or restricting docking analyses to the head groups of lipids (Lee, Wang et al. 2013; Rosenhouse-Dantsker, Noskov

et al. 2013) (Barbera, Ayee et al. 2017). Furthermore, this limitation can be overcome through the use of molecular dynamics simulations which use the docked pose of the ligand as a starting point. This has been done for a variety of proteins, and allows more detailed explorations into the protein-ligand interactions. (Rosenhouse-Dantsker, Noskov et al. 2013; Fürst, Nichols et al. 2014; Hénin, Salari et al. 2014) However, even with these limitations, docking analyses are a powerful approach to provide initial insights and screening into potential ligand binding sites, including cholesterol binding sites.

1.5.2. Molecular Dynamics Simulations

Molecular dynamics simulations are a family of computational approaches used to simulate the movement of atoms and molecules. At their core, MD simulations involve numerically solving Newton's equation of motion for a set of particles over a given period of time. By specifying the initial positions and velocities of a set of particles and defining the rules for intermolecular interactions between particles (via a forcefield), the acceleration of each particle can be calculated. This in turn allows for calculating new velocities and positions of each particle in the system. By iterating this process over millions of time steps, the temporal evolution of the system can be calculated. In the context of protein-ligand interactions, MD simulations can provide a molecular-scale view of these binding interactions, offering insight into the mechanisms of ligand binding, the kinetics and energetics of binding favorability, and the potential shape and location of binding sites on the target protein.

There are a number of important considerations to be made when using MD simulations to interrogate protein-lipid interactions. Central to the validity of MD simulation results is the choice and accuracy of the force field (Guvench and MacKerell 2008; Lopes,

Guvench et al. 2015). The force field parameterizes the intramolecular forces between the atoms or particles in the simulation system, and is based on experimental data, higher resolution quantum mechanical simulations, and chemical intuition. Multiple force fields have been parameterized specifically for biological systems, including AMBER (Case, Ben-Shalom et al. 2018), CHARMM (Brooks, Brooks III et al. 2009), GROMOS (Scott, Hünenberger et al. 1999), OPLS (Jorgensen, Maxwell et al. 1996), and Martini (Marrink, Risselada et al. 2007). In addition to the choice of force field, another important consideration in protein-lipid simulations is that of sampling size. Sampling size can refer to a number of different system attributes, including simulation size (either number of particles or simulation dimensions), simulation runtime, and number of replicates. For each of these system attributes, there is a tradeoff. Larger systems, longer simulations, and more simulation replicates yield more data, but at increasing computational cost. Consequently, in studying protein-lipid interactions with MD simulations, care must be taken in explicitly defining the research question and the simulation objectives. In the context of protein-lipid interactions, the most useful types of simulations are atomistic simulations, where every atom is explicitly described and simulated, and coarse-grained simulations, which group together or average in some form over multiple atoms.

1.5.2.1. Atomistic Simulations

As stated above, atomistic simulation force fields parameterize every atom in the system, providing a high resolution and explicitly detailed molecular system. Consequently, atomistic MD simulations can be a powerful tool in identifying the specific interactions between a sterol and its protein or ion channel target. Indeed, atomistic MD simulations have been used to identify or confirm the cholesterol binding site on a number of membrane

proteins, including the β_1-adrenergic receptor (β_1AR) (Cang, Yang et al. 2014), rhodopsin (Khelashvili, Grossfield et al. 2009), and the A_{2A} adenosine receptor (Lee and Lyman 2012). However, although an explicit atomistic system can closely model the chemistry and physics underlying protein-lipid interactions, the maximum length- and time-scales achievable with current computational power are still limited. In many studies, simulations are limited to a single protein in a small, simple model lipid membrane, often comprised of only 2 or 3 separate components. Likewise, the timescale achievable with atomistic simulations is on the order of hundreds of nanoseconds to microseconds. When the binding site of a ligand is already known, such as after a docking analysis or from a crystal structure, these limitations are less of an issue. However, in the case of lipids like cholesterol, which have less explicitly defined binding sites and a higher abundance in the membrane, atomistic simulations are often not long enough to capture the relevant dynamics (Sengupta and Chattopadhyay 2015; Hedger and Sansom 2016).

1.5.2.2. Coarse-grained Simulations

Coarse-grained (CG) simulations offer a complimentary approach to atomistic simulations that offset some of the aforementioned issues with atomistic simulations. In coarse-grained simulations, groups of atoms are approximated as single particles. In this way, the number of particles in a simulation can be dramatically reduced, significantly reducing the computational load and allowing for larger simulations and longer simulation times. In my studies, I have utilized a coarse-grained force field called the Martini force field (Marrink, Risselada et al. 2007; Monticelli, Kandasamy et al. 2008). The Martini force field has been the most widely applied coarse-grained force field to study lipid-protein interactions. The general philosophy of the martini model is to map groups of on average 4

heavy atoms together into interaction particles with distinct physiochemical properties. These particles come in 4 different types, with 4 to 5 subtypes in each particle, giving a total of 18 different particle types. This parameterization allows for constructing coarse-grained systems in a modular way, providing a means to compare between protein and lipid systems. Consequently these types of CG simulations have seen a rapid expansion in their use for determining the molecular mechanics of lipid membrane-protein interactions: in the context of cholesterol, interaction sites have been determined for several types of G-protein Coupled Receptors (GPCRs) as well as nAChR, and serotonin receptors (Lee and Lyman 2012; Cang, Du et al. 2013; Genheden, Essex et al. 2017; Rouviere, Arnarez et al. 2017).

It is important to note that, as a coarse-grained model, there are certain built-in limitations to using the Martini force field. Grouping atoms together into coarse-grained particles reduces degrees of freedom in a system to speed up simulation time, but results in a smoothened energy landscape. This tradeoff leads to longer timescales but at the loss of fine molecular detail. Furthermore, it has been shown that membrane proteins need an elastic network to stabilize their tertiary structure, restricting dynamics to a single conformational state (Marrink and Tieleman 2013; Grouleff, Irudayam et al. 2016; Hedger and Sansom 2016).

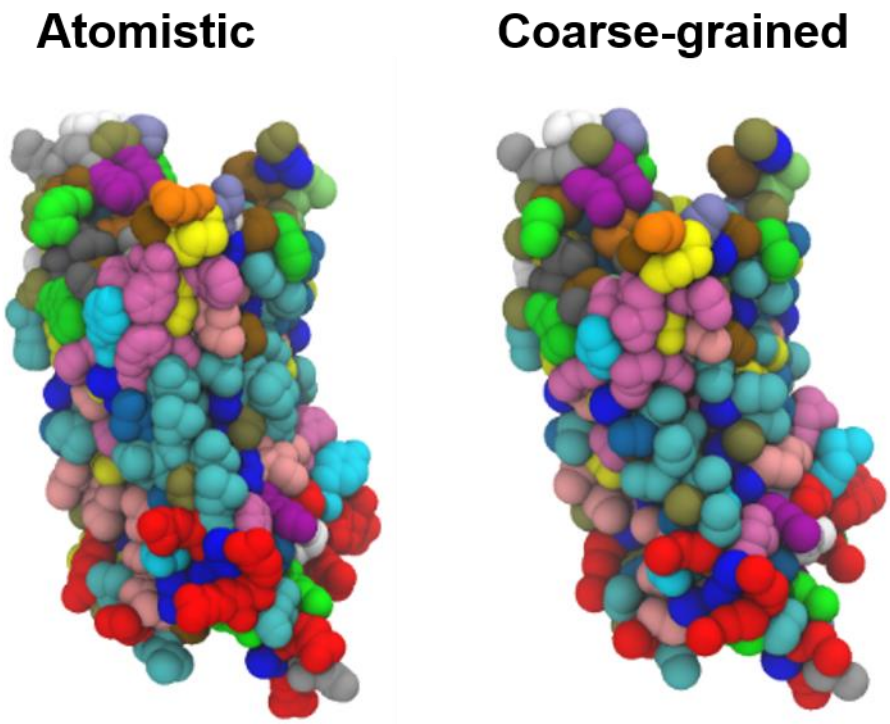

Figure 1-6. Visualization of a protein. Spheres are colored by residue type, at both the atomistic (left) and coarse-grained (right) scale.

1.5.3. Network Theory

In addition to the use of molecular dynamics simulations, a significant portion of the methodology in this thesis involves using principles and approaches from network theory to identify potential cholesterol binding sites and elucidate the mechanisms of cholesterol-mediated regulation of potassium channels. Network theory is an approach to studying complex systems which represents agents of the system and interactions between them as a graphical model consisting of nodes (agents) and edges (pairwise interactions) (Borgatti and Halgin 2011). The agents in these networks can vary considerably based on the system of interest, and network theory has been used to study a wide range of subjects including gene

transcription networks (Pavlopoulos, Secrier et al. 2011), social networks (Bianconi, Pin et al. 2009), proteins (Jacobs, Rader et al. 2001), and transit networks (Ding, Ujang et al. 2015). In each of these different systems, the choice of network and its construction are important considerations. Edges connecting nodes can be given directionality, such as in the case of transcription networks, to indicate causality or directional correlation. Likewise, edges between nodes can be assigned varying weights, signifying stronger or weaker ties. Conversely, connections between nodes can be non-directional and equally weighted.

In the context of studying protein-ligand binding, networks are typically used to map out intra- and inter-molecular structure, such as ligand-residue or residue-residue proximity. (De Ruvo, Giuliani et al. 2012; Hu, Zhou et al. 2013). In the case of ligand-residue interactions, the resulting graph is often analyzed to score potential binding sites. Likewise in the case of residue-residue or intra-protein interactions, these networks are analyzed to characterize changes in protein structure and protein dynamics, such as conformational changes and allostery (De Ruvo, Giuliani et al. 2012). Relationships between residues can also be defined functionally, dictated in part by the concurrent interaction of groups of residues with a given ligand, as in the interpretation of NMR data, where individual amino acids are assessed for their importance in protein function and protein-protein interaction (Kurzbach 2016). While a network approach based on structure is sufficient for 'tight' ligand binding to a single site, as in the case of a drug-like molecule, functional network analysis helps to parse larger datasets, such as the ones I will later show for cholesterol-Kir2.2 interactions. In this thesis I detail two approaches I developed to 1) identify cholesterol binding sites on the Kir2.2 channel and 2) predict the functional consequences of this binding which utilize this network theory-based methodology.

1.6. Approaches to Identify Cholesterol Binding Sites

In general, two different approaches have been used in previous investigations to identify direct cholesterol interaction sites on ion channels: 1) by searching for known cholesterol-binding motifs in the primary sequence of the channel, such as CRAC or CARC (Fantini and Barrantes 2013; Di Scala, Baier et al. 2017; Dopico and Bukiya 2017), or 2) using molecular docking to identify candidate binding sites in an unbiased way (Brannigan, Hénin et al. 2008; Rosenhouse-Dantsker, Noskov et al. 2013; Weiser, Salari et al. 2014).

1.6.1. Cholesterol Recognition Sites

Cholesterol recognition sites are regions of a protein hypothesized to be sites of direct cholesterol binding. These sites are identified in transmembrane proteins through their specific primary acid sequence. For cholesterol, the most well-known site is the Cholesterol Recognition Amino acid Consensus motif (CRAC), and its mirror image CARC. CRAC is a short, linear motif in the N-terminus to C-terminus direction which follows a simple, loose algorithm defined in Fantini and Barrantes 2013: "a branched, apolar Leu or Val residue, followed by a segment containing 1–5 of any residues, then an aromatic residue that is mandatory, Y, then again a segment containing 1–5 of any residues, and finally a basic Lys or Arg." This sequence (L/V)-X_{1-5}-(Y)-X_{1-5}-(K/R) is an oriented motif. That is to say, if the CRAC motif is in the transmembrane domain, it must be oriented such that the residue at the c-terminus must be located at the lipid-water interface. Likewise its mirror image, CARC, follows the opposite requirement. Both CRAC and CARC were explored in detail in nicotinic acetylcholine receptor (nAChR) (Di Scala, Baier et al. 2017) and have been identified in a variety of membrane proteins. (Baier, Fantini et al. 2011; Fantini and Barrantes 2013; Di Scala, Baier et al. 2017). Furthermore, using site-directed mutagenesis and functional

studies, CRAC/CARC-related cholesterol binding sites were also identified in BK channels (Singh, McMillan et al. 2012), P2X7 (Murell-Lagnado 2017), TRPV1 channels (Picazo-Juarez, Romero-Suarez et al. 2011), and voltage-gated potassium channels Kv1.3 (Balajthy, Hajdu et al. 2017).

It is important to note however that while multiple instances of these motifs have been found in a number of different ion channels, in many cases it is not clear whether the identified sequences truly comprise a cholesterol binding site. Indeed a recent analysis of crystal structures containing bound cholesterol showed that the known cholesterol-binding motifs only make up a subset of cholesterol binding regions, and the majority of identified cholesterol-protein complexes did not feature any of these motifs (Rosenhouse-Dantsker 2017).

1.6.2. Combined Computational and Experimental Approach

An alternative approach to identifying cholesterol binding sites on ion channels, not involving binding motifs, involves using a combination of unbiased docking analysis with molecular dynamic simulations. Here, docking of cholesterol is performed on the entire channel structure and the resulting conformations are tested for stability by the MD simulations. This approach, which is unbiased for any motifs or sites, has been successful in identifying cholesterol binding sites on nAChR, VDAC, and $GABA_A$ Receptors (Brannigan, Hénin et al. 2008; Hénin, Salari et al. 2014; Weiser, Salari et al. 2014). Furthermore, as will be detailed in the following section, this approach was combined with site-directed mutagenesis and electrophysiology to identify cholesterol binding regions of Kir2.1 channels (Rosenhouse-Dantsker, Noskov et al. 2013).

1.7. Cholesterol Regulation of Inwardly Rectifying Potassium Channels

1.7.1. Inwardly Rectifying Potassium Channels: Their Structure and Function

This thesis focuses on the regulation of inwardly rectifying potassium channels by cholesterol. Inwardly rectifying potassium (Kir) channels form a family of transmembrane proteins that help regulate resting membrane potential, selectively allowing the influx or efflux of K+. They are found in a wide variety of cells, including endothelial cells (Silver and DeCoursey 1990) (Fang, Schram et al. 2005), epithelial cells (Hebert, Desir et al. 2005), cardiac myocytes (Kurachi 1985; Hibino, Inanobe et al. 2010), and neurons (Brown, GÃ¤hwiler et al. 1990). Kir channels play a key role in regulating the action potential duration in electrically excitable cells and in maintaining the resting membrane potential (Sakmann and Trube 1984) by permitting less current flow at potentials positive to the equilibrium potential E_K and large K+ conductance at negative potentials (Noble 1965). Overall, there are 7 subfamilies of Kir, Kir1-Kir7, with multiple members in each family.

Structurally, Kir channels are tetramers with four identical subunits, shown in **Figure 1-7**, with the subunits arranged around a central axis to form a pore. Each subunit contains a number of structural motifs common to all Kir channels, including (i) two membrane-spanning alpha helices (TM1 and TM2) connected by an extracellular pore-lining region, (ii) cytosolic NH_2 and COOH termini, (iii) a slide helix at the membrane interface, and (iv) a selectivity filter comprised of the sequence T-X-G-Y(F)-G. This last motif is a signature sequence in K+ selective ion channels (Bichet, Haass et al. 2003). As a membrane-embedded protein, the channel structure can also be divided into two domains, the cytosolic and transmembrane (TM) domains, as shown in **Figure 1-7**.

To regulate the flow of potassium ions through its central pore, Kir channels undergo conformational changes between open and closed states, a process which is regulated by the binding of phosphatidylinositol 4,5-bisphosphate (PIP2) to specific sites on each subunit. PIP2 binding yields a corresponding structural rearrangement of the cytosolic and transmembrane domains (Tao, Avalos et al. 2009; Hansen, Tao et al. 2011). Although crystal structures of Kir channels have been discovered for a number of different conformations, these static structures are only snapshots of the gating process, and the mechanism underlying transition from one state to another is not fully known. Furthermore, the functional activity of Kir channels does not lend itself to simple binary on/off model of gating. Rather, it has been shown that there are two distinct gating modes in Kir channels, slow gating and fast gating (Hibino, Inanobe et al. 2010). These two modes correspond to the two types of activity observed in single channel recordings of Kir channels: 1) sustained periods of inactivity, followed by 2) periods of "burst" activity where the channel rapidly opens and closes. Slow gating mechanisms govern the transition from the period of inactivity to burst activity, while fast gating governs the rapid flickering. Previous experiments have shown that mutations in the cytosolic domain of the protein tend to modulate the behavior of slow gating, while mutations around the selectivity filter cause alterations in fast gating, indicating that the different sections of the protein play distinct roles in gating (Trapp, Proks et al. 1998; Proks, Capener et al. 2001; Yi, Lin et al. 2001; Hibino, Inanobe et al. 2010).

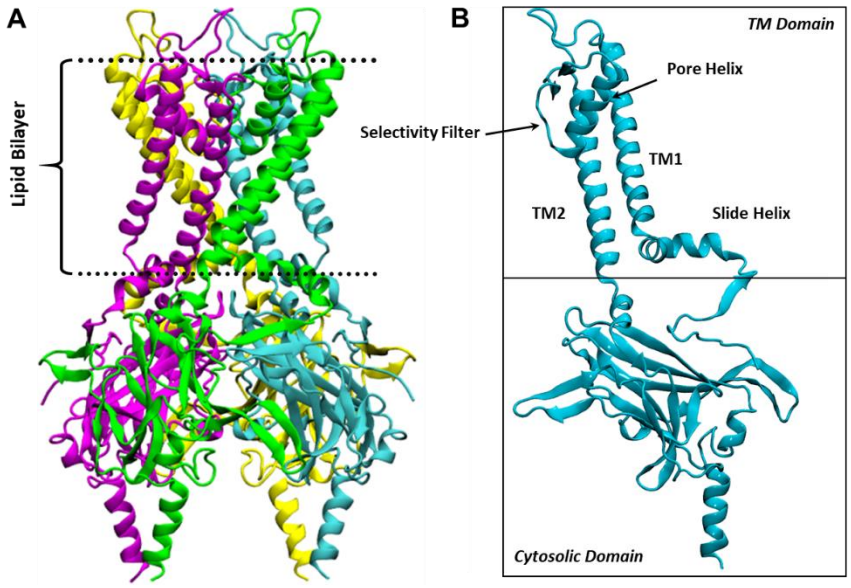

Figure 1-7. Shematic of a Kir Channel. A) The structure of a Kir tetramer, with the location of the lipid bilayer marked by dashed lines. B) A single subunit of the Kir channel, with the separate domains and structural features highlighted

The results contained in this dissertation focus on Kir2 channels, a major sub-family of Kir that is ubiquitously expressed in a variety of cell types, including neurons, cardiomyocytes, smooth muscle cells, endothelial cells and macrophages (Levitan 2009). Kir2 channels are known to be critically involved in regulating membrane excitability in cardiac and smooth muscle cells (Zaritsky, Eckman et al. 2000; Miake, Marban et al. 2003; Piao, Li et al. 2007) and neurovascular coupling (Filosa, Bonev et al. 2006). Early studies from the Davies group also showed that Kir channels expressed in vascular endothelial cells are sensitive to a mechanical force generated by fluid shear stress (Olesen, Clapham et al. 1988) leading to the hypothesis that endothelial Kir channels may be one of the putative shear stress sensors (Davies 1995). As expected from their biophysical profiles, endothelial Kir channels were later identified as Kir2.1 and Kir2.2 (Fang, Schram et al. 2005; Ahn, Fancher

et al. 2017) and recent studies from the Levitan group demonstrated that Kir2.1 channels play a major role in endothelial control of vascular tone via activation of endothelial nitric oxide synthase (eNOS) regulation of NO release (Ahn, Fancher et al. 2017). Furthermore, most recently, the Levitan group established that cholesterol-induced suppression of endothelial Kir2.1 channels has a major impact on vascular function in dyslipidemia: it is responsible for the impairment of flow-induced vasodilation and augments the development of atherosclerosis (Fancher, Ahn et al. 2018). It is clearly critical, therefore, to elucidate the molecular basis of cholesterol regulation of these channels.

1.7.2. Cholesterol Regulates Kir2 Function through Direct Interactions

In previous studies by the Levitan group, increases in cellular cholesterol were found to strongly suppress Kir2.1 channels in endothelial cells (Romanenko, Rothblat et al. 2002) and in a heterologous expression system. (Romanenko, Fang et al. 2004) However, as described above, there are three different ways in which cholesterol can regulate ion channel function. This necessitated further experiments to elucidate the mechanism of cholesterol regulation. To test whether cholesterol regulated Kir2 channel function through protein intermediaries, Kir channel activity was measured in liposomes that contained none of the possible regulatory proteins or lipids. As mammalian Kir2 channels were not available in a purified form at the time, they used a purified bacterial homologue of Kir, KirBac1.1, which could be incorporated (Enkvetchakul, Bhattacharyya et al. 2004) (Singh, Rosenhouse-Dantsker et al. 2009). With this approach they showed that purified Kir channels are suppressed by an increase in cholesterol level of the bilayer, even the absence of intermediates. Additional experiments further demonstrated that that there is no correlation between the activity of these channels and membrane fluidity, as modulated by an array of

different sterols (Singh, Rosenhouse-Dantsker et al. 2009). Later, when purified mammalian Kir2.1 was available, it was likewise shown that cholesterol suppresses channel activity when incorporated into liposomes (D'Avanzo, Hyrc et al. 2011).

In addition to having shown that cholesterol does not regulate channel function through intermediaries or through membrane fluidity, experiments were also performed using chiral isomers to discern whether cholesterol directly interacts with Kir to suppress function. It was found that while loading cells with cholesterol decreased channel function, loading cells with the chiral isomer epicholesterol had the opposite effect. Here, removing ~50% of endogenous cholesterol and substituting it with a similar amount of epicholesterol resulted in a strong increase in Kir current density that was much higher than in cells depleted of cholesterol to the same degree (Romanenko, Rothblat et al. 2002). This evidence suggested that cholesterol regulated Kir function via direct interactions, and that epicholesterol competes with cholesterol for a binding site. Likewise, in another study it was shown that ent-cholesterol has no effect on Kir activity (D'Avanzo, Hyrc et al. 2011), further supporting the conclusion that cholesterol regulates Kir channels by specific direct interactions. Together, all of these studies strongly suggest that cholesterol regulates Kir2 channel function through direct interactions with the protein.

1.7.3. Molecular Simulations and Site-directed Mutagenesis Reveal Residue Candidates for a Putative Binding Site

Having established that cholesterol negatively regulates Kir channel function through direct interactions, the next challenge was to identify where cholesterol is binding and elucidate how this binding affects channel function mechanistically. To identify the direct interaction sites of cholesterol on Kir channels, previous studies from the Levitan lab used a

combination of computational analyses and electrophysiological experiments (Rosenhouse-Dantsker, Noskov et al. 2013). In this method, docking analyses and short-timescale atomistic simulation are used to generate initial predictions for binding sites. As described in the preceding sections, a docking analysis is a common technique in structure-based drug design which generates predictions of the conformation of a ligand within a potential binding site on a protein (Chaudhary and Mishra 2016). In the study by Rosenhouse-Dantsker et al., docking analyses were used to predict pockets in Kir2 where cholesterol could favorably interact (Rosenhouse-Dantsker, Noskov et al. 2013). The predictions of these docking analyses were then refined through atomistic simulations to identify the most energetically favorable binding conformations and potential cholesterol-binding residues. Once these amino acid residues were identified, they were tested through site-directed mutagenesis and electrophysiological recordings. Residues important for cholesterol sensitivity were then defined as those whose modification abrogated the ability of cholesterol to inhibit channel activity. Using this strategy, Rosenhouse-Dantsker et al. identified putative cholesterol binding regions located at the non-annular hydrophobic pockets of Kir2.1 formed by the transmembrane helices, which do not contain any known cholesterol binding motifs (Rosenhouse-Dantsker, Noskov et al. 2013). A similar cholesterol binding region was identified more recently for Kir2.2 channels (Fürst, Nichols et al. 2014).

However, while this previous work successfully identified a putative cholesterol binding site, a number of questions regarding the mechanism of cholesterol regulation still remain. First, the mechanism underlying cholesterol stereospecificty remain unclear. Although the general assumption of stereospecificity has been that chiral isomers do not bind, previous experiments have challenged this and showed that replacing cholesterol with

epicholesterol leads to an increase in channel activity, suggesting a competitive inhibition mechanism. With respect to identifying the putative cholesterol binding site, computational experiments were limited to docking analyses and short-timescale MD simulations. The limitation here is that docking analysis neglect to consider the effects of the surrounding membrane environment on ligand binding favorability, and fail to consider potential binding sites on the surface of the protein (Sousa, Fernandes et al. 2006; Huang and Zou 2010). Likewise, although the short timescale MD simulations can confirm the stability of predicted binding sites, they cannot account for diffusion of cholesterol from the membrane to the channel surface (Ingólfsson, Lopez et al. 2014; Hedger and Sansom 2016).

In this dissertation I addressed these questions and further characterized cholesterol-Kir interactions. I focus my analysis on Kir2.2 because of the recently identified crystal structure (Hansen, Tao et al. 2011) and because it was shown previously that all subtypes of Kir2 channels (2.1, 2.2, 2.3, and 2.4) are suppressed by cholesterol – with Kir2.1 and Kir2.2 being equally sensitive (Romanenko, Fang et al. 2004). Moreover, the homology between 2.1 and 2.2 sequences (70% sequence identity) allows for the comparison of cholesterol binding regions between the two channels. I approach this problem in two ways. First, I performed extensive docking analyses of cholesterol and its chiral isomers, epicholesterol and ent-cholesterol, on five ion channels whose response to cholesterol was shown to be stereospecific: Kir2.2, KirBac1.1, TRPV1, $GABA_A$ and BK. Second, I employed coarse-grained molecular dynamics simulations of Kir2.2 in a model membrane environment of cholesterol and POPC.

2. COMPARATIVE DOCKING OF CHOLESTEROL ANALOGUES

(Previously published as *Barbera, Nicolas A., Baruch Minke, and Irena Levitan. "Comparative docking analysis of cholesterol analogs to ion channels to discriminate between stereospecific binding vs. stereospecific response." Channels 13.1 (2019): 136-146.*)

2.1. Introduction

As has been described above, cholesterol is an important regulator of many ion channels. This regulation is thought to operate either indirectly, by altering the physical properties of the membrane or localizing the protein to lipid rafts, or directly, via specific interactions with the channel. A common approach to elucidate mechanisms of cholesterol regulation and differentiate between direct and indirect methods of cholesterol regulation has been through the comparative analysis of different sterols. This comparative analysis takes advantage of the chirality of cholesterol isomers, whose different "handedness" means their structures are non-superimposable even if their chemical formulas are identical. The governing logic of this approach is that if chiral isomers alter membrane properties in a similar way, but have different effects on protein function, then it's more likely that cholesterol acts via direct interactions. Likewise, the assumption has been that if cholesterol has an effect on channel function while its chiral isomers do not, then these isomers do not bind to the channel. (Romanenko, Rothblat et al. 2002; Addona, Sandermann et al. 2003; Romanenko, Fang et al. 2004; Singh, Rosenhouse-Dantsker et al. 2009; Bukiya, Singh et al. 2011; Picazo-Juarez, Romero-Suarez et al. 2011; Fürst, Nichols et al. 2014). However, previous studies with both mammalian and bacterial Kir channels have challenged this assumption. In these experiments, replacing 50% of the endogenous cholesterol with epicholesterol led to increases in channel activity, suggesting instead that epicholesterol is in fact binding and is a competitive inhibitor (Romanenko, Rothblat et al. 2002; Singh, Shentu

et al. 2011). These results lead to an alternative hypothesis: chiral isomers do bind to the channel, but do not interact with the cholesterol binding site in the same manner as cholesterol, either by occupying a different binding orientation or having a different set of interactions with binding site residues. To test this hypothesis, I performed docking analyses of cholesterol, epicholesterol, and ent-cholesterol on ion channels found to be stereoselective, namely Kir2.2, KirBac1.1, TRPV1, $GABA_A$, and BK (Sooksawate and Simmonds 2001; Romanenko, Rothblat et al. 2002; Addona, Sandermann et al. 2003; Romanenko, Fang et al. 2004; Singh, Rosenhouse-Dantsker et al. 2009; Bukiya, Singh et al. 2011; Picazo-Juarez, Romero-Suarez et al. 2011).

2.2. Methods

2.2.1 Docking Analyses

Docking analyses were performed using AutoDock Vina (Trott and Olson 2010) on five different ion channels, all of which were shown previously to have cholesterol stereospecificity: *Kir2.2, KirBac1.1, TRPV1, $GABA_A$, and BK*. Structures for these channels were taken from the PDB databank (PDB IDs: 3SPI, 1P7B, 3J9J, 4COF, 5TJ6, respectively). The crystal structure resolution of each structure is shown in **Table 2-1.** The general methodology of the AutoDock program is a multi-step process. First, a search space was defined on the target receptor, which was then discretized into a three dimensional grid. Here, the search space was defined such that the center of the search space aligned with the center of the transmembrane region of each tested channel. Likewise, boundaries of the search space were set at the lipid-water interface, as defined by the OPM database (Lomize, Pogozheva et al. 2011). Because these tested channels were multimeric proteins, the dimensions of the search space were chosen to cover both a single subunit and the regions

between subunits. Specifically, the dimensions for each system were: 32.25 Å x 33 Å x 42.75 Å (Kir2.2), 46.5 Å x 33 Å x 36.75 Å (KirBac1.1), 47.25 Å x 47.25 Å x 33.75 Å (TRPV1), 29.25 Å x 45 Å x 47.25 Å ($GABA_A$), and 42.75 Å x 42.75 Å x 42.75 Å (BK). Once the search space was defined, the ligand (cholesterol, epicholesterol, or ent-cholesterol) was placed into the grid and a conformational search was run. This search was run with a genetic algorithm and an exhaustiveness of 40 to ensure adequate sampling of the configurational space. Docking analyses were repeated three times for each sterol on each channel. The results of the docking analysis consist of a list of poses with associated scores. For this study, the top scoring pose was chosen. To determine reproducibility, the RMSD and estimated binding energies of predicted binding poses were compared for all three runs for each sterol,

$$RMSD = \sqrt{\frac{1}{N}\sum_{i=1}^{N}\delta_i^2}$$

where δ_i is the distance between atom i of one predicted pose (excluding hydrogen atoms) and the corresponding atom in the predicted pose of another run.

Additionally, residues interacting with the sterol were defined as those within 4.5 Å of the predicted binding pose.

Structure	**PBD**	**Resolution**
Kir2.2	3SPI	3.307 Å
KirBac1.1	1P7B	3.65 Å
TRPV1	3J9J	3.275 Å
$GABA_A$	4COF	2.97 Å
BK	5TJ6	3.5 Å
β2AR	5D6L	3.2 Å

Table 2-1. Crystal Structure Resolutions

2.2.2 Validation of cholesterol docking procedure

Before docking the sterols to each ion channel, the method was validated by performing a docking analysis of cholesterol to a crystal structure with a known cholesterol binding site, the β2-adrenergic receptor. The crystal structure for this protein was taken from the PDB databank (PDB: 5D6L), and all solvents and ligands were removed from the structure file. Following the procedure outline above, 3 separate docking analyses were performed with cholesterol on the TM region, with x- and y- dimensions of 38.25 Å and 37.5 Å, and the results were compared with the crystal structure binding site. As expected, we found that the top-scoring binding pose from the docking analysis showed good agreement with the crystal structure pose, having an RMSD of 3.83 Å.

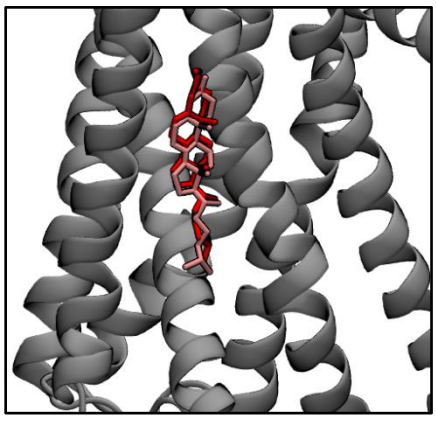

Figure 2-1. Docking analysis prediction versus crystal structure. The results of the docking analysis on the receptor are shown in red, while the crystal structure pose of choelsterol is shown in pink.

2.3. Results

2.3.1. Stereoisomers Interact Similarly in Kir2.2 and KirBac1.1

Docking analyses were performed for cholesterol, epicholesterol, and ent-cholesterol on the transmembrane regions of Kir2.2 and KirBacc1.1 and the highest scoring pose was chosen to analyze. For each sterol, three docking analyses were run to ensure reproducibility of results. Predicted binding energies for the three sterols were found to be very similar on Kir2.2, with predicted binding energies of -9.75 kcal/mol, -9.8 kcal/mol, and -9.9 kcal/mol for cholesterol, epicholesterol, and ent-cholesterol respectively. In addition to having very similar binding energies, the predicted binding poses showed considerable overlap. The RMSD between cholesterol and epicholesterol was equal to .79 Å and the RMSD between cholesterol and ent-cholesterol was 3.12 Å. All three sterols were oriented in a similar manner, with their hydroxyl groups facing toward the cytosolic membrane side of the channel. For cholesterol, the orientation was such that the methyl groups of the "rough" face, at carbon atoms C18 and C19, were facing away from the slide helix and towards the center of the protein and the center of the membrane. In contrast, the orientation of ent-cholesterol mirrored that of cholesterol: while the tetracyclic rings of cholesterol and ent-cholesterol overlapped with one another, their methyl groups faced opposite directions. As might be expected, the consequence of this is a difference in residue interactions. Indeed, I found that while both cholesterol and epicholesterol were predicted to interact with 10 residues, only 8 of these residues overlap, meaning there are two unique residue interactions for each sterol (**Fig. 2-2**). These unique interactions are a consequence of the different methyl and hydroxyl group orientations. In the case of cholesterol, the hydroxyl group is oriented towards Lys^{189}, on the adjacent subunit, while for ent-cholesterol, this group is predicted to

interact with Trp^{79} on the adjacent subunit. Likewise, cholesterol is predicted to interact with Ala^{68}, while ent-cholesterol is predicted to interact with Cys^{74} through one of its methyl groups. Similarly to ent-cholesterol, the predicted orientation of epicholesterol overlapped with cholesterol, specifically in the arrangement of the tetracyclic rings. Here however, the difference between cholesterol is solely between the placements of the hydroxyl groups. This difference in placement meant the hydroxyl group in epicholesterol was oriented in the opposite direction to its counterpart in cholesterol, instead facing Ala^{68}, not Lys^{189}.

As with Kir2.2, the predicted binding energies for these sterols on KirBac1.1 were close to one another: -9.8, -9.4, and -10 kcal/mol. Notably, these values are also similar to the corresponding values in Kir2.2. Likewise, the predicted binding poses of these chiral isomers are structurally similar to one another, with the RMSD difference between the poses of cholesterol and epicholesterol in KirBac1.1 equal to 3.93 Å and the RMSD difference between cholesterol and ent-cholesterol equal to 3.82 Å. The predicted binding site on KirBac1.1 is also analogous to the site on Kir2.2, being situated on the inner leaflet side of the protein near the slide helix, with all three sterols oriented such that their hydroxyl groups face the cytosolic side of the membrane. The predicted binding poses of cholesterol, epicholesterol, and ent-cholesterol also show significant overlap in their interacting residues, with all three predicted to interact with Trp^{48}, Leu^{51}, Tyr^{52}, Trp^{60}, Leu^{67}, Leu^{70}, Phe^{71}, Gly^{137}, Leu^{140}, Ser^{141}, and Leu^{144}. However, each sterol also has unique residue interactions: cholesterol uniquely interacts with residues Ala^{55} and Arg^{153}, while epicholesterol interacts with Phe^{132}, and ent-cholesterol interacts with Ala^{109}, Gly^{134}, Met^{135}, and Ile^{138}.

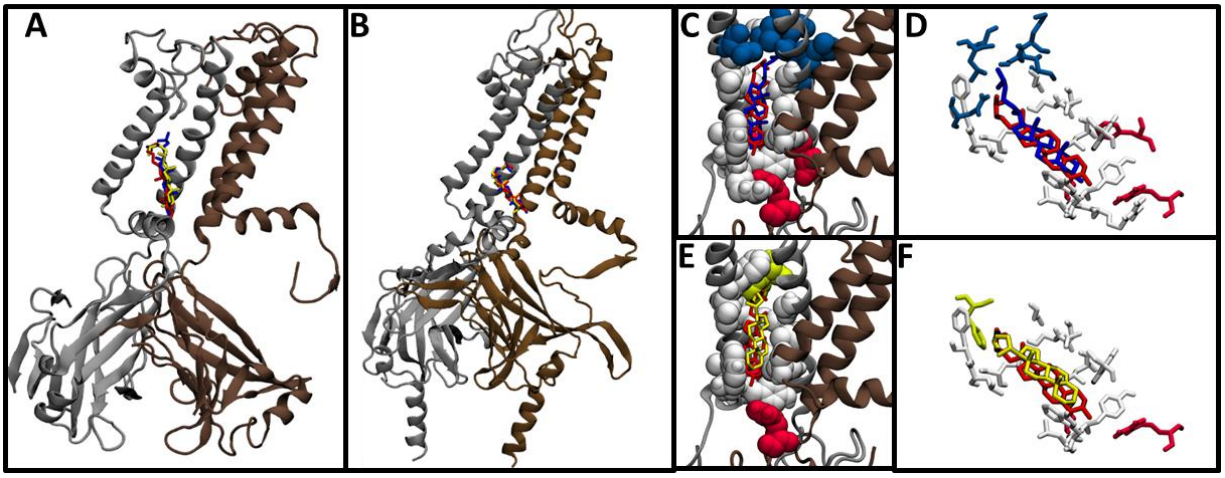

Figure 2-2. Docking results of cholesterol and its chiral isomers on Kir channels ***A)*** *KirBac1.1 channel, showing the predicted binding poses of cholesterol (red), ent-cholesterol (blue) and epicholesterol (yellow)* ***B)*** *Kir2.2 channel, showing the predicted binding poses for cholesterol, ent-cholesterol, and epicholesterol.* ***C)*** *Comparison of the binding poses of cholesterol and ent-cholesterol.* ***D)*** *The specific residues predicted to interact with both cholesterol and ent-cholesterol (white), only cholesterol (red) and only ent-cholesterol (blue).* ***E)*** *Comparison of the binding poses of cholesterol and epicholesterol.* ***F)*** *The specific residues predicted to interact with both cholesterol and ent-cholesterol (white), only cholesterol (red) and only epicholesterol (yellow).*

2.3.2. An Overlap of Cholesterol Stereoisomers Interacting in TRPV1

Docking analyses were also performed for cholesterol, epicholesterol, and ent-cholesterol on the transmembrane region of TRPV1. Following the same procedure as before, the top scoring pose for each sterol was compared. Similar to Kir channels, I found that all three isomers are predicted to bind to TRPV1 in a similar location with almost identical binding energies: -8.3, -8.3, and -8.36 kcal/mol, respectively (**Fig 2-3**). These energies are comparable to what was predicted for Kir2.2 and KirBac1.1. However, while all three isomers were predicted to interact within a similar site, the predicted binding poses

between the sterols do not overlap. Unlike with Kir channels, where the tetracylic rings of all three sterols overlap in their binding poses, here the sterol rings are oriented more orthogonally to one another. Consequently, the RMSD scores were much larger, with the RMSD of cholesterol and epicholesterol being 8.81Å and the RMSD of cholesterol and ent-cholesterol being 6.5Å.

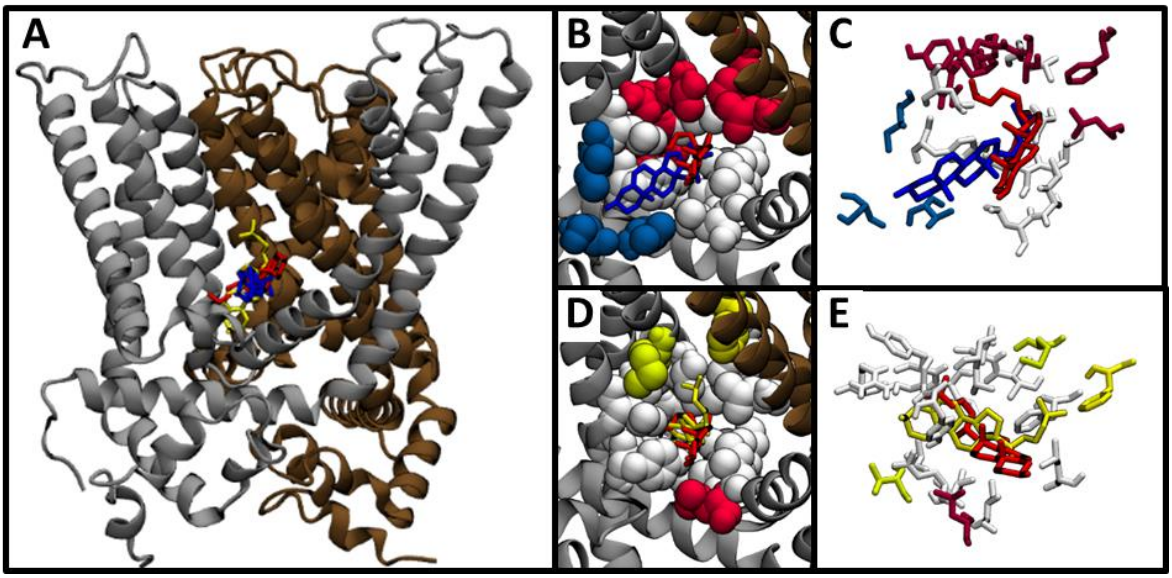

Figure 2-3. Docking results of cholesterol and its chiral isomers on TRPV1 ***A****) The TRPV1 channel along with the top binding poses of cholesterol, ent-cholesterol, and epicholesterol. The binding site of all three sterols overlaps, but each occupies a different pose compared to the others. A comparison of the binding poses* ***B****) of cholesterol and ent-cholesterol, as well as the specific resides predicted to interact with each* ***C****). Residues colored white are those predicted to interact with both sterols, while those colored red are predicted to interact with only cholesterol and those in blue are predicted to interact with only ent-cholesterol. A comparison of the binding poses* ***D****) of cholesterol and epicholesterol, as well as the specific resides predicted to interact with each* ***E****). Residues colored white are those predicted to interact with both sterols, while those colored red are predicted to interact with only cholesterol and those in yellow are predicted to interact with only epicholesterol.*

While the binding poses did not overlap in the same was as in Kir, there was still overlap in the predicted binding residues. There were seven residues predicted to interact with cholesterol, epicholesterol, and ent-cholesterol: Tyr^{131}, Leu^{135}, Leu^{173}, Ala^{186}, Ile^{189}, Glu^{190}, and Ile^{193}. Likewise, similar to Kir, there were residues that were unique to each sterol. Specifically, 7 residues, Ser^{132}, Thr^{170}, Asn^{171}, Tyr^{174}, Arg^{177}, Phe^{207}, and Leu^{266}, were predicted to interact with cholesterol, but not ent-cholesterol while a single residue, Leu^{194}, was predicted to interact with cholesterol, but not epicholesterol.

2.3.3. $GABA_A$ and BK Predict Partial Overlap of Cholesterol Isomers

In the same manner as Kir channels and TRPV1, triplicate docking analyses were performed with cholesterol, epicholesterol, and ent-cholesterol on the $GABA_A$ channel and the BK channel, two other channels for which cholesterol stereospecificity was shown experimentally (Sooksawate and Simmonds 2001; Bukiya, Belani et al. 2011). I found that, as before, all three sterols were predicted to bind to $GABA_A$ and BK channel with similar binding energies. For $GABA_A$, the predicted binding energies for cholesterol, epicholesterol, and ent-cholesterol were -8.1, -8.4, and -9.3 kcal/mol, while for BK channel they were -7.53, -7.47, and -7.0 kcal/mol. Likewise, for both channels there was overlap in the predicted binding sites of the sterols but, similarly to TRPV1, this overlap is partial. In particular, there is one sterol in each case of $GABA_A$ and BK where there was overlap, while the other sterol occupied a more orthogonal position (**Fig. 2-4**). For $GABA_A$, the predicted interaction sites for cholesterol and ent-cholesterol overlap closely, while epicholesterol only partially overlaps. Here, the calculated RMSDs were 3.29Å and 9.72Å. On the BK channel, all three sterols occupy the same spot, but epicholesterol is oriented anti-parallel to cholesterol, with

the RMSDs calculated to be 8.62Å and 4.0Å. This partial overlap of binding sites is also reflected in the different interactions between each sterol and the residues on the $GABA_A$ (**Fig. 2-5**) and BK channels (**Fig. 2-6**).

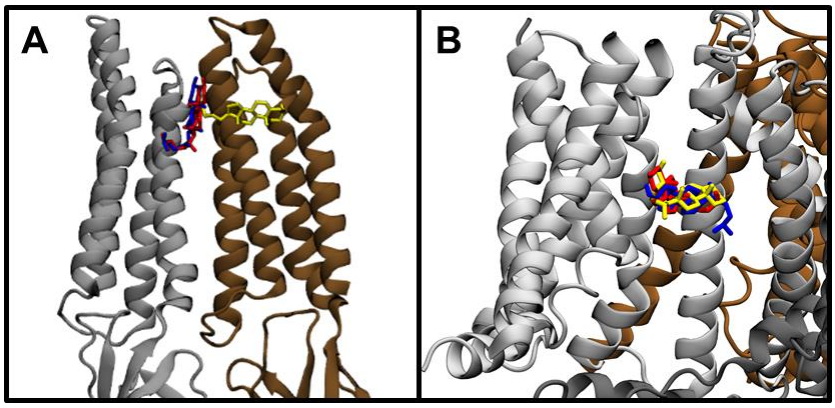

Figure 2-4. Docking results of cholesterol and its chiral isomers on $GABA_A$ and BK channel. Predicted binding poses of cholesterol (red), epicholesterol (yellow), and ent-cholesterol (blue) on the $GABA_A$ channel. Two sterols, cholesterol and ent-cholesterol, show overlap in predicted binding location, while epicholesterol shows partial overlap. B) Predicted binding poses of cholesterol (red), epicholesterol (yellow), and ent-cholesterol (blue) on the BK channel.

2.3.3.1. $GABA_A$

Similar to Kir2.2 and KirBac1.1 where the predicted binding poses of the sterols overlapped along their tetracyclic rings, the poses for cholesterol and ent-cholesterol on the $GABA_A$ receptor showed the same high degree of overlap, with the main difference being the orientation of their methyl groups. As a result, cholesterol and ent-cholesterol interact with many of the same residues, sharing Ile^{234}, Trp^{237}, Val^{238}, Arg^{428} Leu^{297}, Ala^{300}, Phe^{301}, Tyr^{304},

Arg^{428}, and Pro^{432}. Furthermore, cholesterol was predicted to interact with Arg^{312}, while ent-cholesterol is predicted to interact with Phe^{240}. In contrast, because there is only partial overlap between the predicted binding sites for cholesterol and epicholesterol, they only share the residues Trp^{241}, Leu^{297}, Ala^{300}, Phe^{301}, and Tyr^{304}. Likewise, as a consequence of the sterols' anti-parallel orientations with respect to one another, these overlapping residues were predicted to interact with very different portions of each sterol: residues that were predicted to interact near the hydroxyl group for cholesterol were predicted to interact with the tail group of epicholesterol. Additionally, residues Ile^{234}, Trp^{237}, Val^{238}, Arg^{428}, and Pro^{432} are unique to cholesterol and residues Glu^{298}, Ile^{423}, Trp^{426}, Ser^{427}, Val^{430}, and Phe^{431} are unique to epicholesterol (**Fig. 2-5**).

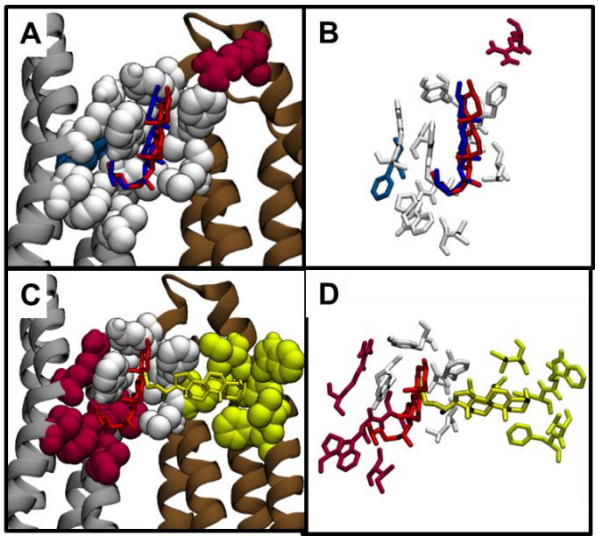

*Figure 2-5. Binding pose comparison on GABA$_A$. **A**) Comparison of the binding poses of cholesterol and ent-cholesterol. **B**) The specific residues predicted to interact with both cholesterol and ent-cholesterol (white), only cholesterol (red) and only ent-cholesterol (blue). **C**) Comparison of the binding poses of cholesterol and epicholesterol. **D**) The specific residues predicted to interact with both cholesterol and ent-cholesterol (white), only cholesterol (red) and only epicholesterol (yellow).*

2.3.3.2. BK Channel

The predicted binding sites for the three isomers on the BK channel follow a similar pattern to those on the $GABA_A$ receptor. All three sterols occupy similar sites with comparable binding energies listed above (**Fig. 2-6**). Additionally, I found that ent-cholesterol has an additional favorable binding site distinct from the shared sight, which might be important for interpreting experiments where cholesterol effects on BK are compared to the effects of ent-cholesterol. In the overlapping site, cholesterol and ent-cholesterol share residues Leu^{170}, Phe^{173}, Phe^{177}, Phe^{195}, Phe^{197}, Leu^{198}, Leu^{201}, Leu^{234}, Thr^{237}, Ala^{238}, Phe^{241}, Phe^{292}, and Phe^{300}, with Leu^{241} unique to cholesterol and Phe^{299} and Leu^{303} unique to ent-cholesterol. Cholesterol and epicholesterol share residues Phe^{173}, Phe^{177}, Phe^{197}, Leu^{198}, Leu^{234}, Thr^{237}, Ala^{238}, Phe^{241}, Phe^{292}, and Phe^{300}, with epicholesterol having no unique residues and cholesterol interacting uniquely with Leu^{241}, Leu^{170}, and Leu^{201}. However, although epicholesterol has no unique residues, its inverted orientation with respect to cholesterol and ent-cholesterol means its hydroxyl group interacts with a different set of residues from the overlapping list.

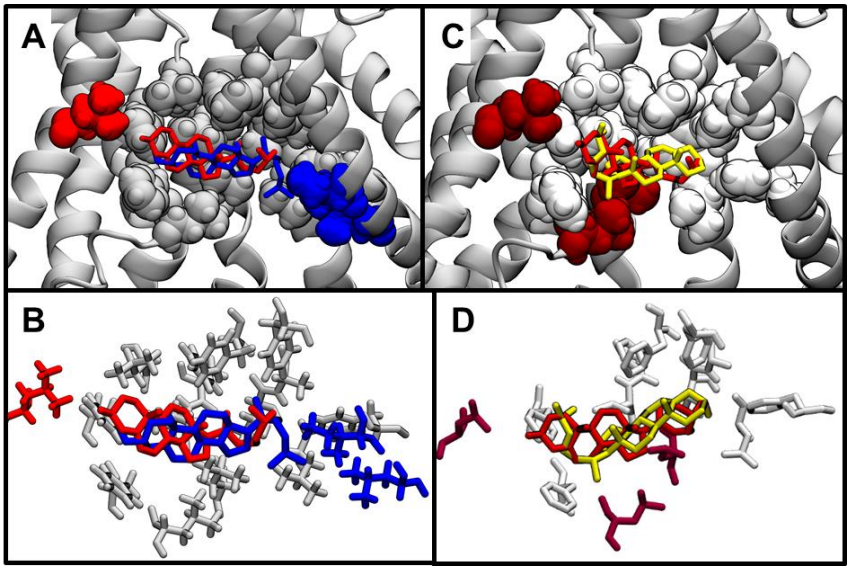

Figure 2-6. Binding pose comparison on BK channel. ***A****) Comparison of the binding poses of cholesterol and ent-cholesterol.* ***B****) The specific residues predicted to interact with both cholesterol and ent-cholesterol (white), only cholesterol (red) and only ent-cholesterol (blue).* ***C****) Comparison of the binding poses of cholesterol and epicholesterol.* ***D****) The specific residues predicted to interact with both cholesterol and ent-cholesterol (white), only cholesterol (red) and only epicholesterol (yellow).*

2.3.4. Residue Makeup of Predicted Binding Sites on Stereoselective Ion Channels

In addition to analyzing the binding energies and predicted binding poses of cholesterol and its chiral isomers on these ion channels, I also quantified the differences in the types of residues comprising their respective binding sites (**Fig. 2-7**). As might be expected, I found that for all three sterols, hydrophobic residues such as Leucine and Phenylalanine account for ~60-90% of the binding sites on the different ion channels.

Likewise, aliphatic residues such as alanine, leucine, and isoleucine appear in almost every site. Phenylalanine occurs the most frequently, being absent only from the ent-cholesterol binding sites of TRPV1 and the BK channel. Conversely, there were very few polar or charged residues in the predicted binding sites, with cysteine being entirely absent. Glutamic acid appeared in all three sterol cites on TRPV1 as well as the epicholesterol binding site on $GABA_A$, while Aspartic acid only appeared in Kir2.2. Asparagine was also rare, appearing only in the cholesterol and epicholesterol sits on TRPV1 and the ent-cholesterol and epicholesterol sites on KirBac1.1. For some of the ion channels, there are differences in the total numbers of residues comprising the predicted sites for different sterols. For KirBac1.1, there are respectively 17, 15, and 18 residues that make up the cholesterol, epicholesterol, and ent-cholesterol binding sites. For TRPV1, there are 15, 19, and 9 residues. For $GABA_A$ and BK there are 11, 11, 11, and 13, 10, and 15 respectively.

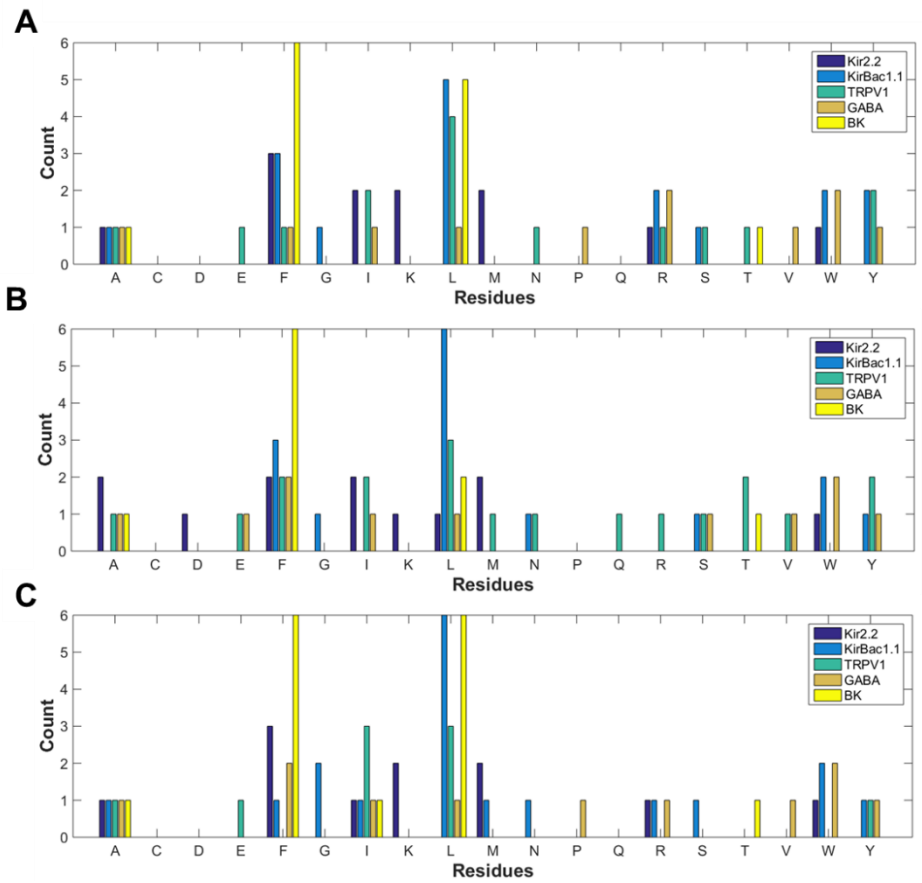

*Figure 2-7. Comparison of binding site residues. Histogram of different amino acid residues identified in the predicted binding sites on Kir2.2, KirBac1.1, TRPV1, $GABA_A$, and BK for **A)** cholesterol, **B)** epicholesterol, and **C)** ent-cholesterol*

2.4. Discussion

The main finding in my work here is that the chiral isomers epicholesterol and ent-cholesterol dock to several types of stereoselective ion channels in the same putative sights as cholesterol. These observations suggest that sterol binding to these proteins is only partially stereoselective. That is to say, the stereoselectivity of these ion channels is not due to an absence of binding for these chiral isomers. Rather, these chiral isomers have different interactions with their putative binding sites than cholesterol. Indeed, I found that ent-cholesterol and epicholesterol are predicted to interact with these channels with similar interaction energies to cholesterol, suggesting comparable binding favorability. This result is in contrast to previous assumptions about stereoselectivity, where it was believed that the chiral isomers of cholesterol did not bind to these ion channels. Specifically, for the ion channels studied here, while cholesterol suppresses the function of Kir, BK, and TRPV1, the chiral isomers epicholesterol and ent-cholesterol had either the opposite or no effect. Similarly, cholesterol supports $GABA_A$ function while epicholesterol does not. My analysis predicts that the main functional difference between cholesterol and its chiral isomers is not due to binding, but rather due to the specific interactions between cholesterol and the residues of its binding site. These specific interactions are not accessible to either epicholesterol or ent-cholesterol, due to their different structures.

My analysis utilizes molecular docking, which is a well-established approach to identifying potential binding sites of ligands on target proteins and characterize their interactions (Kitchen, Decornez et al. 2004; Chaudhary and Mishra 2016; de Ruyck, Brysbaert et al. 2016). This approach has been successfully been used to identify binding sites on the Kir2.1(Rosenhouse-Dantsker, Noskov et al. 2013) and Kir2.2 (Fürst, Nichols et

al. 2014; Barbera, Ayee et al. 2017) channels, as well as TRPV1 and $GABA_A$ (Picazo-Juarez, Romero-Suarez et al. 2011; Hénin, Salari et al. 2014). With respect to Kir channels, these docking analyses were then further verified by site-directed mutagenesis and electrophysiological recordings. Given these previous results, it is important to compare the predictions for cholesterol binding sites I made in this study with the reported sites based on docking and simulations. As might be expected given the similar methodologies, my predictions for Kir2.2 are similar to results already shown for Kir2.1 and Kir2.2 (Rosenhouse-Dantsker, Noskov et al. 2013; Fürst, Nichols et al. 2014). Likewise, my analyses identified cholesterol binding sites on TRPV1 and $GABA_A$ that are similar, but not identical, to what was predicted previously. This is not surprising however, as these predictions were made before crystal structures of TRPV1 or $GABA_A$ were discovered and used homology models (Picazo-Juarez, Romero-Suarez et al. 2011) (Hénin, Salari et al. 2014). Additionally, the existence of transmembrane proteins co-crystallized with cholesterol offered an opportunity to validate my approach. Specifically, I performed cholesterol docking analyses on the β2-adrenergic receptor, one of the well characterized cholesterol binding sites that was confirmed by crystal structure (Hanson, Cherezov et al. 2008; Ma, Weichert et al. 2017), and was able to recapitulate the crystal structure binding site. Thus overall, my current predictions for cholesterol binding sites described above are consistent with previous studies.

Although my current approach was validated against experimental results, it is important to understand the limitations of docking analysis in general. One important consideration is protein structure resolution. In this study, the resolutions of all structures were ~3Å, which is recognized to provide the contours of the protein with the atomic

structure being inferred (https://pdb101.rcsb.org/learn/guide-to-understanding-pdb-data/resolution). Although higher resolution structures are preferred, nevertheless, the crystal structures I used here have been used to obtain significant insights into the ligand binding to the channels (Fürst, Nichols et al. 2014; Elokely, Velisetty et al. 2016; Brannigan 2017) and in some cases represent the highest resolution structures currently available. Another important limitation is that molecular docking approaches typically predict binding favorability via molecular forcefields or turnkey methods, which are by nature are an approximation (Morris, Huey et al. 2009; Chaudhary and Mishra 2016). Likewise, molecular docking requires static protein structures. This is a major limitation, as proteins can be highly flexible in their native environments, with amino acids in a binding pocket being able to rotate and shift position to accommodate different ligands (Arkin, Randal et al. 2003). This limitation can be overcome through molecular dynamics simulations, wherein predicted binding poses are used as starting points for simulation runs. These simulations allow for a more detailed study of binding dynamics, and have been employed with a variety of proteins (e.g. (Rosenhouse-Dantsker, Noskov et al. 2013; Fürst, Nichols et al. 2014; Hénin, Salari et al. 2014). Although preferable, this was not feasible for my current comparative study, which included multiple sterols binding to multiple proteins. However even with the aforementioned limitations, docking analyses can be a powerful approach to uncovering and screening potential sterol-protein binding sites

It is interesting to note that recent atomistic simulations of the β2-adrenergic receptor found that the cholesterol analogues and oxysterols cholesteryl hemisuccinate, 4β-OH-cholesterol and 27-hydroxycholesterol, are also capable of binding to the same binding sites as cholesterol, and that the sterols compete for these binding sites when present

together with cholesterol (Manna, Niemelä et al. 2016). However, it is not known whether these sterols have a functional effect on the receptor. This is an important distinction, because if these sterols bind to the same spot, then the binding site is non-discriminatory. In contrast, if these isomers bind lead to significantly different responses, it means that the differences between the functional interactions of the sterols within the site is significant.

In summary, I propose that ion channel stereospecificity is not caused by cholesterol binding, but rather by the specific interactions cholesterol has with the amino acid residues in its binding site, as compared to its chiral isomers. Or, in other words, sterol binding is a necessary but not sufficient condition for regulation of channel function. In all of the ion channels tested here, I observed specific amino acids that were predicted to interact solely with cholesterol or were predicted to interact with cholesterol in a unique manner relate to the other chiral isomers. I therefore propose that further analysis of these specific residue interactions would provide useful insight into the nature of cholesterol-mediated regulation of ion channels.

3. CHARACTERIZING KIR2.2-CHOLESTEROL INTERACTIONS IN A DYNAMIC ENVIRONMENT

(Previously published as *Barbera, N., M. A. Ayee, et al. (2018). "Molecular Dynamics Simulations of Kir2.2 Interactions with an Ensemble of Cholesterol Molecules." Biophysical journal 115(7): 1264-1280.*)

3.1. Introduction

By mass, cholesterol is one of the biggest components of the mammalian cell membrane. Consequently, the interplay between cholesterol and ion channels constitutes one of the major mechanisms for regulating ion channel function, as numerous ion channels have been shown to be modulated by cholesterol levels in the membrane (Rosenhouse-Dantsker, Mehta et al. 2012; Fantini and Barrantes 2013; Levitan, Singh et al. 2014). An increasing number of studies over the past two decades have shown that cholesterol-mediated regulation acts predominantly through direct, specific interactions between the channel and sterols (Romanenko, Rothblat et al. 2002; Addona, Sandermann et al. 2003; Romanenko, Fang et al. 2004; Bukiya, Singh et al. 2011; Barbera, Ayee et al. 2017). With respect to the focus of this dissertation on Kir channels, previous studies in the Levitan lab have shown that these direct, stereospecific interactions of choleserol suppress the function of Kir channels in both mammalian cells (Romanenko, Fang et al. 2004) and reconstituted liposomes (Singh, Rosenhouse-Dantsker et al. 2009). Furthermore, this mechanism acts on not only mammalian Kir channels, but also bacterial KirBac1.1 channels (Singh, Shentu et al. 2011), further indicating the existence of a cholesterol binding site.

Previous studies sought to identify cholesterol binding sites through a combination of: 1) docking analyses of cholesterol to a Kir2.1 homology model, 2) short-timescale atomistic simulations, and 3) experimental validation via site-directed mutagenesis and

electrophysiology (Rosenhouse-Dantsker, Noskov et al. 2013). Using this approach, putative cholesterol binding regions were identified within non-annular, hydrophobic pockets on the Kir channel, distinct from any cholesterol binding motifs. A similar cholesterol binding region was also identified for Kir2.2 channels (Fürst, Nichols et al. 2014). However, while this previous work was able to identify a putative binding region with amino acids important for cholesterol sensitivity, there were a number of limitations. The computational approach to identify novel sites was limited to docking analyses, with the atomistic simulations serving as a fine-tuning and validation step. This approach is constrained by the limitations of docking analyses in general. In particular, docking analyses are typically performed on a rigid protein structure, in the absence of a membrane environment. Consequently, these analyses may be biased towards deeper binding pockets on the protein, failing to consider more shallow sites on the protein surface. They also will fail to consider the dynamic nature of proteins in a membrane environment, and will likely not identify any ligand binding sites formed by induced fitting (Sousa, Fernandes et al. 2006; Huang and Zou 2010). Likewise, although the atomistic simulations successfully predicted the binding favorability of the docked cholesterol poses, owing to the limited size and time scale these simulations they did not take into account the larger membrane environment or the diffusion of cholesterol to and from the surface of the channel (Ingólfsson, Lopez et al. 2014; Hedger and Sansom 2016). Therefore in this study, I used coarse-grained molecular dynamic simulations of Kir2.2 to study these cholesterol interactions in the context of a larger membrane environment, resulting in a 200-fold increase in timescale and an 8-fold increase in simulation size to what was done previously. Kir2.2 was chosen be because of the recently identified crystal structures of the open and closed states (Tao, Avalos et al. 2009; Hansen, Tao et al. 2011),

and because it was previously shown that all subtypes four subtypes of Kir 2 channels (2.1, 2.2, 2.3, and 2.4) are suppressed by cholesterol, with Kir2.1 and Kir2.2 being equally sensitive (Romanenko, Fang et al. 2004). Moreover, the homology between 2.1 and 2.2 sequences (~70% sequence identity) allows for the comparison of cholesterol binding regions between the two channels.

In this study, I simulated both the open and closed states of Kir2.2 in a model membrane of POPC and varying levels of cholesterol. I found that in this membrane environment, Kir2.2 interacts with an ensemble of cholesterol molecules which have varying degrees of interaction strength and duration with the channel. These varying interactions form a complex milieu, with some individual sterol molecules interacting transiently with the channel surface, while others segregate into discrete and more non-annular pockets. Using a network theory-based approach I developed, I uncovered novel, discrete cholesterol-binding sites distinct from the surrounding "noise". Furthermore, I found that these binding sites are different in the open and closed configurations of the channel.

3.2. Methods

3.2.1. Martini Coarse-grained Simulations

Crystal structures for two states of the Kir2.2 channel, the "open" and "closed" states, were obtained from the RCSB protein data bank (PDB IDs: 3SPI and 3JYC). In both crystal structures, missing residues were modeled with the Modeller9.16 program (Webb and Sali 2014). Atomistic protein structures were converted to a Martini coarse-grained topology using the martinize.py script, downloaded from the Martini website (http://cgmartini.nl/index.php/tools2/proteins-and-bilayers/204-martinize). In the Martini scheme, sets of typically 4 heavy atoms are grouped together to form interaction

particles, each with specific particle type that dictates their physio-chemical properties. Due to the nature of this coarse-grained topology, inter-residue interactions that govern higher order protein structure such as hydrogen bonds are lost. To compensate for this, quantitative recapitulation of dynamics can be facilitated by the use of elastic networks to constrain secondary and tertiary structure. A common elastic network approach for Martini simulations used here is the ElneDyn approach (Periole, Cavalli et al. 2009). Here, a network of elastic bonds is constructed between Martini backbone particles, which represent the Cα atoms of amino acids. Although there are common parameters for bond length and bond strength, the parameters chosen are ultimately system-specific, and should be chosen to best reflect the dynamics of the protein in question.

Two possible elastic network parameterizations were initially compared for the martinized Kir channel. In the first case, a "full" elastic network was constructed, such that all backbone (Cα) particles within ten angstroms of one another (excluding nearest and next-nearest neighbors) are connected with a force constant of 1000 kJ/mol nm^2. In the second case, the elastic network was divided into two "domain-specific" networks, with the cytosolic and transmembrane domains each being interconnected with separate networks. The residues comprising each domain were determined by the CATH database (Sillitoe, Lewis et al. 2014). In both the "full" and "domain specific" parameterizations, elastic networks were defined for each subunit separately. In order to determine which parameterization would be used, both of these networks were evaluated with regard to their ability to predict the binding site of phosphatidylinositol 4,5-bisphosphate, a well-studied Kir ligand.

Having converted the Kir channel to a coarse-grained structure, it was then embedded in a bilayer containing either 7:3 POPC:CHOL or 85:15 POPC:CHOL using the insane.py script (http://cgmartini.nl/index.php/tools2/proteins-and-bilayers).

In the Martini scheme, POPC molecules are represented by choline and phosphate particles, two glycerol linkage particles, and 9 particles making up the acyl tails (Marrink, Risselada et al. 2007). Cholesterol molecules are represented by a polar head group particle, five ring particles, and two tail particles (Ingólfsson, Melo et al. 2014). The bilayer was constructed such that cholesterol was randomly distributed in the xy plane, subject to a zone of exclusion extending radially 75 Angstroms beyond the Kir channel. Simulations were run using the GROMACS simulation package version 5.0.7 (Abraham, Murtola et al. 2015) with the MARTINI 2.2 force field (de Jong, Singh et al. 2012).

3.2.2. PIP2 simulations

A three step equilibration protocol was used, with each step executed for 100 nanoseconds with a time-step of 20 fs. All three equilibration steps employed a Berendsen pressure coupling algorithm set to 1 atm and a velocity-rescale temperature coupling algorithm set to 310.15 K. A reaction field straight cutoff was used (De Jong, Baoukina et al. 2016). In the first step, position restraints were applied to the backbone particles of Kir2.2, and a flat-bottom position restraint was applied to membrane PIP2 to prevent PIP2-protein contacts. In the second step, the protein position restraints were replaced with a flat-bottom restraint, allowing the protein to move, but constraining its lateral diffusion and maintaining separation from PIP2. In the final step, all restraints were removed. After equilibration a 20 μs NPT simulation was run using a Parrinello-Rahman pressure coupling algorithm instead of the Berendsen pressure coupling algorithm. Snapshots were taken every 200 ps.

This simulation protocol was repeated 4 times, with particle velocities re-initialized before each run.

3.2.3. Cholesterol simulations

Simulations with cholesterol were run in the same manner as PIP2, with a 3-step equilibration followed by a 20 μs NPT simulation. Position restraints were applied to Kir2.2 in the first 100 ns equilibration step, replaced by a flat-bottom restraint in the second. A flat-bottom position restraint was applied to membrane cholesterol in steps 1 and 2 to prevent sterol-protein interaction prior to protein and membrane equilibration. In the final step, all restraints were removed. As before, the Berendsen pressure coupling algorithm was replaced with a Parrinello-Rahman coupling algorithm during the subsequent 20 μs NPT production run. Snapshots were taken every 200 ps. This simulation protocol was repeated 4 times, in each case with re-initialized velocities. Simulations were run for both the open and closed states of the channel.

3.2.4. Quantifying Cholesterol-Residue Contacts

In this dissertation, cholesterol-protein interactions in CG MD systems were interrogated on a per-residue basis, using a 6Å contact distance cutoff. This cutoff was used because it approximates the first energy minimum of the Leonard-Jones potential in the Martini force field and is a commonly used cutoff for determining contact between particles (de Jong, Periole et al. 2012; Schmidt, Stansfeld et al. 2012; Sengupta and Chattopadhyay 2012). Furthermore, given the high mobility of the cholesterol tail, for purposes of calculating occupancy I chose to define the center of mass of a given cholesterol molecule such that the two tail particles of the coarse-grained cholesterol molecule are excluded. The

prevalence of cholesterol-residue interactions was quantified in two ways: contact duration and maximum occupancy. Contact duration quantifies the total amount of time individual amino acid residues are within 6 Å of any cholesterol molecule's center of mass, irrespective of how long each individual pairwise contact lasts. In contrast, maximum occupancy is a measure of the persistence of individual cholesterol-residue interactions. It quantifies the longest continuous contact a given amino acid residue has with any cholesterol molecule. Because the Kir2.2 channel is a homotetramer, there are four copies of each subunit, one per residue. These residues were treated as independent for the purposes of calculating average occupancy values. To calculate a mean of each metric for each residue, the aggregate of these samples across all simulation replicates was used.

3.2.5. Identifying Binding Sites by Functional Network Analysis

As described in the introduction, network theory is an approach to studying complex systems by representing agents of the system and interactions between them as a graphical model consisting of nodes (agents) and edges (pairwise interactions) (Borgatti and Halgin 2011). Here I detail the approach I developed to identify binding sites based on creating networks of functionally correlated nodes (residues) and edges (connections indicating likelihood of simultaneous sterol contact).

The network analysis was applied to those sterol molecules regarded as binders, defined here as those molecules that met a quantitative criterion for persistent binding. Specifically, persistent binding was defined by looking at both the duration of a given sterol's contact with the protein and the number of cholesterol-residue interactions present during that contact event. In this way the weighted-time metric was able to select for those ligands that form prolonged and morphologically stable interactions with the ion channel.

Sterol-protein interactions defined as binding events were investigated individually. For each binding event, amino acid residues were likewise examined individually for their contact with the sterol in question. A binary data array $C_i(t)$ was created for every residue *i*, which indicated whether or not sterol contact occurred during that frame *t* of the simulation (1 if present; 0 if absent).

$$C_i(t) = \begin{cases} 1 & residue\ i\ is\ within\ 6\text{Å}\ of\ sterol \\ 0 & residue\ i\ is\ not\ within\ 6\text{Å}\ of\ sterol \end{cases}$$

Equation 3-1

For each pair of residues *i* and *j*, it was then possible to evaluate the likelihood of concurrent ligand contacts by quantifying the similarity of their respective arrays. To determine this similarity, a phi coefficient was generated for each pair. This phi coefficient is analogous to a linear correlation coefficient, but applied to dichotomous data.

$$\varphi = \frac{n_{11}n_{00} - n_{10}n_{01}}{\sqrt{n_{1\bullet}n_{0\bullet}n_{\bullet 0}n_{\bullet 1}}}$$

Equation 3-2

Here *n* is the number of frames, and the subscripts correspond to each possible combination of outcomes, as described in the following table.

	$C_j(t) = 1$	$C_j(t) = 0$	total
$C_i(t) = 1$	n_{11}	n_{10}	$n_{1\bullet}$
$C_i(t) = 0$	n_{01}	n_{00}	$n_{0\bullet}$
total	$n_{\bullet 1}$	$n_{\bullet 0}$	n

Table 3-1. Contingency table comparing binary variables $A_i(t)$ and $A_j(t)$.

By examining the resulting phi coefficients and their corresponding p-values, it was possibly to identify those pairs of residues whose contacts with the sterol are positively correlated with $p < 0.05$. Here, a positive correlation coefficient indicates a likelihood that

two residues will be in simultaneous contact with the bound cholesterol molecule, while a negative correlation coefficient indicates a likelihood that contact with one residue precludes contact with the other. For each separate binding event, the results of these phi coefficients were collated into an adjacency matrix, where every non-zero entry indicates the positively-valued correlation coefficient between residue i and residue j (Borgatti and Halgin 2011).

$$A(i,j) = \begin{cases} \varphi(i,j) & if\ \varphi(i,j) > 0 \\ 0 & if\ \varphi(i,j) \leq 0 \end{cases}$$

Equation 3-3

This adjacency matrix was then used to create a graphical representation of the contact network for each sterol binding event. In this representation, every contact residue is represented as a node whose size indicates the relative duration of contact between the sterol of interest and the residue in question. Edges connecting these nodes indicated concurrent contacts with the sterol, and were weighted according to their relevant correlation coefficients. Once a graph was generated for the binding event in question, it was segregated by modularity class (Blondel, Guillaume et al. 2008). Modularity is a metric that quantifies the interconnectivity within sub-regions of a network, with each modularity class being a cluster of nodes that are more connected to each other than they are to nodes of other classes (Blondel, Guillaume et al. 2008). Given the previous definition of edges as indicating concurrent contact, this clustering by modularity class therefore provides a quantitative means of grouping residues which show a strong tendency to form simultaneous contact with an individual sterol molecule.

In each segregated graph (i.e., each binding event), the binding site for that sterol was identified as the modularity group containing the largest nodes (corresponding to the longest contacts). It is important to note that, due to the observed flexibility of cholesterol within its binding site, not all residues in the identified binding cluster exhibit long contact times.

Once binding residues were identified for each binding sterol, two approaches were used to determine whether the binding events clustered into distinct binding sites. First, pairwise phi coefficients were calculated to quantify the similarity between identified residue networks. Second, a k-means unbiased learning approach was employed to group the networks into clusters characterizing different binding sites (Bishop 1995; Nasrabadi 2007). This k-means clustering approach can be used to determine both an appropriate number of clusters to describe the data and the particular cluster to which each sterol's network belongs. Additionally, for each cluster, the algorithm returns a centroid, which we used to define the binding site.

3.3. Results

3.3.1. Model Validation of Domain Specific Elastic Network

An important consideration for Martini coarse-grained simulations of proteins is the parameterization of the elastic network used to constrain secondary and tertiary structure. Here, I compared three different parameterizations: 1) a "full" elastic network for each subunit, 2) a "domain-specific" elastic network, where the transmembrane and cytosolic domains of each subunit are constrained by separate networks, and 3) no network. In both the full and the domain-specific elastic network the force constant for the elastic network

remains the same. To determine the optimal parameterization for this system and validate my model I first simulated the interactions of Kir2.2 with phosphatidylinositol 4,5-bisphosphate (PIP2). PIP2 is an important agonist for Kir channel activity whose interactions with Kir have been well studied computationally (Stansfeld, Hopkinson et al. 2009; Schmidt, Stansfeld et al. 2012), with the crystal structure of PIP2 bound to Kir known (Hansen, Tao et al. 2011). In each of the simulation conditions, I determined the PIP2 binding site by identifying the amino acid residues in contact with the PIP2 headgroup using a similar methodology to what was used previously (Stansfeld, Hopkinson et al. 2009; Schmidt, Stansfeld et al. 2012). A contact was defined as the center of mass of a residue side chain being within 6 of a particle in the PIP2 headgroup. These were aggregated over the entire simulation. Each amino acid was evaluated for its number of PIP2 contacts, which was expressed as a percentage of total number of ligand-protein contacts. All those amino acids constituting at least 5% of total contacts were considered to be binding residues.

To evaluate the different elastic network parameterizations, I compared the results of all three simulation conditions with each other and with the atomistic reference simulations reported in Schmidt et al (**Fig 3-1**). All three network parameterizations showed good agreement with the reference simulations, with the simulations using the full and domain-specific networks showing the most fidelity. The simulations using no elastic network predicted only 4 of the 7 residues, Arg^{78}, Arg^{80}, Lys^{188}, and Lys^{189}. Four additional residues were also identified which were not in the reference simulation: Arg^{65}, Ile^{77}, $Arg^{190,}$ and Lys^{220}. In the full elastic network simulations, 6 of the 7 residues from the reference simulations were identified, with the 7^{th} residue (Trp^{79}) being just below the 5% cutoff. Additionally, the full elastic network simulations identified two residues, Ala^{68} and Gln^{192},

which were not predicted in the reference. The domain-specific elastic network simulations also identified 6 of the 7 residues. Similar to before, the seventh residue, Trp^{79}, was just below the 5% cutoff. Only one additional residue was identified, Ala^{68}, the same as one of the residues identified in the full elastic network simulations. As the domain-specific elastic network simulations produced the closest results to the atomistic simulations with the fewest "false positives", I used this network parameterization for the subsequent POPC/cholesterol simulations.

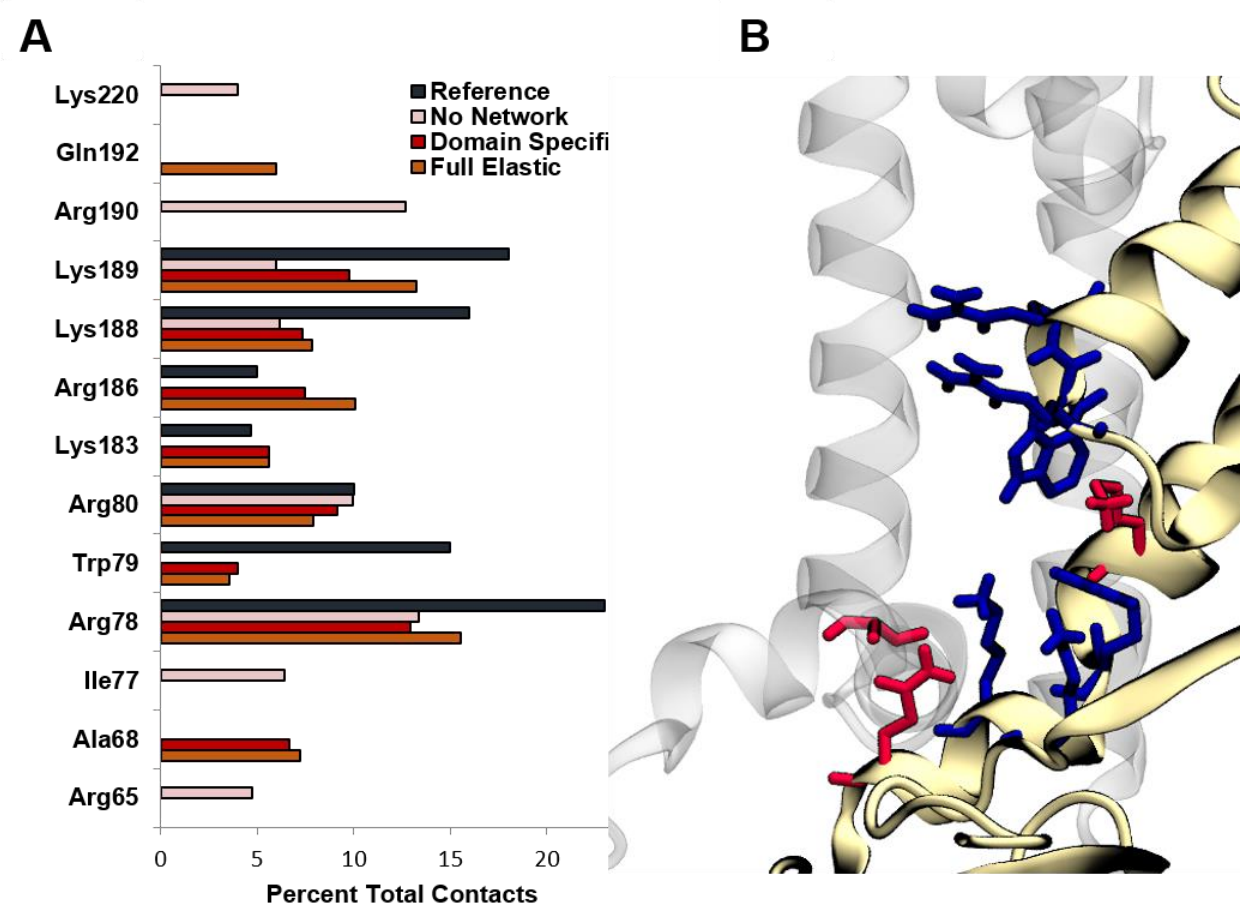

Figure 3-1. PIP2 Binding Results. ***A****) Residues comprising >5% of total contacts with PIP2 in simulations using three different parameterizations of an elastic network for coarse-grained Kir2.2, compared to results from reference atomistic simulations in blue.* ***B****) Visualization of binding site residues identified from atomistic simulations (blue) as well as those identified in coarse-grained simulations (red)*

3.3.2. Kir2.2 Dynamically Interacts with an Ensemble of Cholesterol Molecules in the Membrane Environment

In this study, I investigated the interactions of Kir2.2 in a POPC model membrane with two different levels of cholesterol: 30 mol% and 15 mol%. I first looked at the interactions in simulations 30 mol% cholesterol in the membrane, which is the average molar concentration of cholesterol in mammalian plasma membranes (Yeagle 1991). My simulations showed that in a membrane environment, Kir2.2 is interacting with an ensemble of cholesterol molecules simultaneously, an average of 22±1 separate sterols, with multiple cholesterol molecules interacting per subunit (**Fig. 3-2A**). This ensemble is composed of a very diverse set of interactions, including both very transient interactions on the surface of the protein and persistent interactions within hydrophobic pockets deep in the membrane between alpha helices of separate subunits. A representative snapshot of a simulation illustrating this phenomenon is shown in **Figure 3-2B**. In this snapshot, 8 cholesterol molecules can be seen in contact with the channel, with additional sterols obscured by the protein and membrane lipids. I also observed that cholesterol molecules were free to associate with and disassociate from the surface of the channel, with examples of this unbiased diffusion shown in the individual trajectories in **Figure 3-2C**. A detailed analysis of the interacting residues is presented in the following section of this dissertation.

Rather than localizing to one specific region, cholesterol was found to interact with the entire transmembrane region of the channel that is accessible to the surrounding lipid environment. To determine where there are any preferential interactions, I first calculated

the fractional occupancy of each amino acid in the transmembrane region. I defined fractional occupancy as the amount of time a given amino acid is in contact with any particle of any cholesterol molecule, as a fraction of total simulation time (**Fig 3-2D**). Overall, I found a largely contiguous region of 27 amino acids with a fractional occupancy of 0.5 or higher. This region spans the whole transmembrane region of the protein, including the residues of more recessed pockets (**Fig 3-2E**). Additionally, I found that cholesterol-residue interactions form a continuum of different behaviors, with roughly half the residues in contact with a large number of residues at once (6 or more), and roughly half in contact with relatively few residues (**Fig 3-2F**).

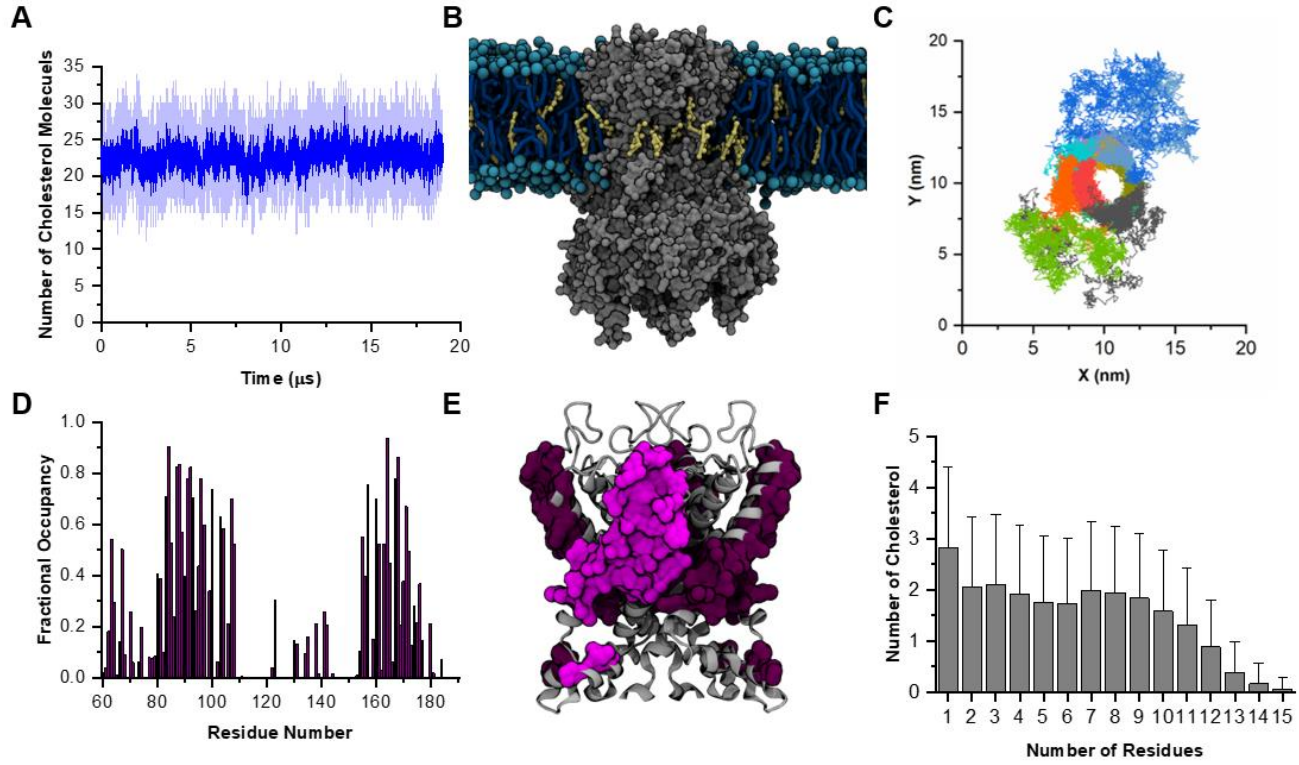

Figure 3-2. Kir2.2 interactions with the surrounding lipid environment. ***A****) Average number of cholesterol molecules within 6Å of the channel as a function of time. Dark blue represents the average of all simulations. Individual simulations are shown behind in light blue.* ***B****) Cholesterol interacting with the lipid bilayer-exposed surface of the channel, as shown in a representative snapshot.* ***C****) Example trajectories of cholesterol molecules showing association with and dissociation from the channel. Each cholesterol trajectory is colored separately. Shown as top-down view of the channel in the membrane.* ***D****) The average fractional occupancy of each residue in the transmembrane region (Asp^{60} to Arg^{190}).* ***E****) Visualization of residues with a fractional occupancy of 0.5 or greater. The residues on a single subunit are highlighted in lighter purple for clarity.* ***F****) Average number of cholesterol molecules in contact with between1-15 separate residues simultaneously.*

3.3.3. Segregating Kir2-Cholesterol Contacts

Generally speaking, molecular dynamics simulation studies have identified binding residues by quantifying contact time between a ligand and the residues of a target protein (Gimpl 2016; Hedger and Sansom 2016). This contact time can be defined in two different

ways: contact duration or maximum occupancy. Because the cholesterol molecules in these simulations exhibit a broad range of different interaction time-scales, I quantified cholesterol-Kir interactions with both metrics. I calculated the contact duration and maximum occupancy of residues Asp60 to Arg190, which comprise the transmembrane domain of the protein, including the slide helix, both TM helices, and the pore domain. Residues outside this range were not included in the analysis because they showed no contact with cholesterol.

I found that for contact duration there were 21 residues in the upper quartile. Visualization of these residues from a side view and top down view of the channel can be seen in **Figure 3-3A**. As might be expected, the corresponding histogram of contact durations contains two prominent peaks, which correspond to the two transmembrane alpha helices (Arg80 to Ile107 and Phe156 to Met184), of the Kir2 subunit, as well as a smaller peak corresponding to the slide helix (Met70 to Arg78). Typically, binding residues would be identified as those with long contact times. However, I observed here a broad range of contact durations across the residues of the TM domain, with no statistical outliers. This is perhaps unsurprising, as the contact duration metric is agnostic to whether the interactions are short (~1-10 ns) but frequent, or less frequent but longer in duration (~1-10 μs). Notably, while this analysis identified 5 residues which overlap strongly with the previously identified cholesterol recognition (Rosenhouse-Dantsker, Noskov et al. 2013), it also identified several other residues which exhibit frequent interaction with cholesterol.

In contrast to this, the calculated maximum occupancy values for the TM residues showed a heavily-tailed distribution. Thirteen residues were identified as statistical outliers (τ = 1.5*IQR + 3rd Quartile). These residues are visualized in red in **Figure 3-3B**, with the

corresponding histogram shown below it in **Figure 3-3E**. As might be expected, the majority of the residues (11 out of 13) identified as outliers from the maximum occupancy analysis overlap with the residues identified in the contact duration analysis. Only one residue, Ile^{177}, is identified through maximum occupancy and not contact duration.

Notably, there is also a subset of residues identified as having long contact duration but low maximum occupancy that do not overlap with the previously identified cholesterol binding site. As can be seen in **Figure 3-3C** in yellow, these residues are concentrated primarily on the surface of the protein, at the protein-bilayer interface. These residues are characterized as having frequent but brief interactions with individual cholesterol molecules.

Interestingly, I also found that contact durations for individual cholesterol molecules with the channel spanned several orders of magnitude. When plotting a histogram of the distribution of all cholesterol contact times, the resulting aggregate forms a power law distribution, similar to what has been described for cholesterol interactions with the B2A receptor (Rouviere, Arnarez et al. 2017).

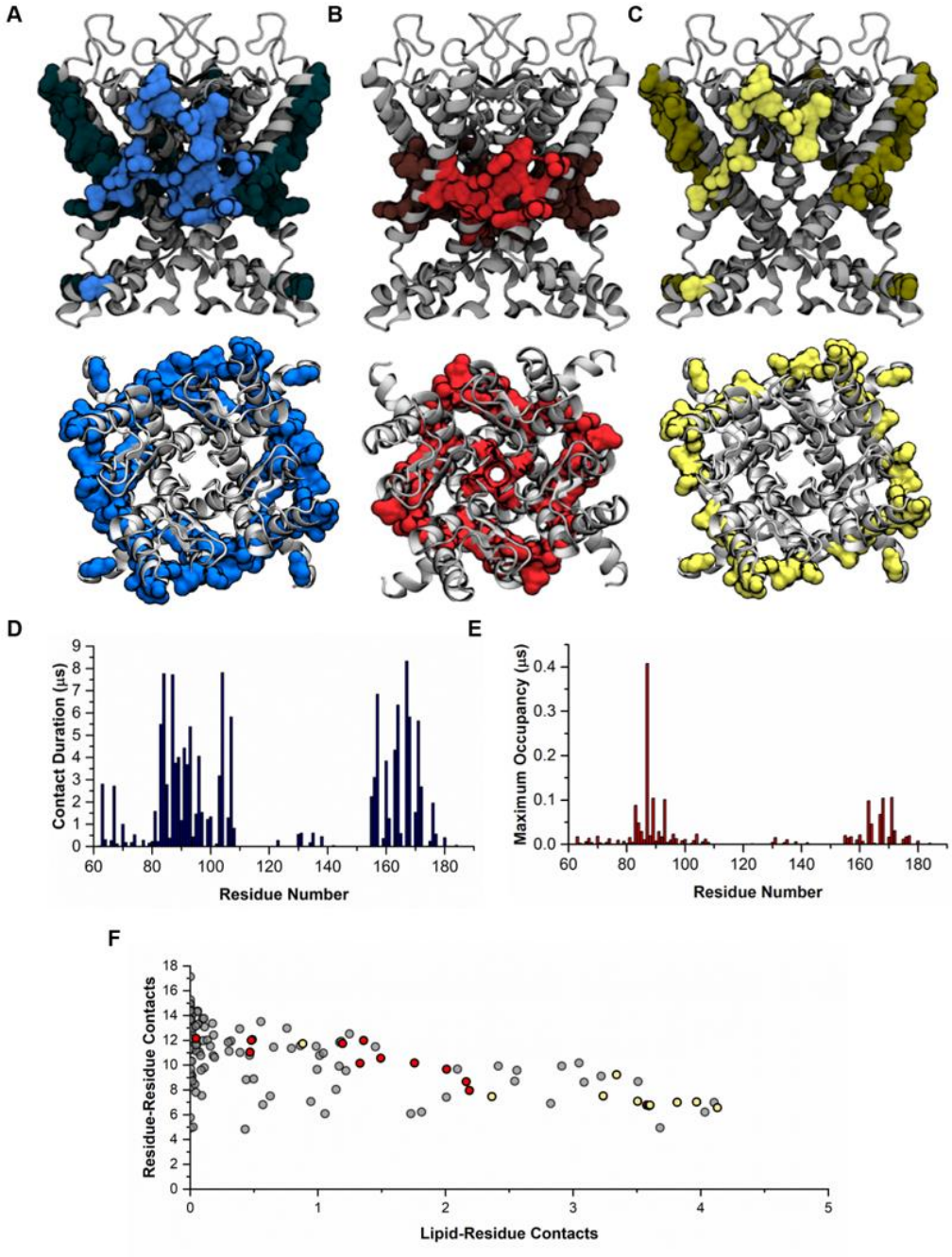

Figure 3-3. Segregating Kir2.2-cholesterol interactions. ***A****) Residues that comprise the upper quartile of contact durations.* ***B****) Residues that comprise statistical outliers of maximum occupancy. C) Residues identified via contact duration that are not maximum occupancy outliers.* ***D****) Histogram of contact durations for each residue in the transmembrane region (Asp60 to Arg190).* ***E****): Histogram of average maximum occupancy for each residue in the same transmembrane region.* ***F****) Average number of residue-residue contacts and residue-POPC contacts per nanosecond for the residues in the transmembrane region. Residues identified in B and C are colored red and yellow respectively.*

3.3.4. Re-defining Annularity as a Continuum

As described in detail in the introduction of this dissertation, cholesterol binding sites on transmembrane proteins have typically been characterized as either annular or non-annular (Fantini and Barrantes 2013; Levitan, Singh et al. 2014; Sengupta and Chattopadhyay 2015). However, given the dynamic nature of protein-lipid interactions in the membrane and the complexities observed in my simulations, defining sites as annular or non-annular, especially from a crystal structure, might not be reflective of the actual dynamics of the interactions. Using coarse-grained MD simulations allows for analyzing the annularity of cholesterol-Kir2.2 interactions over longer timescales than previously accessible. To this end, I ran an additional 20 us simulation of Kir2.2 in a pure POPC bilayer to quantify the accessibility of every TM domain residue to the surrounding lipid environment. I evaluated for each residue over the course of the simulation the number of its residue-residue contacts and the number of its residue-lipid contacts. For those residues in the TM region, I calculated the mean number of contacts per nanosecond, show in **Figure 3-3F** as a 2D plot. As can be seen from this figure, strict definitions of "annular" and "non-annular" are not meaningfully distinct. Rather, there appears to be a gradient of "annularity", with residues possessing relative degrees across the spectrum.

Taking this result into account, I then examined the relative annularity of residues identified from the maximum occupancy and contact duration analyses. Specifically, I looked at the distribution of annularities for those residues with high maximum occupancy (in red) and those residues with low maximum occupancy, but high contact duration (in yellow). I found that the overall trend is as follows: those interactions that are persistent over long periods of time occur in regions of the protein that are less exposed to the lipid environment

(more “non-annular”), while those that are frequent but shorter in duration occur in more “annular” regions. Thus, my current analysis suggests that cholesterols not only interact with the previously determine non-annular binding pockets (Rosenhouse-Dantsker, Noskov et al. 2013; Fürst, Nichols et al. 2014), but also with annular interaction sites on the Kir2channel.

3.3.5. The Microenvironment of Cholesterol Molecules Interacting with the Channel

The results of my simulations suggest that cholesterol-Kir2.2 interactions exhibit a wide range of different timescales and patterns of contact, defying a simple categorization. Given this, I decided to interrogate the microenvironment of these different interactions. Specifically, for each individual cholesterol interaction with the channel I looked at the relative degree of sterol-channel contacts versus sterol-phospholipid contacts. To do this, I calculated the number of sterol-residue contacts and sterol-phospholipid contacts at each instant of time, and aggregated the results for all sterols into a population density map. This density map, shown in **Figure 3-4A**, represents the likelihood of a cholesterol molecule being in contact with *n* residues versus *m* lipid particles. Here, it is visualized as a heat map with a pseudo-color scheme. As might be expected given the previous results regarding annularity, there is an inverse relationship between the number of residue contacts vs. the number of phospholipid contacts. Likewise, it is unsurprising that the highest density region correspond to cholesterol molecules experiencing contact with a single residue, as these make up the short (< 2ns) interactions and are likely due to incidental contacts between cholesterol and the channel, rather than being functionally relevant binding events.

More interestingly, the cholesterol density map suggests that the existence of discrete behaviors segregated by number of concurrent residue contacts. Consequently, I next investigated whether these instances of concurrent residue contacts – hereafter called "residue cohorts" – mapped to distinct regions on the channel or to particular amino acid residues. Similar to what was done with PIP2, for each residue cohort (1-12 concurrent residue contacts) I counted the frequency with which each amino acid residue appears as a member of that cohort. This frequency is reported as a percentage of total contacts. Histograms for each cohort are shown in **Figure 3-4**. Based on the general shape of these histograms, there appears to be at least two qualitatively different behaviors. For residue cohorts with fewer than 8 residues, there is a broad distribution with few if any residues making up more than 5% of the total contacts (**Fig 3-4Aa-Ah**). In contrast, for cohorts of greater than 10 residues, there appear to be two narrow sets of residues making up the majority of the contacts (**Fig. 3-4Ai-4.5Al**). The differences between these two behaviors was further quantified with a chi squared distance metric, shown in **Figure 3-4B**. These results confirm that, indeed, there were two characteristic behaviors: one corresponding to cohorts with 8 or fewer residues, one corresponding to cohorts with 9 or more. Notably, the residues corresponding to these two behaviors also closely correspond to those identified in the previous section (Figures 4-4C and 4-4B, respectively). Nine of the ten largest peaks in the histograms for cohorts 1-8 are residues with frequent, but short-lived contacts and nine of the ten largest peaks for cohorts 9-12 are maximum occupancy outliers.

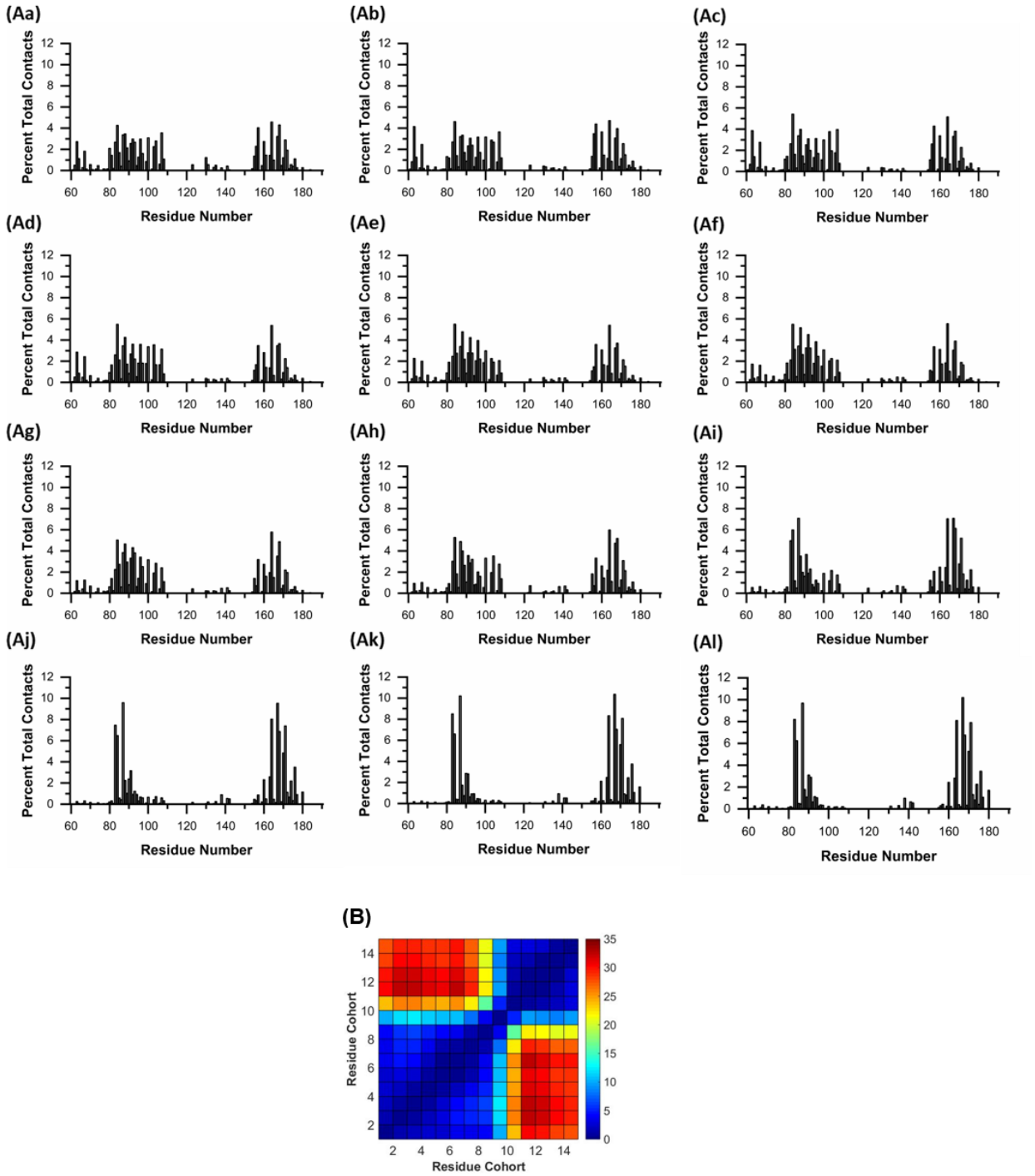

Figure 3-4. Residue cohort interactions. (Aa-Al): Histograms for residue cohorts 1 – 12, for 30 mol% cholesterol simulations in the open state. (B): A pseudo-color plot showing the chi squared calculation for each pairwise combination of cohorts.

In addition to analyzing the residues comprising these cohorts, I also considered frequency with which each one appears in my simulations and the lengths of time for which they persist. For every sterol channel interaction, I calculated the duration of contact and the average size of the contact residue cohort, and found that the vast majority of these contacts (95%) occur with 3 or fewer residues (**Fig. 3-5D**). Furthermore, I found that cholesterol interactions with 9 or more residues are more stable, with interaction times that are orders of magnitude larger than the other contacts involving fewer residues (**Fig. 3-5E**).

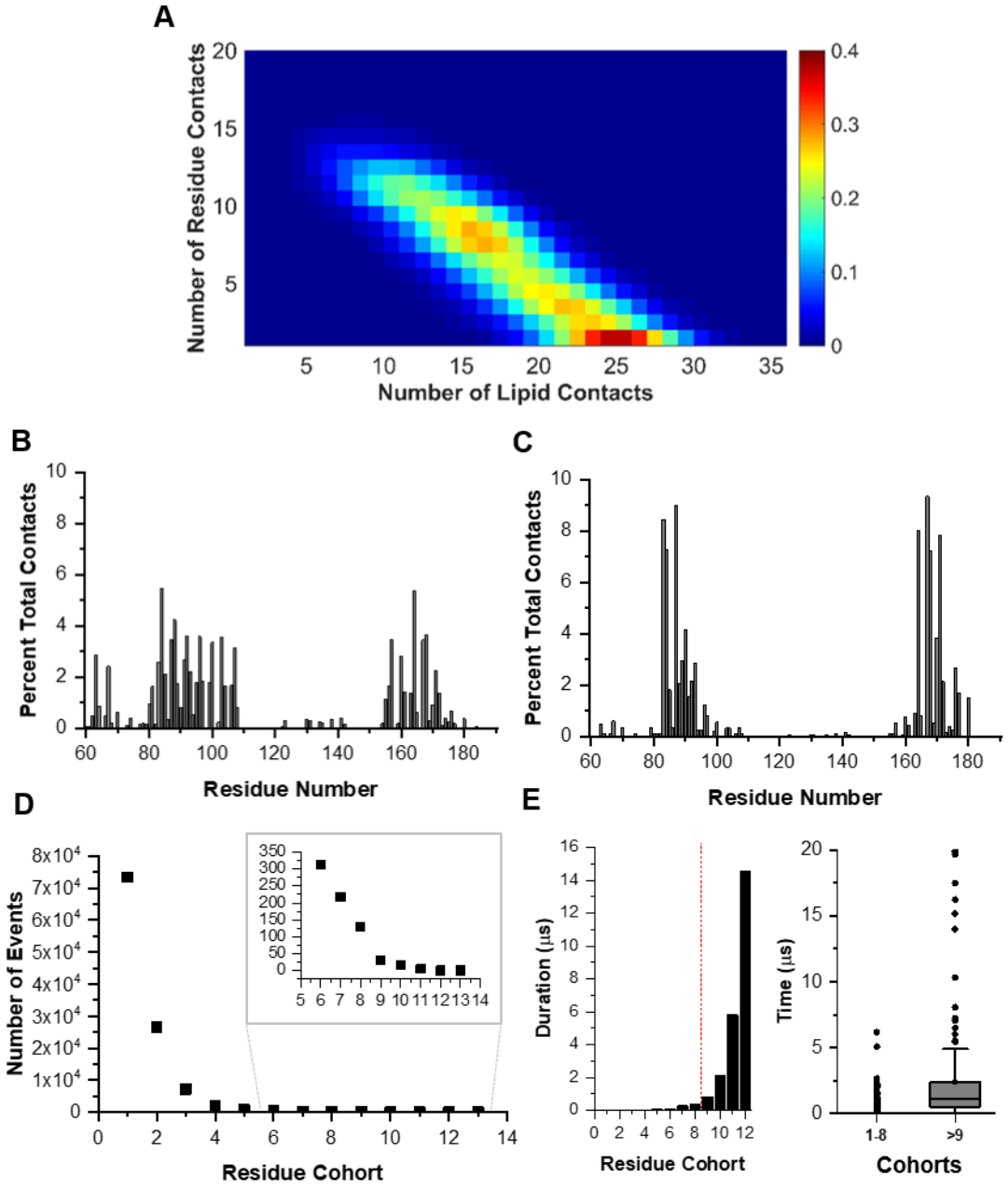

Figure 3-5. Quantifying the cholesterol microenvironment. ***A****) A bivariate histogram showing the average number of cholesterol in contact with X POPC particles and Y separate residues, shown in a pseudo-color plot.* ***B****): A histogram of residue contacts for the 11 residue cohort.* ***C****): A histogram of residue contacts for the 4 residue cohort.* ***D****) The average number of interaction events for a given cohort in a simulation.* ***E****) The average interaction time for each cohort (left) and a boxplot showing the averages and distributions for cohorts 1-8 and >9.*

3.3.6. Concentration Dependence of Cholesterol-Channel Interactions

Previous studies have shown that a 50% depletion of cholesterol from the membrane with MβCD leads to a significant increase in Kir2 channel activity (Romanenko, Fang et al. 2004; Han, Rosenhouse-Dantsker et al. 2014). Given the above results regarding the complexity of Kir-cholesterol interactions in the membrane, I ran additional simulations of Kir2.2 with a similar 2-fold decrease in cholesterol (15 mol% from 30 mol%) to test the effects of cholesterol depletion on these interactions. As might be expected, I found that decreasing the cholesterol content in the membrane decreased the number of cholesterol molecules interacting with the channel by a proportional amount, with an average of 11 ± 1 interacting with the channel, compared to 22± 1 found for 30 mol% (**Fig 3-6A**).

Additionally, I repeated the microenvironment analysis described above to quantify the contact patterns of cholesterol in the 15 mol% condition. I found that despite the decrease in the average number of interactions between the cholesterol and the channel, the segregation of patterns was still present, as was the inverse relationship between the number of cholesterol contacts and the number of residue contacts (**Fig 3-6B**). This segregation was validated by a chi squared analysis. Furthermore, I found that the residues dominating the 1-8 and 9+ cohorts in the 15 and 30 mol% conditions were nearly identical. This similarly was likewise validated by a chi squared analysis comparing the interactions between the higher and lower cholesterol levels simulations (**Fig 3-6C**).

While the overall pattern of residue contacts was consistent between simulation conditions, the average duration of cholesterol contacts was found to decrease in the simulations with lower cholesterol levels. This was found to be the case for both the small (1-9) and large (>9) residue cohorts, as shown in the boxplots in **Figure 3-6D**. In the left plot,

cholesterol contact times for the 9+ cohorts are compared. In both conditions, the 9+ cohorts represent a comparatively small number of events with long contact times. However, the median contact duration in the 15mol% simulations is significantly shorter than in the 30 mol% simulations. This is likewise true for the contacts in the 1-8 residue cohorts. (**Fig 3-6D**).

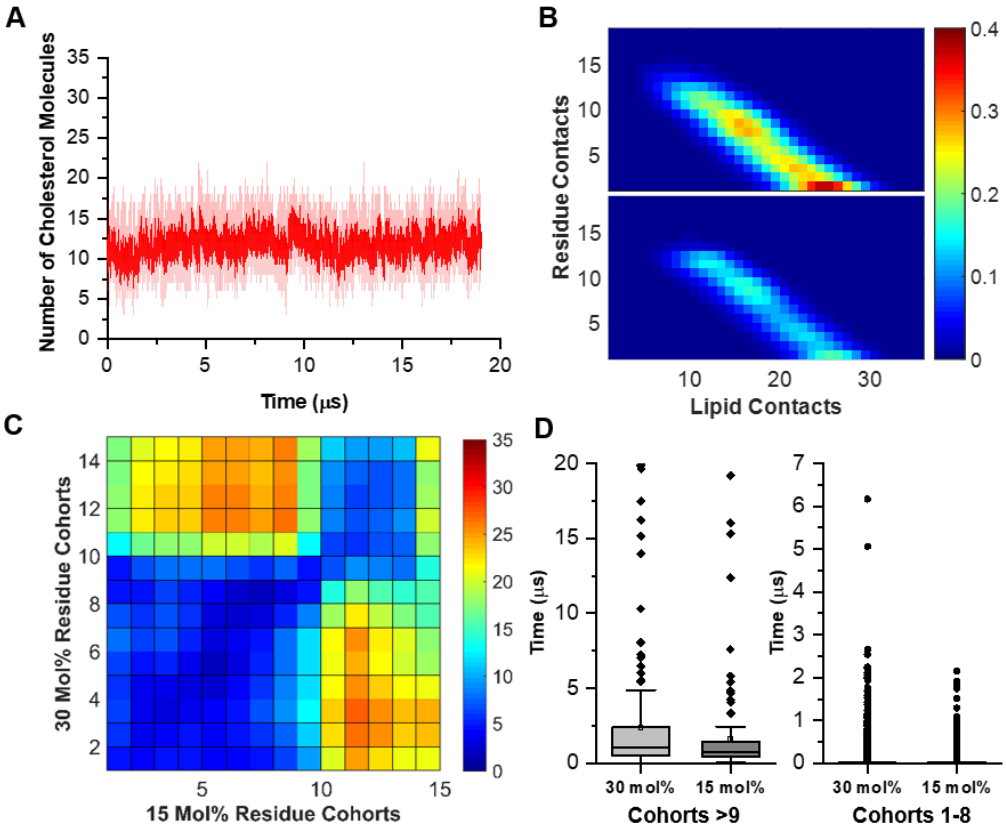

Figure 3-6. Effects of cholesterol concentration on channel-sterol interactions. ***A****) Average number of cholesterol molecules within 6Å of the channel as a function of time in 15 mol% simulations. Dark red represents the average of all simulations. Individual simulations are shown behind in light red.* ***B****) Bivariate histogram showing the average number of cholesterol in contact with X POPC particles and Y separate residues, shown in a pseudo-color plot. The top histogram is from 30 mol% cholesterol simulations, the bottom histogram is from 15 mol% cholesterol simulations.* ***C****): A pseudocolor plot of the chi-squared distances calculated for each pair of residue cohorts at 15 and 30 mol%.* ***D****): Boxplots showing the interaction times of cohorts >9 (left) and 1-8 (right) for 30 and 15 mol%.*

3.3.7. Cholesterol Recognition Region Maps to Discrete Binding Sites

Having shown that multiple cholesterol molecules interact with the Kir2 channel simultaneously and identifying a set of residues that show frequent and persistent interactions with cholesterol, a new question arose: do residues form distinct cholesterol binding sites, or a continuous, cholesterol-favorable environment? To address this question, I posited that a binding site is a set of residues that have a high likelihood of simultaneous contact with a particular bound sterol and used principles from network theory to identify these highly correlated 'neighborhoods' of residues. In this analysis, I generated contact patterns for every bound sterol by representing its interaction as a network of nodes (residues) and edges (connections indicating likelihood of simultaneous contact). Moreover, this network can be further segregated on the basis of modularity (interconnectivity) to identify cholesterol binding sites. I performed this analysis on those cholesterol molecules that were persistently bound to the channel, as defined by both duration of contact and the average number of cholesterol-residue interactions present. Through this metric, I identified 25 cholesterol binding events in the 30 mol% simulations. In my approach, each cholesterol binding event is represented as a separate network, two examples of which are shown in **Figure 3-7A,B**. In this representation, the size of the node reflects the duration of its contact with cholesterol. The edges connecting nodes indicate concurrent contacts with the sterol, and are weighted by the magnitude of their correlation as calculated by their correlation coefficient. This variation in correlation coefficients and the network structure itself reflects the inherent flexibility of cholesterol within its interaction site.

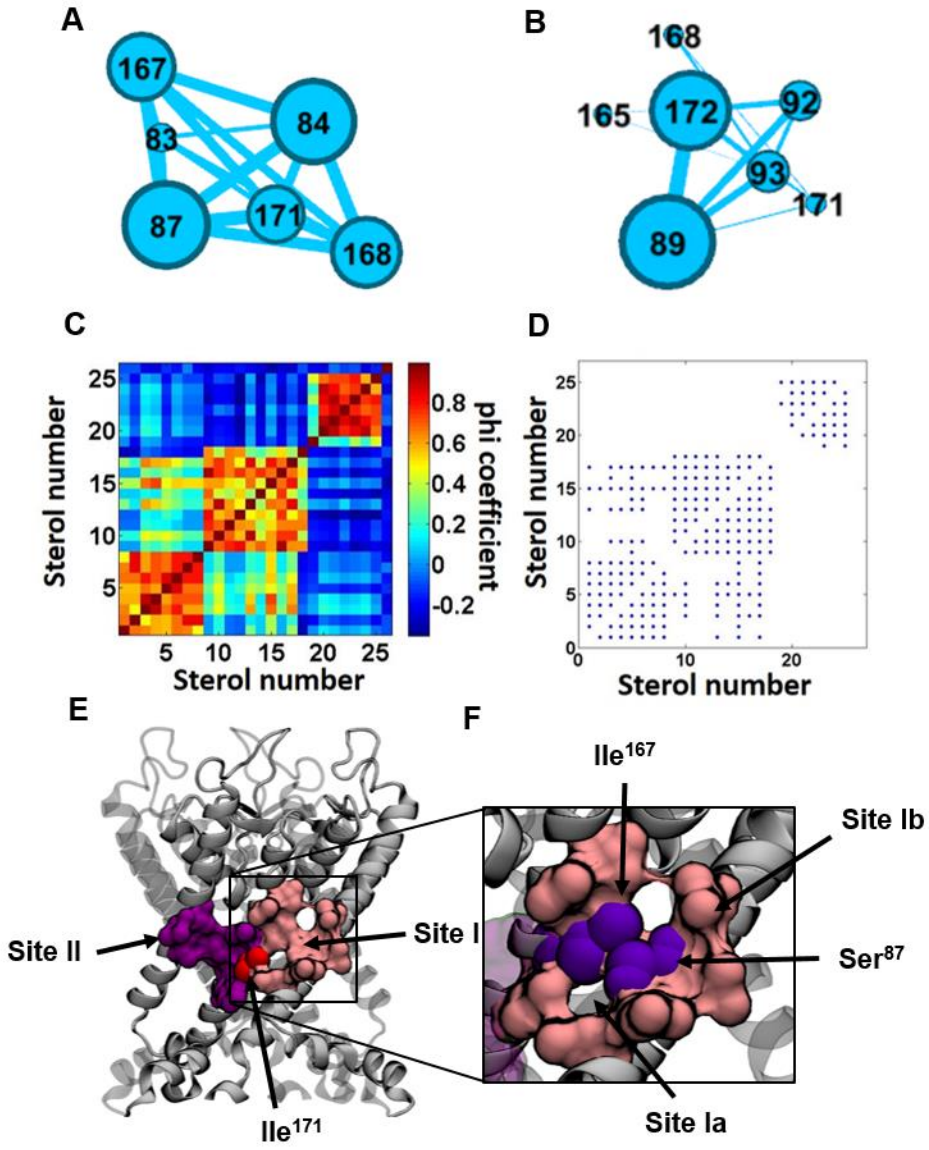

*Figure 3-7. Network representations of cholesterol binding events. Two examples are shown in **A** and **B**. Nodes are sized according to total contact time, and edges between nodes are sized according to the corresponding correlation coefficient. **C**) Phi coefficients for each pair of binding events, represented in a pseudo-color plot. **D**) Corresponding P-values for the correlation coefficients. Those with $P < 0.05$ are shown. **E**) Visualization of sites I (pink) and site II (purple). Their shared residue, Ile171, is shown in red. **F**): A close up of site I. Sub sites Ia and Ib are colored separately. Their shared residues are colored in purple.*

After applying this analysis to all of the identified sterol binding events, each of the 25 sterols had an associated set of "binding residues". To determine whether these residues represented one or multiple sites, I used a similarity analysis to compare the sets of residues. Here, binding events were grouped according to their k-means clustering, shown in **Figure 3-7C,D**. As can be seen from the figure, the grouping of statistically significant phi coefficients indicates that there are two separate binding events in these simulations. These two sites together form a contiguous region, but are distinct from one another. Comparing the residues identified for each site, only one residue, Ile^{171}, is present in both. The residues comprising these sites are shown in **Table 3-2**. Of the two sites, site I is situated at the interface between two subunits, while site II falls between the alpha helices of a single subunit. Both of these sites are visualized in **Figure 3-7E**. With respect to binding frequency, I found that site I was occupied more frequently, with an average rate of 4.5 instances per simulation (17 total events: 8 at site Ia, 9 at site Ib), whereas only 7 instances of binding at site II were observed, for an average rate of 1.75. Furthermore, I observed that binding at these two sites could occur simultaneously, and that these sites were replicated across the different subunits of the homotetramer protein.

In addition to reinforcing the existence of sites I and II, use of the unbiased clustering approach also identified two sub-regions within site I, denoted as sites Ia and site Ib. These subgroups are likewise evident from the phi coefficient analysis. The two sub-sites are located atop one another, occupying the groove at the subunit-subunit interface and sharing residues Ser^{87} and Ile^{167} (**Fig 3-7E,F**). As mentioned above these two sub sites were occupied at a similar rate in the simulations, with 8 binding instances at site Ia and 9 at site Ib. Here I also observed concurrent occupation of the 2 sub-sites by separate cholesterol molecules.

3.3.8. Cholesterol Segregates into Different Sites on the Open and Closed States of the Channel

As an ion channel protein, Kir2.2 undergoes conformation changes between "open" and "closed" states, which in turn regulate the flux of potassium through its central pore. To explore the effect of conformational state on the interactions of the channel with cholesterol, I performed additional simulations of Kir2.2 in a POPC/cholesterol bilayer using the closed state of the channel (PDB: 3JYC). Following the same methodology as the open state simulations, I ran three sets of simulations of the closed state of the channel at two different membrane concentrations of cholesterol (15 and 30 mol%). As with the open state, I observed for the closed state that numerous cholesterol molecules interact with the channel simultaneously. On average, 24 cholesterol molecules interact with the closed state of the channel, which is similar to the number interacting with the open state (22). Likewise, these interacting cholesterol molecules exhibited a broad range of interaction phenomena, and their contact times follow a similar power law distribution to that of the closed state.

I then applied my network theory approach to identify cholesterol binding sites on the closed state of the channel. Using the same binding criterion as with the open state, I found 21 cholesterol binding events. After generating networks for each sterol, I performed similarity analyses to determine the number of distinct binding sites. Interestingly, the similarity analysis identified 3 binding sites, with only one of them (site Ib) appearing in the open state simulations (**Fig 3-8**). These new sites, named sites III and IV, represent distinct binding sites from those determined in the open state of the channel. This was further confirmed by the k-means clustering algorithm in the similarity analysis. It is interesting to note that, although sites III and IV are distinct from sites I and II, there is a partial overlap in

the residues identified for these separate sites. Specifically, in each pair, Ia vs. III and II vs. IV, there is an overlap of 3 residues. The amino acid residues comprising all of the Kir2.2 binding sites in both open and closed conformations of the channel are presented in **Table 3-2**.

Site Ia	**Site Ib**	**Site II**
Leu^{83}, **Ser^{87}**, Ile^{167}, **Cys^{170}**, Ile^{171}	Leu^{84}, Ser^{87}, Leu^{88}, Leu^{91}, Val^{163}, Val^{164}, Ile^{167}	**Ala^{89}**, Val^{92}, Ser^{93}, Val^{168}, Ile^{171}, **Ile^{172}**, **Phe^{175}**
Site III	**Site Ib**	**Site IV**
Met^{70}, **Leu^{83}**, Leu^{84}, Phe^{86}, **Ser^{87}**, Phe^{90}, **Cys^{170}**, Phe^{175}, Met^{176}, Ile^{180}	Same as above	Met^{70}, Phe^{71}, Cys^{74}, Met^{82}, Leu^{85}, **Ala^{89}**, **Ile^{172}**, **Phe^{175}**, Met^{176}

Table 3-2. Residues comprising the discrete cholesterol binding sites for the open and closed states

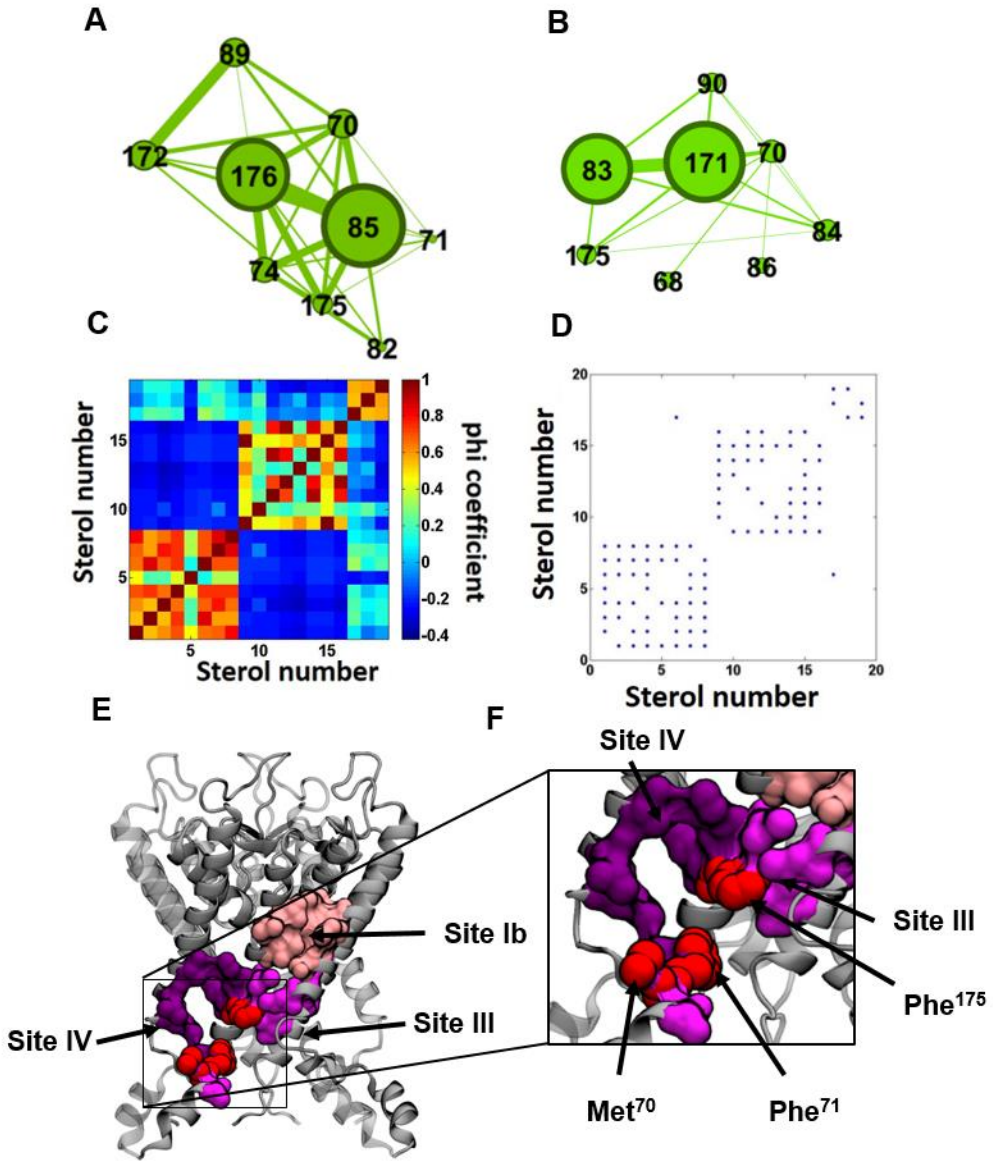

Figure 3-8. Network representations of cholesterol binding events. Two examples are shown in ***A*** *and* ***B****. Nodes are sized according to total contact time, and edges between nodes are sized according to the corresponding correlation coefficient.* ***C****) Phi coefficients for each pair of binding events, represented in a pseudo-color plot.* ***D****) Corresponding P-values for the correlation coefficients. Those with P < 0.05 are shown* ***E****): Visualization of sites Ib (pink), site III (purple), and site IV (magenta). Their shared residues, Met70, Phe71, and Phe175 are shown in a separate color.* ***F****): A close up of sites III and IV, with their shared residues shown in red.*

The similarities between the open and closed binding sites are readily apparent in their 3D structures. Like site I, site III sits at the interface between two subunits, while site IV lies on a single subunit near the slide helix, similar to site II. Furthermore, visual inspection of these sites reveals that the closed state sites are located in spots shifted downward toward the cytosolic domain with respect to their analogues in the open state. Specifically, site III sites just below site Ia in the inter-subunit space, while site IV sites just below site II in the same groove of alpha helixes (**Fig 3-9**).

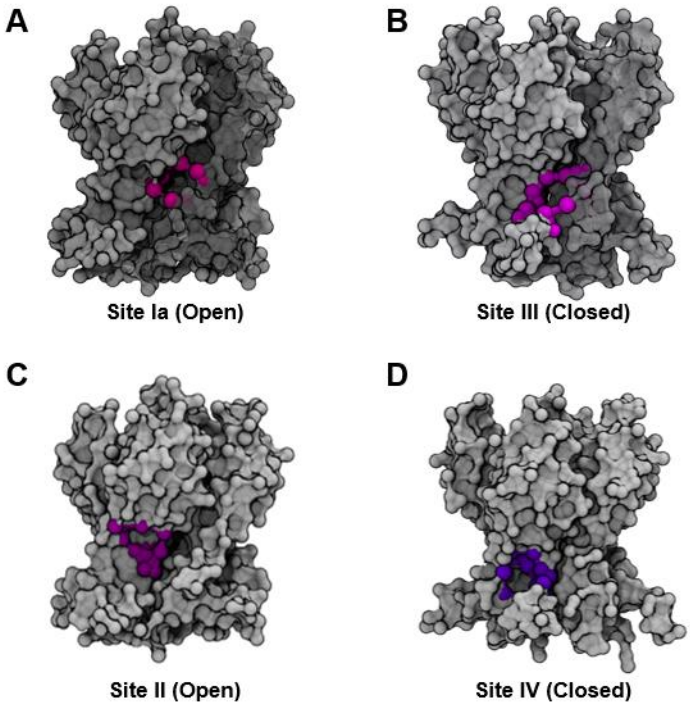

*Figure 3-9.Visualizing analogous cholesterol binding sites on the open and closed states of the channel. **A**) Site Ia on the open channel. **B**) Analogous site III on the closed channel. **C**) Site II on the open channel. **D**) Analogous site IV on the closed channel*

3.3.9. Asymmetric Concentration Dependence of Discrete Sites in both the Open and Closed States

I then repeated the network analysis to interrogate binding events in simulations containing 15 mol% cholesterol for Kir2.2 in its open and closed states.

3.3.9.1. Open State

I identified 13 total binding events in the 15 mol% system, roughly half the number of events observed in the 30 mol% system (25). Interestingly, this analysis also revealed that decreasing the concentration of cholesterol in the membrane prompted an asymmetric decrease in the occupancies of the identified binding sites. While in the 30 mol% system, all of the identified sites were occupied, in the 15 mol% system, cholesterol binding occurred almost exclusively at site Ia, while only a few events were identified at site II, and none at site Ib (**Fig 3-10**). Specifically, I observed 10 binding events at site Ia and 2 at site II, a 5:1 occupancy ratio. In comparison, the occupancy ratio at 30 mol% was 2.4:1. Looking at the sub-sites, there is an even more marked asymmetry, as site Ib was unoccupied. Regardless of the concentration of cholesterol in the membrane, site Ia was occupied for 90% of the total simulation time, while in contrast, the occupancies for sites Ib and II dropped dramatically. The occupancy of site Ib dropped from 60% to 0 and for site II, the occupancy dropped from 50% to 10% (**Fig 3-10**). In summary: reducing membrane cholesterol content by 50% results in a loss of site Ib binding events, a marked decrease in site II binding events, and no change in site Ia binding occupancy.

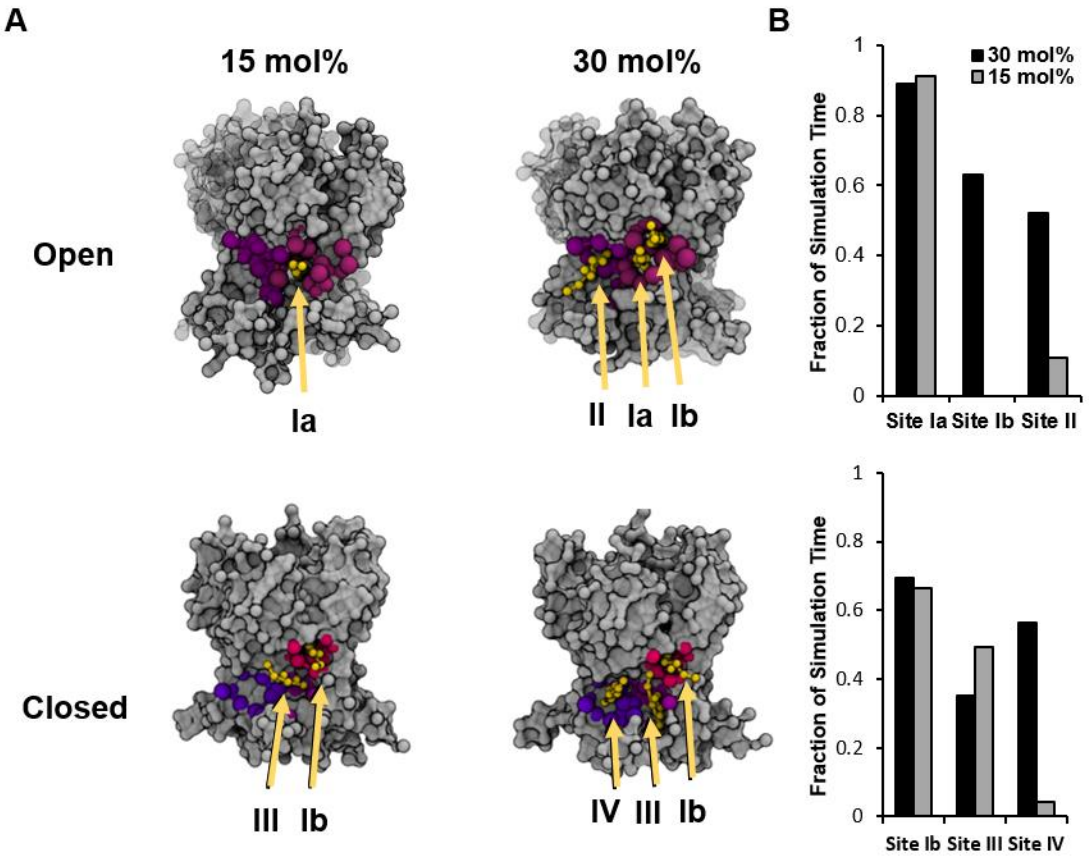

Figure 3-10. Differential occupancy of cholesterol binding sites. ***A****) Representative snapshots of the transmembrane domains of Kir2.2 in all four simulation conditions (open/30 mol%, open/15mol%, closed/30 mol%, and closed/15 mol%). The rest of the protein and the membrane lipids are hidden for clarity. Identified binding sites are colored as previously. Bound cholesterol are shown in yellow.* ***B****) Fractions of simulation time cholesterol occupies sites Ia, Ib, and II at 30 and 15 mol% in the open state simulations (top), and fractions of simulation time cholesterol occupies sites Ib, III, and IV at 30 and 15 mol% in the closed state simulations (bottom).*

3.3.9.2. Closed State

I also observed an asymmetric concentration dependence of the cholesterol binding sites on the closed state of the channel. In these simulations, site Ib was occupied for 60% of the simulation time, comparable to the site's occupancy in the 30 mol% simulations as well

as in the open state simulations at 30 mol%. Interestingly, this suggests that site Ib is concentration dependent in the open state, but not the closed state. Likewise, the occupancy of site III, which is analogous to site Ia in the open state and situated at the subunit interface, remained unchanged at both cholesterol concentrations. In contrast, site IV showed a marked decrease from 56% to 5% occupancy, mirroring the change occupancy of its analogous site on the open channel, site II. Thus, the occupancy of the single subunit site is sensitive to cholesterol concentration in both the open and closed states. These differences in state- and concentration-dependent binding sites offer a new window into understanding cholesterol-Kir channel dynamics, as further examined in the Discussion.

3.4. Discussion

My coarse-grained simulations showed that Kir2.2 exists in a dynamic membrane environment where cholesterol-channel interactions are continuous and present across the entire transmembrane region of the protein. This is a departure from previous conceptions of cholesterol-Kir2.2 interactions, which envisioned cholesterol binding as similar to a drug binding event, wherein there is a strong association between a single molecule at a well-defined binding site (Picazo-Juarez, Romero-Suarez et al. 2011; Singh, McMillan et al. 2012; Rosenhouse-Dantsker, Noskov et al. 2013; Fürst, Nichols et al. 2014; Balajthy, Hajdu et al. 2017; Barbera, Ayee et al. 2017; Morales-Lázaro and Rosenbaum 2017). Here, the use CG-MD to simulate larger system sizes than previous atomistic simulations allowed me to study these interactions in a broader context, by taking into consideration not just cholesterol molecules already bound to the channel, but the entire surrounding membrane environment as well. This allowed me to identify both annular and non-annular interactions between cholesterol and the channel, as well as the dynamics of these contacts. This was essential in

discovering how altering the membrane concentration of cholesterol affects its interactions with the channel. My main findings are: i) multiple cholesterol molecules interact with the Kir2.2 channel concurrently; ii) cholesterol-Kir2.2 interactions can be segregated into persistent, "rare" binding events at deeply embedded, non-annular binding pockets and transient, high frequency events localized at the lipid bilayer-channel interface; iii) that a decrease in membrane cholesterol results in a proportional decrease in the number of cholesterol molecules interacting with the channels and a corresponding decrease in interaction time. Furthermore, applying my network analysis approach to these long-scale simulations allowed me to identify discrete binding sites within a general cholesterol binding region and show that these sites are contingent on the conformational state of the channel. I also discovered that these sites show significant differences in occupancy when cholesterol levels were lowered in the membrane.

Previously, there were two general approaches to identify putative cholesterol binding sites on ion channels: scanning the primary sequence for known cholesterol-binding motifs, such as CRAC and CARC (Fantini and Barrantes 2013; Di Scala, Baier et al. 2017; Dopico and Bukiya 2017), or using an unbiased docking analyses of cholesterol to an ion channel to identify candidate sites, which are then further tested (Brannigan, Hénin et al. 2008; Rosenhouse-Dantsker, Noskov et al. 2013; Weiser, Salari et al. 2014). As described in the Introduction, the CRAC motif and its mirror image CARC have been identified as a potential source of cholesterol binding sites on transmembrane proteins. These motifs and their energetic requirements were explored in detail in nicotinic acetylcholine receptor (nAChR) (Di Scala, Baier et al. 2017), and additional CRAC/CARC-related sites were identified in TRPV1 channels (Picazo-Juarez, Romero-Suarez et al. 2011), BK channels

(Singh, McMillan et al. 2012), P2X7 (Murell-Lagnado 2017), and voltage-gated potassium channels Kv1.3 (Balajthy, Hajdu et al. 2017). However, while these motifs have offered clues into cholesterol binding sites, a recent analysis of crystal structures complexed with cholesterol showed that the cholesterol binding motifs only make up a subset of cholesterol binding regions, with many of these crystal structures showing interactions at novel sites independent of any known motifs(Rosenhouse-Dantsker 2017). In an alternative to this motif-centered approach, previous studies from the Levitan group and others have used a combination of unbiased docking analyses with atomistic simulations. Here, the docking analysis is performed on an unbiased manner on the whole transmembrane region of the channel, with candidate sites tested for stability in atomistic simulations (Brannigan, Hénin et al. 2008; Rosenhouse-Dantsker, Noskov et al. 2013; Hénin, Salari et al. 2014; Weiser, Salari et al. 2014). Using this approach, binding sites were identified in VDAC, nAChR and $GABA_A$ Receptors (Brannigan, Hénin et al. 2008; Hénin, Salari et al. 2014; Weiser, Salari et al. 2014). This unbiased docking approach was also combined with site-directed mutagenesis and electrophysiology to identify cholesterol binding sites on Kir2.1 (Rosenhouse-Dantsker, Noskov et al. 2013). Notably, as with the analysis of the crystal structure database, here the identified cholesterol binding sites do not contain any of the known cholesterol binding motifs.

While the two methods outlined about have successfully identified clusters of "cholesterol-binding" residues, both are limited by the static nature of their approaches, which cannot take into account the inherently dynamic nature of the membrane environment or the relevant timescales. Consequently, previous studies of Kir2 could neither explore cholesterol interactions on the surface of the channel nor provide information about

the dynamics of cholesterol-Kir2 interactions (Rosenhouse-Dantsker, Noskov et al. 2013; Fürst, Nichols et al. 2014). In contrast, the CG simulations I used in this study provided new insights into these interactions by considering the channel in a dynamic membrane environment. However, it is important to recognize the limitations of a coarse-grained simulation approach, and the limitations of the Martini model in particular (Alessandri, Souza et al. 2019). The Martini scheme involves a 4-to-1 mapping of heavy atoms onto coarse-grained "interaction particles". This reduces the degrees of freedom in the simulation and the computational expense of the simulations, but at the cost of a smoothened energy landscape and a loss of fine molecular detail. Likewise, this loss of molecular detail means that proteins in the Martini scheme must be constrained by an elastic network to maintain proper secondary and tertiary structure, restricting the protein to a single conformational state. These limitations are an important consideration when interpreting the results of CG-MD simulations and have been examined in detail in a number of reviews which outline the use of the Martini scheme for protein-lipid and protein-sterol interactions (Marrink and Tieleman 2013; Grouleff, Irudayam et al. 2016; Hedger and Sansom 2016). Nevertheless despite the limitations, coarse-grained simulations – and Martini CG in particular – have been successful in identifying lipid binding sites on a range of membrane proteins which have been further corroborated by crystallography experiments (Arnarez, Marrink et al. 2013; Prasanna, Chattopadhyay et al. 2014). Consequently, these types of CG simulations have seen a rapid expansion in their use for examining the dynamics of lipid-protein interactions. With respect to cholesterol, CG-MD simulations have identified binding sites for several types of G-protein Coupled Receptors (GPCRs) as well as nAChR, and serotonin receptors (Lee and Lyman 2012; Cang, Du et al. 2013; Genheden, Essex et al. 2017; Rouviere,

Arnarez et al. 2017). I found in my simulations that the entire transmembrane region of the channel was not only accessible to cholesterol molecules, but fully sampled by them, and that these cholesterol molecules can undergo both rapid (ns) and slow (μs) exchange with various sites on the channel. The frequency and duration of these interactions follows a power law relationship in line with what has recently been observed for the A2A receptor (Rouviere, Arnarez et al. 2017). Likewise, I found that previously identified "cholesterol sensitive" residues interact with cholesterol for non-uniform lengths of time and frequency, similar to what has been observed for GPCRs (Sengupta and Chattopadhyay 2015). Together, these results lend credence to the idea that the complex milieu of cholesterol and the surrounding membrane environment must be considered altogether and dynamic perspective to fully appreciate the sterol's regulatory effect on ion channels. More specifically, I used two analytical approaches to understand the nature of cholesterol-Kir2.2 interactions. In the first approach, I examined the dynamics of these interactions by quantifying occupancy times and contact frequencies. In the second approach, I analyzed the microenvironment of interaction cholesterol molecules in terms of the ration of sterol-phospholipid and sterol-residue interactions. The results of both of these analyses converged on two types of interactions: 1) persistent, long-lasting (μs) binding events between transmembrane helices, corresponding to the previously identified non-annular sites and 2) previously unidentified, short-lived events occurring on the surface of the channel-lipid bilayer interface.

My current analysis also provides strong evidence for the hypothesis that cholesterol is highly flexible within its binding site and explores a large conformational space. Previously, this hypothesis was based on the multiple overlapping sites identified from

docking analysis. In my simulations I observe this phenomenon directly. Furthermore, this seems to be a common feature of cholesterol-protein interactions, as similar mobility has been reported for cholesterol interactions with A2A Adenosine receptors and β2-Andrenergic receptors, among others (Gimpl 2016; Genheden, Essex et al. 2017; Rouviere, Arnarez et al. 2017). This flexibility meant defining a cholesterol binding site by previously methods was challenging: the list of amino acids in contact with a bound cholesterol molecule was found to continually fluctuate. To overcome this problem, I utilized principles from network theory to create a new analysis method. By defining residue relationships based on their likelihood of concurrent interaction, I could identify those residues that comprise a binding site even when the bound cholesterol molecule in that site was highly flexible. This is a departure from previous uses of network theory in the study of protein-ligand binding, which have predominantly created interactions based in residue-residue and residue-ligand proximity (Pons, Glaser et al. 2011; De Ruvo, Giuliani et al. 2012; Hu, Zhou et al. 2013). My analysis revealed that there are four discrete sites, characterized by distinct sets of binding residues, two of which are present in the open state of the channel and two of which are present in the closed state. Additionally, I found that one of the sites in the open state can be occupied by two cholesterol molecule simultaneously, and can therefore be divided into two sub-sites.

Identification of these binding sites represents a significant improvement over the previously identified cholesterol binding regions. Prior studies from the Levitan group identified a relatively large hydrophobic region in the Kir2.1 channel, which was labeled the “cholesterol binding region” (Rosenhouse-Dantsker, Noskov et al. 2013), while a similar site was identified for Kir2.2 (Fürst, Nichols et al. 2014). In contrast, in using the network

analysis I developed, I could identify discrete sites within the previously identified region, and that these sites were dependent on the conformational state of the channel.

It is also interesting to note the similarities between the identified binding sites in the open and closed states of the channel. Specifically, site Ia and III show partial overlap in their residue composition, as do sites II and IV. Furthermore, these sites are in analogous positions with respect to each other: both sites II and IV sit on a single subunit near the slide helix, while sites Ia and III sit between subunits. In each of these cases, the closed state binding site is shifted downward towards the cytosolic region.

These simulation results also provide the first insights into the effect of altering membrane cholesterol concentration on the specific binding of the sterol to sites on the channel. In the 15 mol% simulations, I saw a proportional decrease in the number of cholesterol molecules interacting with the channel. Likewise, lowering the membrane cholesterol concentration caused a decrease in the average contact time. Of the sterol molecules that did interact with the channel however, the microenvironments of their interactions remained consistent with the 30 mol% simulations: segregation into frequent, annular binding events and persistent, non-annular binding events. Most interestingly, I observed that lowering the levels of cholesterol in the membrane led to significant differences in the occupancy of the identified binding sites. Specifically, I found that site Ia in the open state is occupied at both cholesterol levels, while sites II and Ib see a significant drop in occupancy. Likewise, for the closed channel, sites Ib and III remained equally occupied at both cholesterol levels, while site IV saw a large decrease. This asymmetry in occupancy implies a difference in affinity for cholesterol to these sites, possibly dictated by cholesterol-mediated perturbations to the conformation of the protein.

In conclusion, I ran CG-MD simulations of the open and closed states of Kir2.2 in a membrane with varying levels of cholesterol. I found that the interactions between cholesterol and Kir are more complex and numerous than previously conceptualized, with cholesterol molecules interacting for a range of timescales and in various locations across the protein. I created a novel analytical framework by utilizing network theory to identify cholesterol binding sites, and found that these sites are conformation state-specific. Furthermore, I found that these sites experience significantly different responses to membrane cholesterol levels, suggesting a more complex cholesterol-mediated regulation process.

4. UNCOVERING FUNCTIONAL EFFECTS OF CHOLESTEROL BINDING

4.1. Introduction

This dissertation has thus far focused primarily on the identification and characterization of cholesterol binding sites on Kir2. The studies in the previous chapters and in recent publications from the Levitan lab have successfully identified multiple state- and concentration-depending binding sites across different conformations of the channel (Rosenhouse-Dantsker, Noskov et al. 2013; Barbera, Ayee et al. 2018). However, although putative binding sites have been identified, the question remains: what is the molecular mechanism through which cholesterol alters channel gating and function?

The previous studies outlined above and in the Introduction show that cholesterol interacts exclusively with the transmembrane region of Kir channels. However, there is significant evidence showing that gating among the different Kir sub-families is regulated predominantly in the cytosolic domain, via a diverse set of different ligands and regulators (Na+, Gβγ, ethanol, ATP, sulfonylurea receptor subunits), including the necessary agonist PIP2 (Hibino, Inanobe et al. 2010). This has been confirmed via multiple high-resolution structures of Kir channels which have been elucidated in complex with different combinations of ligands (Hansen, Tao et al. 2011; Whorton and MacKinnon 2011; Whorton and MacKinnon 2013) (Lee, Wang et al. 2013). Furthermore, these crystal structures and subsequent molecular dynamics simulations suggest that two major conformational changes occur as part of the opening process during channel gating: 1) rotating/twisting of the cytoplasmic domain with respect to the transmembrane domain, and 2) cytoplasmic domain

tethering to the transmembrane domain, stabilized by PIP2 (Wang, Lee et al. 2012; Wang, Vafabakhsh et al. 2016; Zangerl-Plessl, Lee et al. 2019).

In contrast to these various ligands, the biding of cholesterol to sites within the transmembrane domain suggests a different mechanism of regulation. It has been hypothesized previously that cholesterol acts to stabilize the closed state of the channel, effectively acting to create a population of "silent" channels (Romanenko, Rothblat et al. 2004). Moreover, studies from the Levitan have shown that multiple different pieces of the cytosolic domain of the channel regulate channel sensitivty to choleserol, (Rosenhouse-Dantsker, Noskov et al. 2012; Rosenhouse-Dantsker, Noskov et al. 2013), including "belt" of residues near the interface of with the transmembrane domain (Epshtein, Chopra et al. 2009; Rosenhouse-Dantsker, Logothetis et al. 2011). These studies point to the mechanism of cholesterol regulation acting on: 1) the interactions at the interfaces of the N- and C- termini on the four subunits of the channel, which couple the motions of these subunits, particular during gating, and 2) the cytosolic gating machinery situated around the G-loop, which controls pore opening (Rosenhouse-Dantsker, Noskov et al. 2013). In both cases, the proposed mechanism requires a mechanistic link between cholesterol interactions with the transmembrane domain and corresponding effects in the cytosolic domain.

In this study, I used coarse-grained molecular dynamics simulations to show that cholesterol interactions with the transmembrane region of Kir2.2 do indeed affect the dynamic behaviors of the cytosolic region of the channel, including those that are important for channel gating. Using a network theory-based approach adapted from Yao et al. (Yao, Momin et al. 2018), I identified specific domains of coherent movement within the Kir2 channel which correspond to structures known to be important for gating. I found that

increasing membrane cholesterol levels negatively affects the interactions between these domains, causing them to "de-couple" from one another. Furthermore, I found that this effect is mediated by a series of important residue-residue interactions whose interactions are also altered by increasing membrane cholesterol. Most significantly, the interactions between these specific pairs of residues are contingent on the number of cholesterol bound: when more cholesterol binding sites are occupied, these residue pairs show a correlated decrease in contact probability.

4.2. Methods

4.2.1. Coarse-grained Molecular Dynamics Simulations

For this study, I use the same set of simulations described in Chapter 3, including both conformational states and both membrane cholesterol conditions. However, here I develop an alternative analysis to address the new question posed about the effects of cholesterol on the dynamic behaviors of the channel.

4.2.2. Generating Protein Contact Networks

I again exploit a network theory approach to make sense of structure and dynamics in the membrane protein system. By re-defining the nodes and edges, I address the consequences of cholesterol binding by quantifying the changes in protein dynamic structure that result from state and concentration-dependent binding of cholesterol. Through this analysis, I generated a set of protein contact networks for the Kir2.2 channel in each conformational state (open and closed) and at each membrane cholesterol concentration (15 and 30 mol%). By doing so, effects of cholesterol on the structural dynamics of the channel could be inferred. This approach was adopted from the work of Yao

et al. (Yao, Momin et al. 2018), and offersuseful concept to interrogate changes in the dynamic behavior of a protein.

To determine the effects of cholesterol on the motion of the channel, I first needed to identify the dynamic structural features of Kir2.2 (i.e. domains that move coherently irrespective of cholesterol concentration or channel state). In the previous chapter, I focused my network analysis on sterol-residue interactions. Here, the interactions I choose to examine are those that exist between pairs of residues. Thus, the nodes of interest are residues, and the edges represent contacts, weighted by their probability of occurrence. For each pair of residues in the channel, the contact probability was calculated as per **Equation 4-1**, where $n_{contact}$ is the number of simulation frames in which a pair of residues *i* and *j* were within the 6Å cutoff distance and N is the total simulation length (N).

$$p(C_{ij}) = \frac{n_{contact,ij}}{N}$$

Equation 4-1

Together, these probabilities represent an M-by-M adjacency matrix, hereafter called a Protein Contact Network, *PCN*, where N is the number of residues in a Kir2.2 channel subunit (here, 337) and each index (*i,j*) corresponds to the average contact probability of residues *i* and *j*. A protein contact network was generated for each simulation condition, leading to four separate networks: open channel/30 mol% cholesterol (O30), open channel/15 mol% cholesterol (O15), closed channel/30 mol% cholesterol (C30), and closed channel/15 mol% cholesterol (C15).

The overall goal of this protein contact network analysis is to identify dynamic changes in the protein structure that are caused by cholesterol. Consequently, it is helpful to first identify domains of the protein than move coherently, regardless of channel

conformation or cholesterol concentration. Relative motions of these domains are likely to be implicated in channel gating. Coherent motions were identified using a consensus network, *A(i,j)*, which is defined by those residue-residue interactions that persist for at least 90% of the simulation time in all four simulation conditions **Equation 4-2**.

$$A(i,j) = 1 \; if \; p\left(C_{ij}\right) \geq 0.9 \; in \; all \; 4 \; protein \; contact \; networks$$

Equation 4-2

A is thus a binary adjacency matrix where each element (A_{ij}) corresponds to the presence (1) or absence (0) of persistent contact between residues *i* and *j*. Partitioning the consensus network into communities via the same modularity protocol described in the previous chapter allows the conserved dynamic domains of the Kir2.2 channel to be defined. Having identified those domains, net changes in their motion relative to one another can be quantified using a difference contact network. For each state of the channel (i.e., open or closed), the difference network is defined as:

$$D(i,j) = PCN_{30\ mol\%}(i,j) - PCN_{15\ mol\%}(i,j)$$

Equation 4-3

Thus, the consensus network provides a binary representation of dynamically conserved contacts, while the difference network quantifies dynamic perturbations that are due to increased membrane cholesterol.

Once the consensus network and difference contact networks are created, the effect of cholesterol on interactions both *between* and *within* domains can be assessed. To calculate the change in contact between two domains, $\Delta B_{x,y}$, I used the following equation:

$$\Delta B_{xy} = \sum_{i \in x} \sum_{j \in y} D_{ij}$$

Equation 4-4

where D is the difference contact network, and i and j refer to residues in domains x and y, respectively. Likewise, the change in residue contacts within a single domain, ΔB_x, can be calculated as:

$$\Delta B_x = \sum_{i \in x} \sum_{j \in x} D_{ij}$$

Equation 4-5

4.3. Results

I used the above approach to answer the following questions: 1) does cholesterol binding cause perturbations in the dynamic structure of the channel, and 2) if so, where are these perturbations occurring?

4.3.1. Identifying Domains of Coherent Motion on the Kir2.2 Channel

Protein contact networks encode information regarding both the covalent and non-covalent interactions between amino acid residues within the protein, and provide a relatively simple and straightforward mathematical framework from which to interrogate the dynamics of Kir2.2.

All four protein contact networks (corresponding to the four simulation conditions) are visualized with pseudocolor plots in **Figure 4-1A.**, with higher contact probabilities shown as yellow, and lower probabilities shown as blue. At first glance, the four plots appear similar to one another: the pattern of a given plot shows dense connections in the top right

and bottom left corners, corresponding to the transmembrane and cytosolic domains, and few connections between the two. Furthermore, the qualitative similarity between these protein contact networks implies that there are indeed domains of coherent motion within the channel.

To define these domains, I examined the four protein contact networks and took those interactions between residues that persisted for 90% of the simulation in all 4 conditions. From this I built a consensus network as described in the Methods section **(Figure 4-1B)**. This consensus network represents the average residue interactions within the channel, and is agnostic to conformational state or membrane cholesterol composition. Having defined this consensus network, I partitioned it into 8 separate, self-interacting modularity groups using the algorithm defined in the Methods section. These modularity groups form the aforementioned domains. Encouragingly, they also correspond to known functionally important features of the channel (**Figure 4-1C,D**).

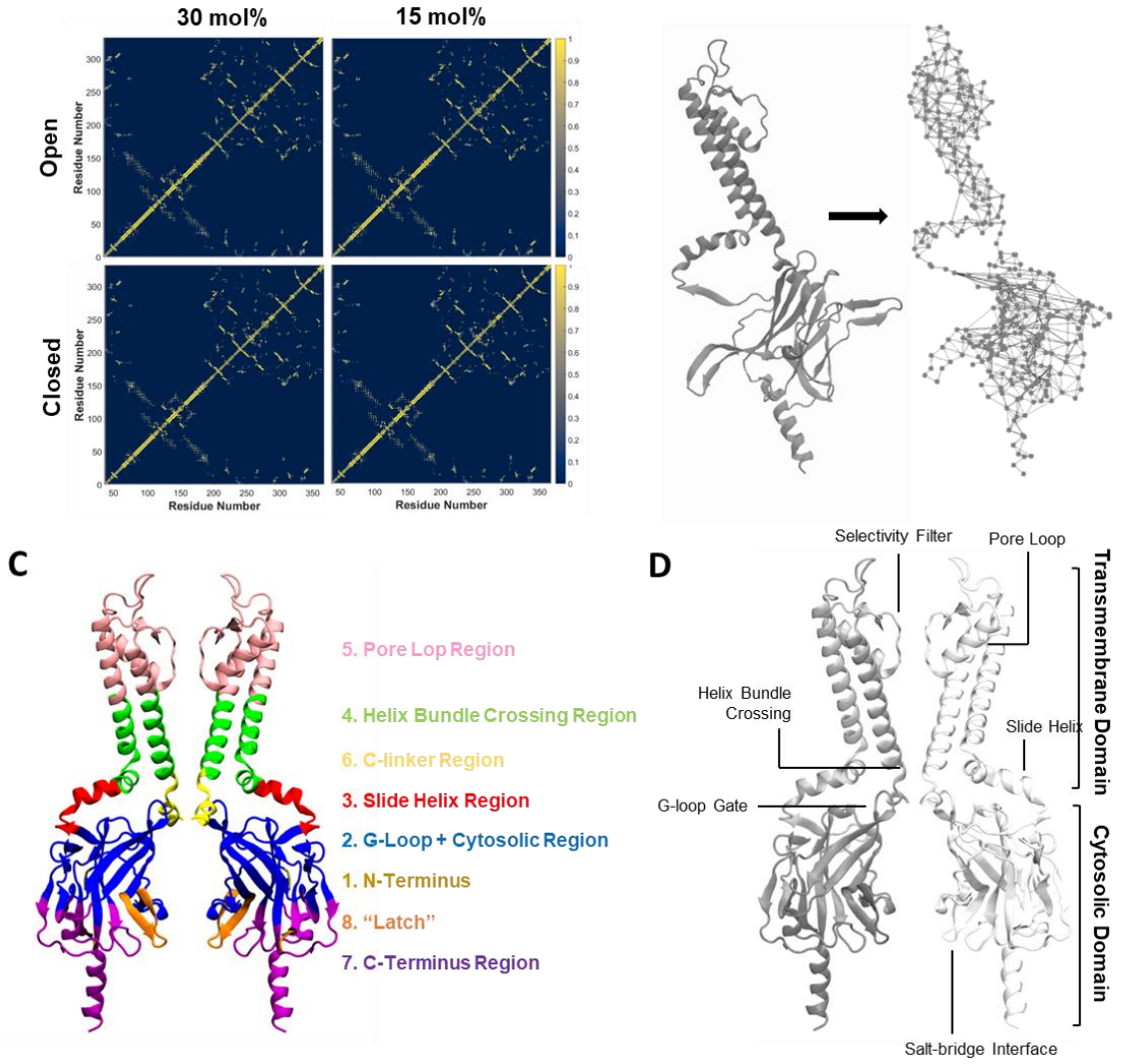

Figure 4-1. Generating a consensus network for Kir2.2. ***A****)Protein contact networks for the 4 simulation conditions: open and closed channel states, 15 and 30 mol% cholesterol. Every index (i,j) in the matrix corresponds to the average contact probability between residues i and j for that simulation condition.* ***B****) Schematic showing a cartoon rendering of the protein and the consensus network. The consensus network is able to capture the essential structural features of the Kir channel.* ***C****) Schematic showing the identified modularity groups on the channel. Two subunits are shown for clarity. Colors on the channel correspond to the labeled modularity groups.* ***D****) Structural schematic of the Kir channel, showing the important features in the cytosolic and transmembrane domains.*

4.3.2. Cholesterol Causes De-coupling Between Dynamic Domains in Kir2.2

Having defined the domains of coherent motion within the Kir2.2 channel, the effects of membrane cholesterol on the channel's dynamic structure could then be identified. I first looked at the effect of increasing membrane cholesterol on the interactions between domains and asked: how does increasing cholesterol affect these interactions? I address this be quantifying the net change in contact probability between the residues comprising each pair of domains.

For each conformational state of the channel (open and closed), I generated a difference contact network as described in the Methods: I calculated the change in contact probability between every residue pair when cholesterol was increased from 15 to 30 mol%. From these difference networks, I identified those pairs of residues connecting specific domains and their changes in contact probability from, and calculated net change of residue interactions connecting these domains to one another. I found that when the concentration of cholesterol in the model membrane bilayer is increased, the primary effect on the interactions between these domains is a "de-coupling" effect. That is to say, there is a net decrease in contact probability between modularity groups in the high cholesterol conditions as compared to the low cholesterol conditions (**Figure 4-2A,B**). In particular, in the open state, communities 1 and 8, and 2 and 4 show large net decreases in their contact probabilities, indicating a de-coupling. Likewise, in the closed state, communities 2 and 3, and 2 and 8 show similarly large decreases. When mapped to their corresponding structures in the channel, it appears that these decreases in interaction happen predominantly at the membrane-cytosol interface and within the cytosolic domain (**Figure 4-2C**). Moreover these decoupled domains are: (1) made of residues distinct from the previously identified

cholesterol binding sites (Rosenhouse-Dantsker, Noskov et al. 2013; Fürst, Nichols et al. 2014; Barbera, Ayee et al. 2018); (2) located in regions of the protein that are distant from cholesterol binding sites; and (3) correspond to regions within the channel where Kir2.2 gating mechanisms are located.

Seeing that cholesterol affected the interactions between dynamic domains, I also looked at the effects of increased membrane cholesterol on the residue-residue interactions *within* each individual domain. I found that the most pronounced effects of increasing cholesterol exist in the closed state (**Figure 4-2D**). Here, cholesterol causes a decrease in contact probability between residues within domain groups 2 and 6. Notably, domain 2 contains the g-loop, which is an important feature of Kir channels that helps govern gating (Hibino, Inanobe et al. 2010; Meng, Zhang et al. 2012). Likewise, domain 6 contains a sequence of residues that undergoes a disorder-to-order transition during the opening of the channel, as can be seen between crystal structures of the open and closed channels, which would be characterized by an increase in inter-community contact probability. Again, it is important to note that these effects occur in the cytosolic region of the channel, separate from the cholesterol binding sites. Overall, these results indicated that although cholesterol interacts with the transmembrane region of Kir2.2, increasing membrane cholesterol does indeed perturb dynamics within the cytosolic region of the protein where gating is regulated.

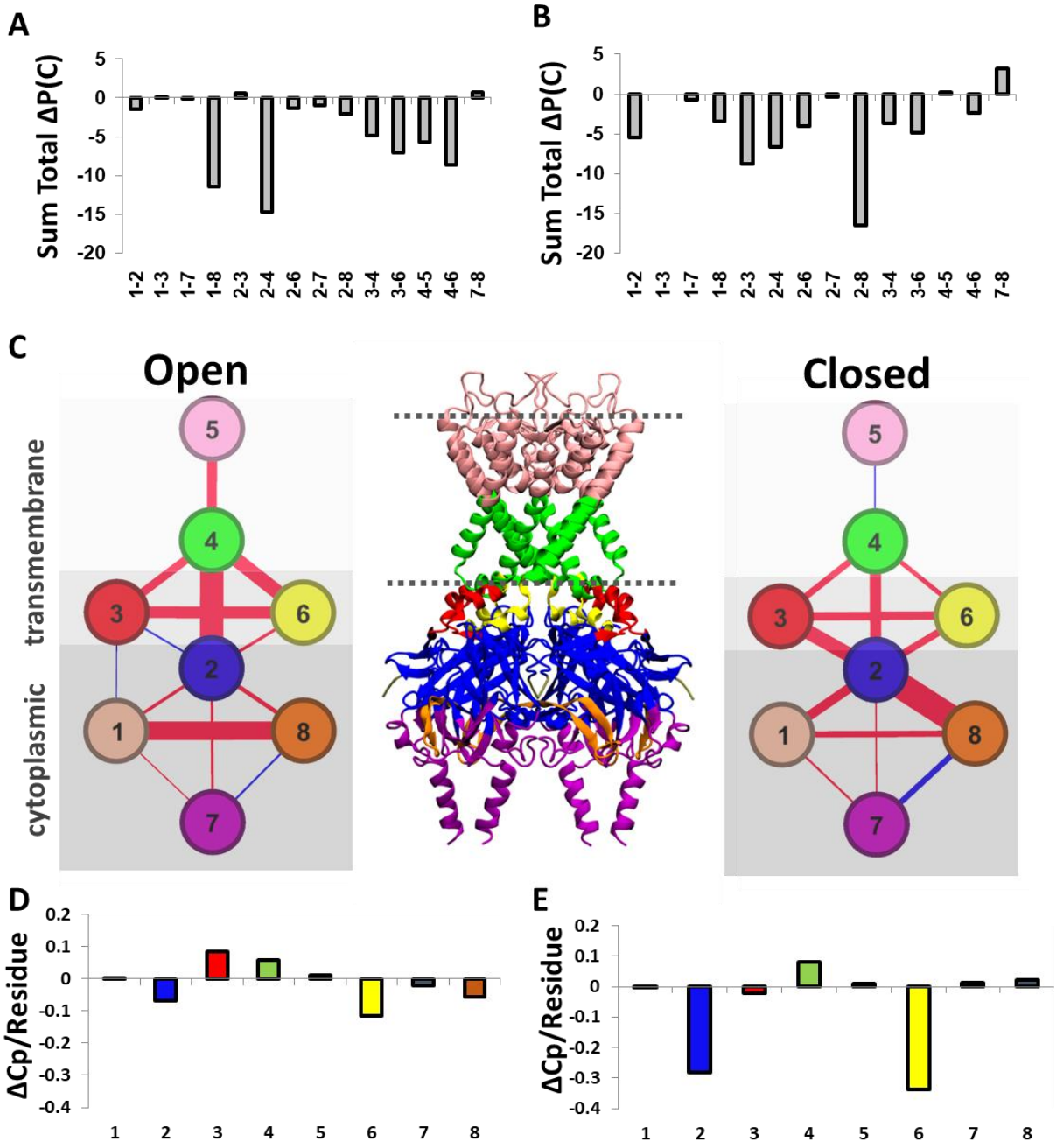

Figure 4-2. Quantifying the effects of cholesterol on dynamic domains of Kir2.2. ***A****) Sum total change in contact probabilities between domain groups within the open state of the channel.* ***B****) Sum total change in contact probabilities between domain groups within the closed state of the channel.* ***C****) Visualization of the domain groups identified in the channel and the changes in sum total contact probability between them. Here, red lines denote a decrease in probability and blue denotes an increase in probability, with the thickness of the line denoting magnitude. Domain groups are colored according to the corresponding domains in the reference image of the channel in the center (dotted lines represent the lipid membrane).* ***D****) The average change in contact probability per residue in each domain of the open state of the channel.* ***E****) The average change in contact probability per residue in each domain of the closed state of the channel.*

4.3.3. Cholesterol Affects a Sub-set of Residue-Residue Pairs

The above results point to a mechanism through which cholesterol mediates channel function by altering the dynamics between structurally important features of the channel. A common way to experimentally investigate structure-function relationships in proteins is through site-directed mutagenesis. In this approach, an amino acid of interest is replaced by one with a different functional group (e.g., one with different physiochemical properties). Changes in protein function are then measured. While we have determined that cholesterol has an overall "de-coupling" or dissociative effect between and within the domains, validation of this result experimentally requires that we translate the domain-level phenomenon into residue-specific events. To this end, I aimed to determine whether specific residue pairs mediated the domain-level decoupling effects, or whether domain de-coupling effects were due to the aggregated contributions of many small changes in pairwise contact probabilities. Representations of these pairwise interactions are shown in **Figure 4-3A**.

To investigate the changes in specific pairs, I turned again to the difference contact networks previously generated and shown here in **Figure 4-3B,C**. As might be expected from a dynamic re-arrangement of the channel, increasing cholesterol causes both increases and decreases in inter-residue contact probability, colored as either red or blue in the difference contact network. However, when I looked at the net total changes for each residue, I again saw that the overall effect is a decoupling one: while some residues show an increase in association with their neighbors, those increases are offset by many more decreases in contact probability. (**Fig. 4-3D,E**).

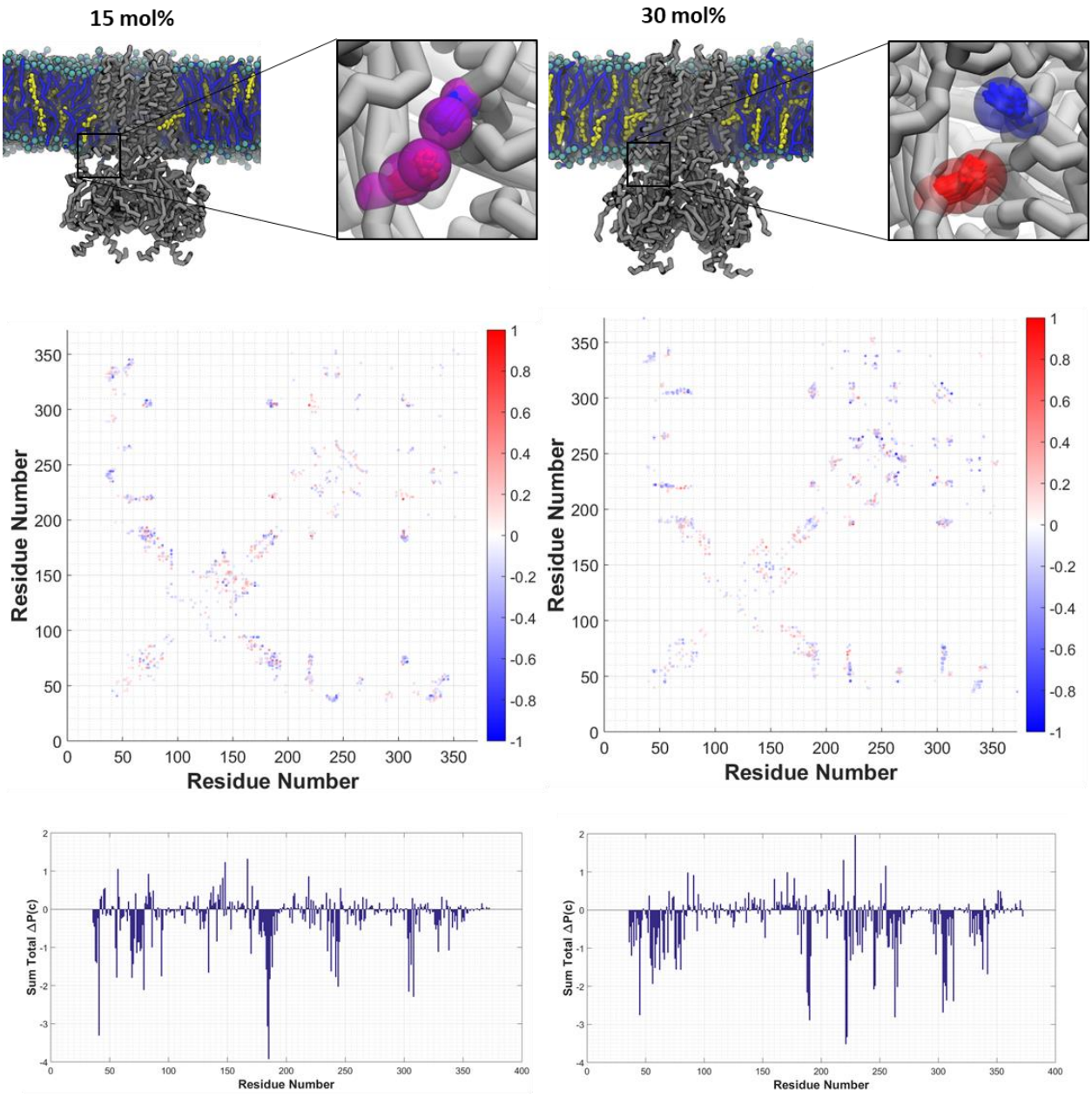

Figure 4-3. Quantifying the effects of cholesterol on residue-residue interactions. ***A)*** *Example of the contact probability between a pair of residues changing from the 15 mol% (left) to 30 mol% (right) condition. In this example, increasing membrane cholesterol causes these residues to move away from one another and for their contact probability to decrease.* ***B)*** *The difference contact network for the open state of the channel.* ***C)*** *The difference contact network for the open state of the channel.* ***D)*** *The sum total change in contact probability for each residue in the open state of the channel.* ***E)*** *The sum total change in contact probability for each residue in the closed state of the channel.*

Because the channel and the surrounding environment are in constant motion and owing to the probabilistic nature of these simulations, it is reasonable to expect that many of the changes in contact probability between residue pairs are relatively small and not functionally relevant. Indeed, when I plotted a histogram of the changes in contact probability for all pairs in each conformation, I found that the vast majority of these changes (90%) are less than a ten percent change in magnitude (**Fig. 4-4A,B**). Furthermore, only 0.5% of contacts constitute changes of -.35 or more, suggesting that the overall domain effects are influenced by a small set of pairwise interactions. These pairs are listed in **Table 4-1** and **Table 4-2**. When I visualized these pairs, I found that these changes are concentrated primarily within the cytosolic region of the channel. In particular, for the closed state, the majority of these interactions are at the subunit-subunit interface, while in the open state they are clustered around the PIP2 binding site. It is also interesting to note that, as with the domain interactions, many of these interactions are in the cytosolic domain of the protein, distant from the previously identified cholesterol binding sites (**Fig. 4-4C,D**).

Pairs		ΔP(c)
Cys^{41}	Pro^{235}	-0.38
Cys^{41}	Pro^{245}	-0.56
Phe^{56}	Pro^{267}	-0.39
Phe^{56}	Asp^{341}	-0.45
Phe^{56}	Phe^{345}	-0.44
Thr^{72}	Met^{308}	-0.62
Asp^{76}	Pro^{187}	-0.40
Trp^{94}	Gly^{169}	-0.49
Trp^{94}	Ile^{172}	-0.47
Trp^{94}	Asp^{173}	-0.47
Gln^{141}	Cys^{170}	-0.67
Glu^{304}	Met^{308}	-0.50
Glu^{304}	Thr^{310}	-0.50

Table 4-1. Residue pairs from the open state of the channel with a net change of -0.35 or greater

Pairs		ΔP(c)
Phe^{45}	Val^{54}	-0.39
Val^{46}	His^{222}	-0.66
Asp^{76}	Thr^{306}	-0.57
Lys^{189}	Val^{224}	-0.36
Arg^{190}	Met^{308}	-0.33
His^{222}	Leu^{264}	-0.36
Ile^{233}	Val^{265}	-0.60
Pro^{235}	Tyr^{338}	-0.48
Ile^{244}	Leu^{331}	-0.47
Leu^{246}	Val^{265}	-0.63

Table 4-2. Residue pairs from the closed state of the channel with a net change of -0.35 or greater

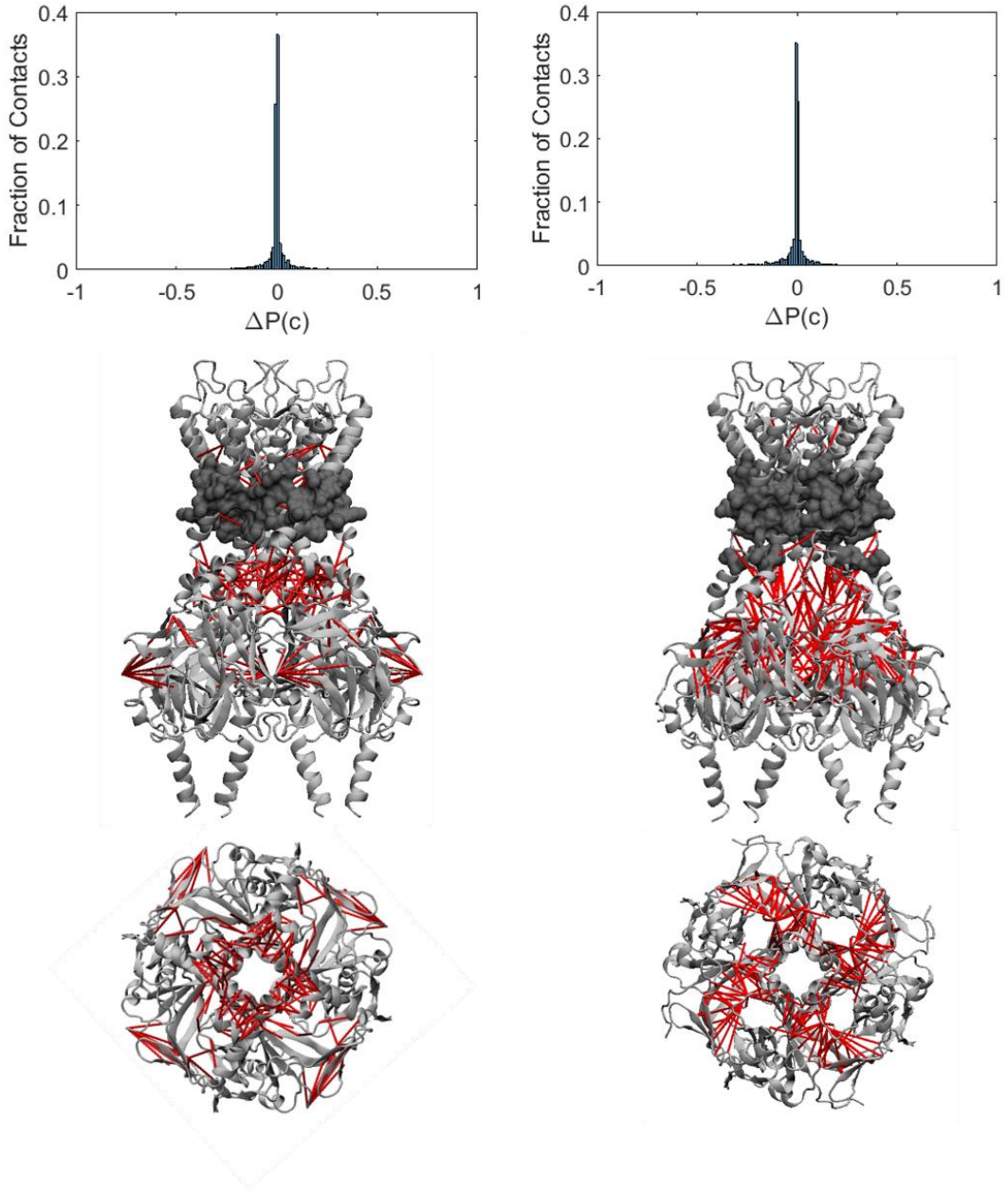

Figure 4-4. Cholesterol predominantly affects residue-residue interactions in the cytosolic domain. ***A****) A histogram of the non-zero changes in contact probability between every pair of residues in the difference contact network from the open state of the channel.* ***B****) A histogram of the non-zero changes in contact probability between every pair of residues in the difference contact network from the closed state of the channel. A side and top-down view of the open* ***C****) and closed* ***D****) states of the channel. The previously determined cholesterol binding regions are shown in grey, while contacts between residue pairs listed in table 4-1 are shown as red lines. In the open state, these are clustered near the PIP2 binding site and the N-terminus, while in the closed state they are clustered at the subunit interfaces*

4.3.4. Residue-residue contact probability is correlated with cholesterol binding

As the results of this Chapter show, interactions with cholesterol and transmembrane indeed show indirect effects on the dynamics cytoplasmic domain. One outstanding question remains: do these perturbations truly reflect a site-specific binding event modulating protein structure, as distinct from a collective, membrane-mechanical effect on structure? Previous studies on the effects of cholesterol on Kir channels have drawn the distinction between direct effects of cholesterol binding and indirect effects of cholesterol on membrane features. In the context of my simulations, I asked a similar question: to what degree are the pairwise decreases in contact probability a product of direct cholesterol binding, and to what degree are they due to indirect membrane effects from increasing cholesterol concentration? To answer this, I looked at those residue interaction pairs in each state of the channel that showed a large negative change in contact probability and quantified the degree of decrease with the number of bound cholesterol. Based on my definition of the cholesterol binding sites described earlier in this thesis, I looked at each duration of time in the simulation where between 1 and 6 cholesterol were bound to the channel, and calculated the average contact probabilities of these residue pairs at each bound condition. Interestingly, I found that there is a correlation between bound cholesterol and contact probability, with increasing numbers of bound cholesterol leading to decreased contact probability for these pairs.

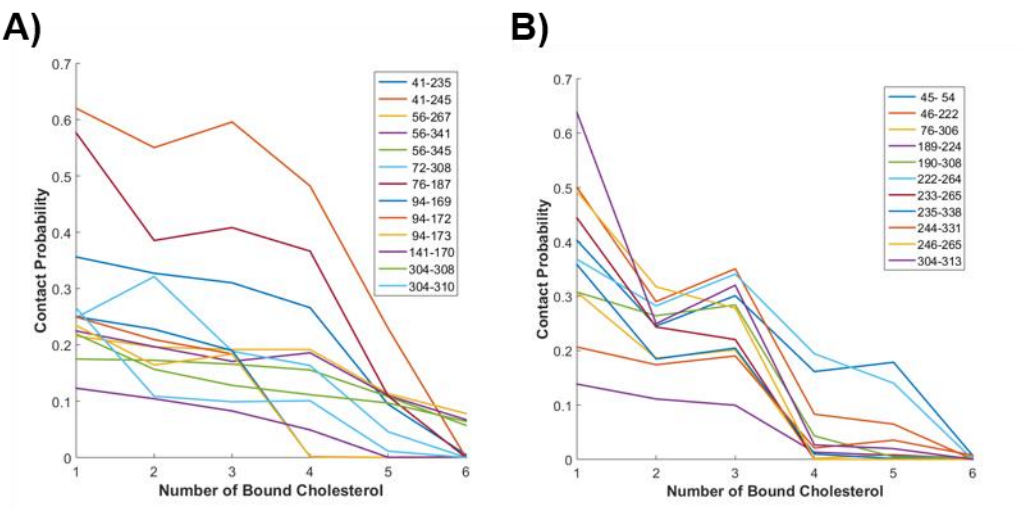

*Figure 4-5. Plots of the contact probability of specific residue pairs vs. the number of bound cholesterol in the **A**) open and **B**) closed state simulations.*

4.4. Discussion

My coarse-grained simulations of different conformational states of Kir2.2 in different levels of membrane cholesterol, combined with a protein contact network-based analysis, showed that increasing membrane cholesterol levels caused a shift in intra-protein interactions within the channel. Specifically, I found that a higher level of membrane cholesterol reduced the likelihood of contact between specific regions of the cytoplasmic and transmembrane domains of the channel, and that these specific regions correspond to structures known to be important for gating. These regions were determined in an unbiased manner by first creating a consensus protein contact network, which represented all of the covalent and non-covalent interactions between residues in the protein averaged over all simulation conditions. This consensus network was partitioned into separate modularity groups which represent distinct, dynamic domains of the channel. From this framework, I

found that increasing membrane cholesterol not only alters interactions between these identified groups, but also within these groups. In both cases, I found that the overall effect was a "de-coupling" one. That is, the predominant effect of increasing membrane cholesterol was a decrease in residue-residue contact probability, which facilitated this dissociative effect. Additionally, I found that while the net overall effect was one of decreasing contact probability, only a small set of residue-residue interactions (comprising 0.5%) saw a large (>30%) decrease in their contact probabilities. This result suggested that the overall domain effects are influenced by a relatively small set of pairwise interactions, which were concentrated predominantly in the cytosolic region of the channel and separate from cholesterol binding sites. Specifically, these sites were found to cluster at the subunit interface of the cytosolic domain in the "closed state" simulations, and near to the PIP2 binding site in the "open state" simulations. Most interestingly, I found that the probability of contact between these residue pairs negatively correlated to the stoichiometry of cholesterol binding events at the previously determined putative sites.

Previous investigations into the interactions of cholesterol and Kir channels focused on three different questions: 1) does cholesterol regulate the function of Kir channels through direct or indirect interactions, 2) what are the interaction sites of cholesterol on the channel, and 3) what is the biophysical mechanism through which cholesterol alters channel gating? The direct regulation of Kir channels by cholesterol was confirmed in studies using chiral isomers, which demonstrated the sterospecificity of Kir as well as the direct interactions between the channel and cholesterol (Romanenko, Rothblat et al. 2002; Singh, Rosenhouse-Dantsker et al. 2009; D'Avanzo, Hyrc et al. 2011). Additionally, later studies by the Levitan group and others utilized a combination of computational and experimental

methods to identify putative binding sites on the channel (Rosenhouse-Dantsker, Noskov et al. 2013; Fürst, Nichols et al. 2014). Most recently, the work outlined in this dissertation showed that the cholesterol binding sites on the channel are dependent on channel conformation, and that the interactions between cholesterol and Kir2 are complex and multifaceted (Barbera, Ayee et al. 2018).

In addition to identifying putative cholesterol binding sites on Kir2, a number of studies from the Levitan lab also investigated the mechanism of cholesterol-mediated regulation by identifying specific segments of the cytosolic domain of the channel which contain residues that are "cholesterol sensitive". Specifically, they found that parts of the CD-loop and G-loop, as well as parts of the C- and N-termini, form a cytosolic "belt" around the channel near the interface with the transmembrane domain that is critical for modulating the sensitivity of the channel to cholesterol (Epshtein, Chopra et al. 2009; Rosenhouse-Dantsker, Logothetis et al. 2011). Furthermore, in subsequent studies they showed that cholesterol regulation of Kir2 channels depends on two features of the cytosolic domain: 1) the interactions at the interfaces of the N- and C- termini on the four subunits of the channel, which couple the motions of these subunits, particular during gating, and 2) the cytosolic gating machinery situated around the G-loop, which controls pore opening (Rosenhouse-Dantsker, Noskov et al. 2013). These facets form a complex relationship between distal parts of the protein, linking the CD loop, EF and GA loops of the C terminus which are far from the TM domain, and the βA sheet of the N-terminus (Rosenhouse-Dantsker, Noskov et al. 2012; Rosenhouse-Dantsker, Noskov et al. 2013).

My simulations provide a new level of detail to the experimental findings outlined above and to cholesterol-Kir2 interaction in general by investigating the structure of the

channel in a dynamic context through a network theory-based approach. Generally speaking, network theory is a method used for the analysis of complex systems, which represents agents in a system and the interactions between those agents as a graphical model of nodes (agents) and edges (the pairwise interactions between them) (Borgatti and Halgin 2011). In my analysis, I employed a type of network called a protein contact network. A protein contact network is type of network that maps the 3-dimensional structure and topology of a protein into a more mathematically tractable space by representing individual residues as nodes and the probability of contact between them as edges. By representing the dynamics of the protein as a single network, protein contact networks have been used to investigate the effects of ligand binding and allosteric communication pathways in proteins (Daily and Gray 2009; Dokholyan 2016), as well as interrogate the effects of small changes – such as the concerted movements of individual amino acids – on the global features of a protein (Daily and Gray 2009). Here I used protein contact network-based analysis based on the protocol laid out by Yao et. al (Yao, Momin et al. 2018) which allowed me to compare the effects of cholesterol on the dynamic structure of the channel across multiple different conditions by generating a common framework in an unbiased way. Furthermore, this framework led to the identification of specific residue interactions that are potentially mediating changes in channel structure, which can be directly tested via electrophysiological experiments. Most importantly, the residue interactions identified in my simulations localize to regions that have been determined from previous experiments to be critical to channel gating and Kir2 cholesterol sensitivity. In particular, I found that these interactions occur in two places: the inter-subunit interface and near the PIP2 binding site. PIP2 is a necessary agonist for channel opening, and its binding is hypothesized to stabilize the open state of the channel (Lee, Wang

et al. 2013; Zangerl-Plessl, Lee et al. 2019). Moreover, previous experiments from the Levitan lab showed that a number of "cholesterol sensitive" residues are also important for the Kir2 channel's sensitivity to PIP2, with alterations to these residues affecting both cholesterol and PIP2-related effects (Rosenhouse-Dantsker, Logothetis et al. 2011). Likewise, inter-subunit interactions like the ones identified in my simulations have been shown to be important in regulating channel gating and in mediating channel sensitivity to cholesterol via a "belt" (Rosenhouse-Dantsker, Logothetis et al. 2011).

In interpreting the results of these simulations, it is important to understand the limitations of the methodology. In particular, the Martini model involves a 4-to-1 mapping of heavy atoms into coarse grained particles, which smoothes the energy landscape at the price of atomic resolution. (Alessandri, Souza et al. 2019). Likewise, this coarse-grained mapping necessitates the use of an elastic network to stabilize the secondary and tertiary structures of the protein, restricting individual simulations to a single conformational state. As has been outlined in a number of reviews (Marrink and Tieleman 2013; Grouleff, Irudayam et al. 2016; Hedger and Sansom 2016), these limitations are an important consideration, particularly when interpreting the results in regards to cholesterol binding on channel dynamics. However, even with these limitations, coarse-grained simulations allow for the simulation lengths not currently accessible by atomistic simulations, but which have been shown to be necessary to investigate the effects of cholesterol binding (Barbera, Ayee et al. 2018).

In conclusion, I ran coarse-grained molecular dynamics simulations of Kir2.2 in a membrane with varying levels of cholesterol. Using a network theory-based approach, I found that increasing membrane cholesterol caused specific domains within the channel to de-couple from one another, similar to what has been seen in experimental studies of Kir2.

This de-coupling was facilitated by the decrease in contact probability between specific pairs of amino acids, predominantly centered on the inter-subunit interface and PIP2 binding site. Furthermore and most interestingly, I found that the contact probabilities of these residues is correlated to the number of cholesterol bound to the channel, with contact probabilities for these pairs decreasing upon increasing numbers of bound cholesterol.

5. CONCLUSION AND FUTURE DIRECTIONS

5.1. Conclusion

In this dissertation, I have primarily focused on three questions: 1) understanding the cholesterol stereospecificity of Kir channels, 2) characterizing the interactions of Kir2.2 and cholesterol in a dynamic membrane environment, and 3) uncovering the effects of altering membrane cholesterol on the intra-protein dynamics of Kir2.2.

To answer the first question regarding cholesterol stereospecificity, I turned to docking analyses. Molecular docking is a well-established approach to identifying potential binding sites of ligands on target proteins and characterize their interactions (Kitchen, Decornez et al. 2004; Chaudhary and Mishra 2016; de Ruyck, Brysbaert et al. 2016), and has been successfully employed to identify binding sites on a number of ion channels, including Kir2, TRPV1, and $GABA_A$ (Rosenhouse-Dantsker, Noskov et al. 2013) (Fürst, Nichols et al. 2014; Barbera, Ayee et al. 2017) (Picazo-Juarez, Romero-Suarez et al. 2011; Hénin, Salari et al. 2014). I tested three different sterols isomers: cholesterol, epicholesterol, and ent-cholesterol, and docked them to five ion channels that are known from prior experiments to be stereoselective in their activity: Kir2, KirBac1.1, TRPV1, $GABA_A$, and BK Channel. The main finding of this work is that, for each ion channel tested, all three isomers dock to the channel with comparable binding energy and with varying degrees of overlap, suggesting that the stereoselectivity of channels is not due to a lack of sterol binding. This result is in contrast to previous assumptions about stereoselectivity, where it was believed that the chiral isomers of cholesterol did not bind to these ion channels. Instead, my analysis predicted that the main functional difference between cholesterol and its chiral isomers is due to the specific interactions between cholesterol and the residues comprising its binding site.

With respect to the second question, I ran CG-MD simulations of the open and closed states of Kir2.2 in a membrane with varying levels of cholesterol. By using the Martini coarse-grained scheme, I was able to run simulations on an order of magnitude longer timescale that what was previously done (Rosenhouse-Dantsker, Noskov et al. 2013). Additionally, I found that the interactions between cholesterol and Kir are more complex and numerous than previously conceptualized, with cholesterol molecules interacting for a range of timescales and in various locations across the protein. This represents a new perspective on cholesterol-Kir2.2 interactions: prior studies viewed cholesterol as a drug-like molecule associating with a well-defined binding site (Picazo-Juarez, Romero-Suarez et al. 2011; Singh, McMillan et al. 2012; Rosenhouse-Dantsker, Noskov et al. 2013; Fürst, Nichols et al. 2014; Balajthy, Hajdu et al. 2017; Barbera, Ayee et al. 2017; Morales-Lázaro and Rosenbaum 2017). In contrast, my simulations here showed that Kir2-cholesterol interactions are more complex, and I identified both annular and non-annular interactions between cholesterol and the channel. Overall, the main findings of this work are: i) multiple cholesterol molecules interact with the Kir2.2 channel concurrently; ii) cholesterol-Kir2.2 interactions can be segregated into persistent, "rare" binding events at deeply embedded, non-annular binding pockets and transient, high frequency events localized at the lipid bilayer-channel interface; iii) that a decrease in membrane cholesterol results in a proportional decrease in the number of cholesterol molecules interacting with the channels and a corresponding decrease in interaction time. Additionally, I created a novel analytical framework to study Kir2-cholesterol interactions by utilizing network theory to identify cholesterol binding sites. Through this analysis, I found that these sites are not only specific to the conformational

state of the channel, but that they experience significantly different responses to membrane cholesterol levels, suggesting a more complex cholesterol-mediated regulation process.

Finally, to answer the third question posed above, I expanded the analyses I used on my CG MD simulations to focus on the effects of cholesterol on intra-protein dynamics. Here, I used protein contact networks to determine – in an unbiased manner – dynamic domains of the channel which persist regardless of conformational state or membrane cholesterol level. I found that increasing membrane cholesterol caused these domains to "de-couple" from one another. Moreover, I found that this de-coupling was facilitated by the decrease in contact probability between specific pairs of amino acids, which experienced much larger decreases in contact relative to the bulk of interactions. These pairs were found to be predominantly centered on the inter-subunit interface and PIP2 binding site, similar to results of previous experimental studies (Rosenhouse-Dantsker, Logothetis et al. 2011) (Rosenhouse-Dantsker, Logothetis et al. 2011). Finally, I found that the contact probabilities of these residue pairs are negatively correlated to the number of cholesterol bound to the channel, pointing to a potential allosteric mechanism of regulation.

5.2. Future Directions

The results contained in this dissertation point to a number of interesting and novel conclusions regarding the interactions of cholesterol and Kir2. Consequently, there are a number of different computational and experimental approaches that I propose as follow-up studies to further support the claims made by my computational work.

5.2.1. Mutagenesis Studies and Multi-scale Simulations

First and foremost, I propose using site-directed mutagenesis and electrophysiological experiments to test the effects of my identified residue interactions on channel function. In particular, the results of Chapter 5 suggest that the functional effect of cholesterol binding is the weakening of interactions between specific residue pairs, which de-couple parts of the channel from one another. This can be directly tested by deliberately mutating identified residues to strengthen their interactions with their respective partners. Indeed, combining site-directed mutagenesis and electrophysiology is a common and effective approach to interrogate cholesterol-Kir interactions, as detailed in the introduction of this dissertation and as numerous studies from the Levitan lab have demonstrated previously (Epstein, Chopra et al. 2009; Rosenhouse-Dantsker, Logothetis et al. 2011; Rosenhouse-Dantsker, Noskov et al. 2012; Rosenhouse-Dantsker, Noskov et al. 2013; Rosenhouse-Dantsker, Noskov et al. 2013). Likewise, the results from my docking analyses suggest that cholesterol interactions with Kir2.2 are unique compared to epicholesterol and ent-cholesterol, which can be interrogate by targeted mutation of these residues as well.

The electrophysiological experiments proposed above would also be bolstered by the use of multi-scale MD simulations. The general principle of multi-scale simulations is to combine the strengths of both coarse-grained and atomistic simulations together: CG MD allow for simulating systems of larger size and for longer timescales than atomistic simulations, while atomistic simulations offer a high level of molecular resolution (Ayton, Noid et al. 2007; Stansfeld and Sansom 2011). In a serial multi-scale approach, CG MD serves as the "seed" for atomistic simulations, with an equilibrated coarse grained system "backmapped" to an atomistic one (Wassenaar, Pluhackova et al. 2014). This approach has

been proven to be useful for the study of protein-lipid interactions, including those between PIP2 and Kir2.2 (Stansfeld, Hopkinson et al. 2009; Schmidt, Stansfeld et al. 2012). As my simulations have shown, the interactions between Kir2 and cholesterol are complex and numerous, requiring microsecond-scale CG MD simulations to properly investigate the surrounding microenvironment. Combining these simulations with complementary atomistic simulations would offer deeper insight into the specific interactions mediating cholesterol sensitivity identified in this dissertation. One way to utilize this multi-scale approach would be to further investigate the correlation between contact probability and bound cholesterol. In this scenario, specific CG MD simulation "snapshots" containing a set number of bound cholesterol would be back-mapped to an atomistic system, which would then be simulated. In these atomistic simulations, the root mean squares of residues can be quantified with respect to bound cholesterol, showing which residues see a greater restriction in their movement after cholesterol binding. Likewise, the dihedral and rotational angles of the channel's residues can be calculated. Using these, free energy landscapes of the channel can be generated that match with bound cholesterol conditions. These types of free energy landscapes have been used in previous computational studies of protein dynamics (Sittel and Stock 2018), and provide detailed information on protein conformational ensembles. With respect to cholesterol-Kir2 interactions, these would show directly the effect of cholesterol binding on the equilibrium distributions of channel structure. Moreover, multi-scale simulations can be combined with *in silico* residue mutations. That is to say, the residues identified for site-directed mutagenesis can also be altered in the proteins of these simulation systems and subjected to the same analyses proposed above, allowing for direct comparison of the experimental results with details at the molecular level.

Atomistic simulations of Kir2-channel interactions can also provide insight into the effects of cholesterol binding by identifying specific allosteric pathways within the channel. Allosteric pathway analysis is a relatively new computational technique which quantifies the degree of mutual information between residues in a protein MD simulation and identifies how these linked residues form "paths" of correlated movement throughout a protein (Bhattacharya and Vaidehi 2014; Vaidehi and Bhattacharya 2016). My current CG MD simulations have identified both cholesterol interaction sites on the channel and residue pairs which de-couple domains of the channel. By treating these as the start and end points, allosteric pathway analysis can be used to identify the specific mechanism through which the binding of cholesterol causes the identified residue pairs to disassociate.

5.2.2. Investigating the Effects of Cholesterol on PIP2 Binding

The results of my simulations suggest that one of the functional effects of cholesterol is the de-stabilization of the PIP2 binding site. This hypothesis can be tested directly through a combination of additional CG MD simulations and electrophysiological experiments. Recent studies by the Sansom group have shown that PIP2 binding affinity to Kir2 can be calculated by a number of different coarse-grained simulation approaches, including potential of mean force calculations, alchemical free energy perturbation, and well-tempered metadynamics (Domański, Hedger et al. 2017; Corey, Vickery et al. 2019). These simulation techniques can be employed in CG MD simulations of Kir2.2 and PIP2 in bilayers with different levels of cholesterol to directly assess the effect of increasing membrane cholesterol on the binding affinity of PIP2. Furthermore, these experiments can be combined with Kir2 current rundown experiments. Previous experiments from the Levitan lab have shown that depleting cholesterol alters the results of neomycin-mediated sequestering of PIP2, delaying

current rundown (Rosenhouse-Dantsker, Epshtein et al. 2014). These experiments can be repeated for cholesterol-enriched conditions to further test this hypothesis, and combined with computation experiments would be strong evidence in favor of the hypothesis presented in this dissertation.

5.2.3. A broader understanding of lipid-ion channel interactions

In addition to providing further insight into the regulation of Kir2 channels by cholesterol, the analytical approaches detailed in this dissertation provide a roadmap for characterizing and understanding the interactions with ion channels and cholesterol more broadly. The concurrent interactions I observed between Kir2.2 and the ensemble of cholesterol molecules is likely a universal one. As membrane-embedded proteins, ion channels are situated in similar environments to those of Kir. It is reasonable therefore to assume that the qualitative phenomena I observed in this dissertation – in particular, the aforementioned interactions with an ensemble of cholesterol molecules as well as the promiscuous, "fuzzy" interaction sites – are features of sterol-ion channel interactions more broadly. Indeed, this assumption is further bolstered by the fact that similar observations have been made for GPCRs (Sengupta and Chattopadhyay 2015; Rouviere, Arnarez et al. 2017).

Few other studies have computationally interrogated sterol-ion channel interactions to the degree that I have in this dissertation: this work necessitated long-timescale simulations of the channel in a lipid environment and a complex network theory-based approach to characterize binding sites and uncover their functional effects. Furthermore, my observation that these binding sites were differentially dependent on cholesterol concentration was surprising. Replicating these analyses for other cholesterol-sensitive ion

channel then is critical, especially for the interpretation of site-directed mutagenesis studies. Likewise, the dynamic domain approach yielded important insights into the functional effects of binding which could be tested via direct experiment. This too can be applied to ion channel studies to better understand the unique functional effects of cholesterol in each different system. Long term, an ideal goal would be a comparative analysis of cholesterol-ion channel interactions similar to the docking results presented in Chapter 2, but utilizing the network methodology in this dissertation, to develop a more general theory of cholesterol-mediated regulation.

Finally, in addition to studying protein-sterol interactions, the network approach I developed can also be used for lipids more broadly. Indeed, the method presented here has already been utilized in a recent study to investigate the interplay between PIP2 and anionic phospholipids on Kir2.2 (Duncan, Corey et al. 2020).

CITED LITERATURE

1. Abi-Char, J., A. Maguy, et al. (2007). "Membrane cholesterol modulates Kv1. 5 potassium channel distribution and function in rat cardiomyocytes." The Journal of Physiology **582**(3): 1205-1217.

2. Abraham, M. J., T. Murtola, et al. (2015). "GROMACS: High performance molecular simulations through multi-level parallelism from laptops to supercomputers." SoftwareX **1**: 19-25.

3. Addona, G. H., H. Sandermann, et al. (2003). "Low chemical specificity of the nicotinic acetylcholine receptor sterol activation site." Biochimica et Biophysica Acta (BBA)-Biomembranes **1609**(2): 177-182.

4. Ahn, S. J., I. S. Fancher, et al. (2017). "Inwardly rectifying K+ channels are major contributors to flow-induced vasodilatation in resistance arteries." The Journal of Physiology **595**(7): 2339-2364.

5. Albert, A. D. and K. Boesze-Battaglia (2005). "The role of cholesterol in rod outer segment membranes." Progress in lipid research **44**(2-3): 99-124.

6. Albert, A. D., J. E. Young, et al. (1996). "Rhodopsin-cholesterol interactions in bovine rod outer segment disk membranes." Biochimica et biophysica acta **1285**: 47-55.

7. Alessandri, R., P. C. Souza, et al. (2019). "Pitfalls of the Martini Model." Journal of chemical theory and computation **15**(10): 5448-5460.

8. Almeida, P. F. (2009). "Thermodynamics of lipid interactions in complex bilayers." Biochimica et Biophysica Acta (BBA)-Biomembranes **1788**(1): 72-85.

9. Andersen, O. S. and R. E. Koeppe (2007). "Bilayer thickness and membrane protein function: an energetic perspective." Annual review of biophysics and biomolecular structure **36**.

10. Antollini, S. and F. Barrantes (1998). "Disclosure of Discrete Sites for Phospholipid and Sterols at the Protein-Lipid Interface in Native Acetylcholine Receptor-Rich Membrane." Biochemistry **37**(47): 16653-16662.

11. Arkin, M. R., M. Randal, et al. (2003). "Binding of small molecules to an adaptive proteinâ€“protein interface." Proceedings of the National Academy of Sciences **100**(4): 1603-1608.

12. Arnarez, C., S. Marrink, et al. (2013). "Identification of cardiolipin binding sites on cytochrome c oxidase at the entrance of proton channels." Scientific reports **3**: 1263.

13. Ayton, G. S., W. G. Noid, et al. (2007). "Multiscale modeling of biomolecular systems: in serial and in parallel." Current opinion in structural biology **17**(2): 192-198.

14. Baenziger, J. E., C. M. Hénault, et al. (2015). "Nicotinic acetylcholine receptor-lipid interactions: Mechanistic insight and biological function." Biochimica et Biophysica Acta (BBA)-Biomembranes **1848**(9): 1806-1817.

15. Baier, C. J., J. Fantini, et al. (2011). "Disclosure of cholesterol recognition motifs in transmembrane domains of the human nicotinic acetylcholine receptor." Scientific reports **1**: 69.

16. Balajthy, A., P. Hajdu, et al. (2017). "Sterol Regulation of Voltage-Gated K^+ Channels." Current topics in membranes(80): 255-291.

17. Barbera, N., M. A. Ayee, et al. (2018). "Molecular Dynamics Simulations of Kir2.2 Interactions with an Ensemble of Cholesterol Molecules." Biophysical journal **115**(7): 1264-1280.

18. Barbera, N., M. A. A. Ayee, et al. (2017). "Differential Effects of Sterols on Ion Channels: Stereospecific Binding vs Stereospecific Response." Current topics in membranes(80): 25 -52

19. Barrantes, F. J. (2007). "Cholesterol effects on nicotinic acetylcholine receptor." Journal of neurochemistry **103**: 72-80.

20. Bhattacharya, S. and N. Vaidehi (2014). "Differences in allosteric communication pipelines in the inactive and active states of a GPCR." Biophysical journal **107**(2): 422-434.

21. Bianconi, G., P. Pin, et al. (2009). "Assessing the relevance of node features for network structure." Proceedings of the National Academy of Sciences **106**(28): 11433-11438.

22. Bichet, D., F. A. Haass, et al. (2003). "Merging functional studies with structures of inward-rectifier K+ channels." Nature Reviews Neuroscience **4**(12): 957.

23. Bishop, C. M. (1995). Neural networks for pattern recognition, Oxford university press.

24. Blondel, V. D., J.-L. Guillaume, et al. (2008). "Fast unfolding of communities in large networks." Journal of Statistical Mechanics: Theory and Experiment **2008**(10): P10008.

25. Borgatti, S. P. and D. S. Halgin (2011). "On network theory." Organization science **22**(5): 1168-1181.

26. Brannigan, G. (2017). Direct interactions of cholesterol with pentameric ligand-gated ion channels: testable hypotheses from computational predictions. Current topics in membranes, Elsevier. **80:** 163-186.

27. Brannigan, G., J. Hénin, et al. (2008). "Embedded cholesterol in the nicotinic acetylcholine receptor." Proceedings of the National Academy of Sciences **105**(38): 14418-14423.

28. Brooks, B. R., C. L. Brooks III, et al. (2009). "CHARMM: the biomolecular simulation program." Journal of computational chemistry **30**(10): 1545-1614.

29. Brown, D. A., B. H. GÃ¤hwiler, et al. (1990). Chapter Membrane currents in hippocampal neurons. Progress in brain research, Elsevier. **83:** 141-160.

30. Bruce, A., J. Alexander, et al. (2002). "Molecular biology of the cell. 4 th." Garland Science: 1313-1362.

31. Bukiya, A. N., J. D. Belani, et al. (2011). "Specificity of cholesterol and analogs to modulate BK channels points to direct sterol-channel protein interactions." The Journal of general physiology **137**(1): 93-110.

32. Bukiya, A. N., A. K. Singh, et al. (2011). "The steroid interaction site in transmembrane domain 2 of the large conductance, voltage-and calcium-gated potassium (BK) channel accessory β1 subunit." Proceedings of the National Academy of Sciences **108**(50): 20207-20212.

33. Cang, X., Y. Du, et al. (2013). "Mapping the functional binding sites of cholesterol in β2-adrenergic receptor by long-time molecular dynamics simulations." The Journal of Physical Chemistry B **117**(4): 1085-1094.

34. Cang, X., L. Yang, et al. (2014). "Cholesterol-β1AR interaction versus cholesterol- AR interaction." Proteins: Structure, Function, and Bioinformatics **82**(5): 760-770.

35. Case, D., I. Ben-Shalom, et al. (2018). "AMBER 2018; 2018." University of California, San Francisco.

36. Chakraborty, H. and A. Chattopadhyay (2015). "Excitements and challenges in GPCR oligomerization: molecular insight from FRET." ACS chemical neuroscience **6**(1): 199-206.

37. Chattopadhyay, A. (2014). "GPCRs: lipid-dependent membrane receptors that act as drug targets." Advances in Biology.

38. Chaudhary, K. K. and N. Mishra (2016). "A Review on Molecular Docking: Novel Tool for Drug Discovery." Databases **3**: 4.

39. Corey, R. A., O. N. Vickery, et al. (2019). "Insights into Membrane Proteinâ€“Lipid Interactions from Free Energy Calculations." Journal of chemical theory and computation **15**(10): 5727-5736.

40. Crowley, J. J., S. N. Treistman, et al. (2003). "Cholesterol antagonizes ethanol potentiation of human brain BKCa channels reconstituted into phospholipid bilayers." Molecular Pharmacology **64**(2): 365-372.

41. D'Avanzo, N., K. Hyrc, et al. (2011). "Enantioselective protein-sterol interactions mediate regulation of both prokaryotic and eukaryotic inward rectifier K+ channels by cholesterol." PLoS One **6**(4): e19393.

42. Daily, M. D. and J. J. Gray (2009). "Allosteric communication occurs via networks of tertiary and quaternary motions in proteins." PLoS computational biology **5**(2).

43. Dart, C. (2010). "SYMPOSIUM REVIEW: Lipid microdomains and the regulation of ion channel function." The Journal of Physiology **588**(17): 3169-3178.

44. Davies, P. F. (1995). "Flow-mediated endothelial mechanotransduction." Physiological Reviews **75**: 519-560.

45. De Jong, D. H., S. Baoukina, et al. (2016). "Martini straight: boosting performance using a shorter cutoff and GPUs." Computer Physics Communications **199**: 1-7.

46. de Jong, D. H., X. Periole, et al. (2012). "Dimerization of amino acid side chains: lessons from the comparison of different force fields." Journal of Chemical Theory and Computation **8**(3): 1003-1014.

47. de Jong, D. H., G. Singh, et al. (2012). "Improved parameters for the martini coarse-grained protein force field." Journal of Chemical Theory and Computation **9**(1): 687-697.

48. De Ruvo, M., A. Giuliani, et al. (2012). "Shedding light on protein-ligand binding by graph theory: the topological nature of allostery." Biophysical Chemistry **165**: 21-29.

49. de Ruyck, J., G. Brysbaert, et al. (2016). "Molecular docking as a popular tool in drug design, an in silico travel." Advances and Applications in Bioinformatics and Chemistry: AABC **9**: 1.

50. Di Scala, C., C. J. Baier, et al. (2017). "Relevance of CARC and CRAC Cholesterol-Recognition Motifs in the Nicotinic Acetylcholine Receptor and Other Membrane-Bound Receptors." Current Topics in Membranes(80): 3-24.

51. Ding, R., N. Ujang, et al. (2015). "Complex network theory applied to the growth of Kuala Lumpur's public urban rail transit network." PLoS One **10**(10): e0139961.

52. Dokholyan, N. V. (2016). "Controlling allosteric networks in proteins." Chemical Reviews **116**(11): 6463-6487.

53. Domański, J., G. Hedger, et al. (2017). "Convergence and sampling in determining free energy landscapes for membrane protein association." The journal of physical chemistry B **121**(15): 3364-3375.

54. Dopico, A. M. and A. N. Bukiya (2017). "Regulation of Ca^{2+}-Sensitive K^+ Channels by Cholesterol and Bile Acids via Distinct Channel Subunits and Sites." Current Topics in Membranes(80): 53-94.

55. Duncan, A. L., R. A. Corey, et al. (2020). "Defining how multiple lipid species interact with inward rectifier potassium (Kir2) channels." Proceedings of the National Academy of Sciences **117**(14): 7803-7813.

56. Elokely, K., P. Velisetty, et al. (2016). "Understanding TRPV1 activation by ligands: Insights from the binding modes of capsaicin and resiniferatoxin." Proceedings of the National Academy of Sciences **113**(2): E137-E145.

57. Enkvetchakul, D., J. Bhattacharyya, et al. (2004). "Functional characterization of a prokaryotic Kir channel." Journal of Biological Chemistry **279**(45): 47076-47080.

58. Epshtein, Y., A. P. Chopra, et al. (2009). "Identification of a C-terminus domain critical for the sensitivity of Kir2. 1 to cholesterol." Proceedings of the National Academy of Sciences **106**(19): 8055-8060.

59. Epstein, Y., A. P. Chopra, et al. (2009). "Identification of a C-terminus domain critical for the sensitivity of Kir2. 1 to cholesterol." Proceedings of the National Academy of Sciences **106**(19): 8055-8060.

60. Fancher, I. S., S. J. Ahn, et al. (2018). "Hypercholesterolemia-induced loss of flow-induced vasodilation and lesion formation in Apolipoprotein E-Deficient Mice Critically Depend on Inwardly Rectifying K+ Channels." Journal of the American Heart Association **7**(5): e007430.

61. Fang, Y., G. Schram, et al. (2005). "Functional expression of Kir2.x in human aortic endothelial cells: the dominant role of Kir2.2." American Journal of Physiology-Cell Physiology **289**(5): C1134-C1144.

62. Fang, Y., G. Schram, et al. (2005). "Functional expression of Kir2.x in human aortic endothelial cells: the dominant role of Kir2.2." Am J Physiol Cell Physiol **289**(5): C1134-1144.

63. Fantini, J. and F. J. Barrantes (2013). "How cholesterol interacts with membrane proteins: an exploration of cholesterol-binding sites including CRAC, CARC, and tilted domains." Frontiers in physiology **4**: 31.

64. Filosa, J. A., A. D. Bonev, et al. (2006). "Local potassium signaling couples neuronal activity to vasodilation in the brain." Nat Neurosci **9**(11): 1397.

65. Fürst, O., C. G. Nichols, et al. (2014). "Identification of a Cholesterol-Binding Pocket in Inward Rectifier K+(Kir) Channels." Biophysical Journal **107**(12): 2786-2796.

66. Ganguly, S., A. H. Clayton, et al. (2011). "Organization of higher-order oligomers of the serotonin1A receptor explored utilizing homo-FRET in live cells." Biophysical journal **100**(2): 361-368.

67. Genheden, S., J. W. Essex, et al. (2017). "G protein coupled receptor interactions with cholesterol deep in the membrane." Biochimica et Biophysica Acta (BBA)-Biomembranes **1859**(2): 268-281.

68. Gerl, M. J., J. L. Sampaio, et al. (2012). "Quantitative analysis of the lipidomes of the influenza virus envelope and MDCK cell apical membrane." Journal of Cell Biology **196**(2): 213-221.

69. Gimpl, G. (2016). "Interaction of G protein coupled receptors and cholesterol." Chemistry and Physics of Lipids **199**: 61-73.

70. Grouleff, J., S. J. Irudayam, et al. (2016). "The influence of cholesterol on membrane protein structure, function, and dynamics studied by molecular dynamics simulations." Biochimica et Biophysica Acta (BBA)-Biomembranes **1848**(9): 1783-1795.

71. Guvench, O. and A. D. MacKerell (2008). Comparison of protein force fields for molecular dynamics simulations. Molecular modeling of proteins, Springer**:** 63-88.

72. Hajdú, P., Z. Varga, et al. (2003). "Cholesterol modifies the gating of Kv1. 3 in human T lymphocytes." Pflügers Archiv

73. **445**(6): 674-682.

74. Han, H., A. Rosenhouse-Dantsker, et al. (2014). "Silencing of Kir2 channels by caveolin-1: cross-talk with cholesterol." The Journal of Physiology **592**(18): 4025-4038.

75. Hansen, S. B., X. Tao, et al. (2011). "Structural basis of PIP2 activation of the classical inward rectifier K+ channel Kir2. 2." Nature **477**(7365): 495-498.

76. Hanson, M. A., V. Cherezov, et al. (2008). "A specific cholesterol binding site is established by the 2.8 Å structure of the human b2-adrenergic receptor." Structure **16**(6): 897-905.

77. Harikumar, K. G., V. Puri, et al. (2005). "Differential effects of modification of membrane cholesterol and sphingolipids on the conformation, function, and trafficking of the G protein-coupled cholecystokinin receptor." Journal of Biological Chemistry **280**(3): 2176-2185.

78. Hebert, S. C., G. Desir, et al. (2005). "Molecular diversity and regulation of renal potassium channels." Physiological reviews **85**(1): 319-371.

79. Hedger, G. and M. S. Sansom (2016). "Lipid interaction sites on channels, transporters and receptors: recent insights from molecular dynamics simulations." Biochimica et Biophysica Acta (BBA)-Biomembranes **1858**(10): 2390-2400.

80. Hénin, J., R. Salari, et al. (2014). "A Predicted Binding Site for Cholesterol on the GABA A Receptor." Biophysical journal **106**(9): 1938-1949.

81. Hibino, H., A. Inanobe, et al. (2010). "Inwardly rectifying potassium channels: their structure, function, and physiological roles." Physiological reviews **90**(1): 291-366.

82. Hibino, H., A. Inanobe, et al. (2010). "Inwardly Rectifying Potassium Channels: Their Structure, Function, and Physiological Roles." Physiol. Rev. **90**(1): 291-366.

83. Hibino, H. and Y. Kurachi (2007). "Distinct detergent-resistant membrane microdomains (lipid rafts) respectively harvest K+ and water transport systems in brain astroglia." European Journal of Neuroscience **26**(9): 2539-2555.

84. Hodgkin, A. L. and A. F. Huxley (1952). "A quantitative description of membrane current and its application to conduction and excitation in nerve." The Journal of Physiology **117**(4): 500-544.

85. Hu, G., J. Zhou, et al. (2013). "The Topology and dynamics of protein complexes: insights from intra-molecular network theory." Current Protein and Peptide Science **14**(2): 121-132.

86. Huang, S.-Y. and X. Zou (2010). "Advances and challenges in protein-ligand docking." International Journal of Molecular Sciences **11**(8): 3016-3034.

87. Ingólfsson, H. I., C. A. Lopez, et al. (2014). "The power of coarse graining in biomolecular simulations." Wiley Interdisciplinary Reviews: Computational Molecular Science **4**(3): 225-248.

88. Ingólfsson, H. I., M. N. Melo, et al. (2014). "Lipid organization of the plasma membrane." Journal of the American Chemical Society **136**(41): 14554-14559.

89. Jacobs, D. J., A. J. Rader, et al. (2001). "Protein flexibility predictions using graph theory." Proteins: Structure, Function, and Bioinformatics **44**(2): 150-165.

90. Jorgensen, W. L., D. S. Maxwell, et al. (1996). "Development and testing of the OPLS all-atom force field on conformational energetics and properties of organic liquids." Journal of the american chemical society **118**(45): 11225-11236.

91. Khelashvili, G., A. Grossfield, et al. (2009). "Structural and dynamic effects of cholesterol at preferred sites of interaction with rhodopsin identified from

microsecond length molecular dynamics simulations." Proteins: Structure, Function, and Bioinformatics **76**(2): 403-417.

92. Kitchen, D. B., H. l. n. Decornez, et al. (2004). "Docking and scoring in virtual screening for drug discovery: methods and applications." Nature Reviews Drug discovery **3**(11): 935.

93. Kurachi, Y. (1985). "Voltage-dependent activation of the inward-rectifier potassium channel in the ventricular cell membrane of guinea-pig heart." The Journal of Physiology **366**(1): 365-385.

94. Kurzbach, D. (2016). "Network representation of protein interactions: Theory of graph description and analysis." Protein Science **25**(9): 1617-1627.

95. Lee, A. (2003). "Lipid-protein interactions in biological membranes: a structural perspective." Biochimica et Biophysica Acta (BBA)-Biomembranes **1612**(1): 1-40.

96. Lee, J. Y. and E. Lyman (2012). "Predictions for cholesterol interaction sites on the A2A adenosine receptor." Journal of the American Chemical Society **134**(40): 16512-16515.

97. Lee, S.-J., S. Wang, et al. (2013). "Secondary anionic phospholipid binding site and gating mechanism in Kir2. 1 inward rectifier channels." Nature communications **4**: 2786.

98. Levental, I., K. R. Levental, et al. (2020). "Lipid Rafts: Controversies Resolved, Mysteries Remain." Trends in Cell Biology.

99. Levitan, I. (2009). "Cholesterol and Kir channels." IUBMB Life. **61**: 781-90.

100. Levitan, I., D. Singh, et al. (2014). "Cholesterol binding to ion channels." Frontiers in physiology **5**(65).

101. Levitt, E. S., M. J. Clark, et al. (2009). "Differential Effect of Membrane Cholesterol Removal on μ-and δ-Opioid Receptors A PARALLEL COMPARISON OF ACUTE AND CHRONIC SIGNALING TO ADENYLYL CYCLASE." Journal of Biological Chemistry **284**(33): 22108-22122.

102. Lomize, M. A., I. D. Pogozheva, et al. (2011). "OPM database and PPM web server: resources for positioning of proteins in membranes." Nucleic acids research **40**(D1): D370-D376.

103. Lopes, P. E., O. Guvench, et al. (2015). Current status of protein force fields for molecular dynamics simulations. Molecular modeling of proteins, Springer**:** 47-71.

104. Lundbæk, J. A., P. Birn, et al. (2004). "Regulation of sodium channel function by bilayer elasticity: the importance of hydrophobic coupling. Effects of Micelle-

forming amphiphiles and cholesterol." The Journal of general physiology **123**(5): 599-621.

105. Lundbæk, J. A., S. A. Collingwood, et al. (2010). "Lipid bilayer regulation of membrane protein function: gramicidin channels as molecular force probes." Journal of The Royal Society Interface **7**(44): 373-395.

106. Ma, P., D. Weichert, et al. (2017). "The cubicon method for concentrating membrane proteins in the cubic mesophase." nature protocols **12**(9): 1745.

107. Manna, M., M. Niemelä, et al. (2016). "Mechanism of allosteric regulation of β2-adrenergic receptor by cholesterol." Elife **5**: e18432.

108. Marrink, S. J., H. J. Risselada, et al. (2007). "The MARTINI force field: coarse grained model for biomolecular simulations." The Journal of Physical Chemistry B **111**(27): 7812-7824.

109. Marrink, S. J. and D. P. Tieleman (2013). "Perspective on the Martini model." Chemical Society Reviews **42**(16): 6801-6822.

110. Marsh, D. and L. Horváth (1998). "Structure, dynamics and composition of the lipid-protein interface. Perspectives from spin-labelling." Biochimica et Biophysica Acta (BBA)-Reviews on Biomembranes **1376**(3): 267-296.

111. Marsh, D. and T. Páli (2004). "The protein-lipid interface: perspectives from magnetic resonance and crystal structures." Biochimica et Biophysica Acta (BBA)-Biomembranes **1666**(1-2): 118-141.

112. Martens, J. R., N. Sakamoto, et al. (2001). "Isoform-specific localization of voltage-gated K+ channels to distinct lipid raft populations Targeting of Kv1. 5 to caveolae." Journal of Biological Chemistry **276**(11): 8409-8414.

113. Meng, X.-Y., H.-X. Zhang, et al. (2012). "The molecular mechanism by which PIP2 opens the intracellular G-loop gate of a Kir3. 1 channel." Biophysical journal **102**(9): 2049-2059.

114. Miake, J., E. Marban, et al. (2003). "Functional role of inward rectifier current in heart probed by Kir2.1 overexpression and dominant-negative suppression." J Clin Invest. **111**: 1529-36.

115. Minor, D. L. (2010). An overview of ion channel structure. Handbook of Cell Signaling, Elsevier**:** 201-207.

116. Mobashery, N., C. Nielsen, et al. (1997). "The conformational preference of gramicidin channels is a function of lipid bilayer thickness 1." FEBS letters **412**(1): 15-20.

117. Monticelli, L., S. K. Kandasamy, et al. (2008). "The MARTINI coarse-grained force field: extension to proteins." Journal of Chemical Theory and Computation **4**(5): 819-834.

118. Morales-Lázaro, S. L. and T. Rosenbaum (2017). "Multiple Mechanisms of Regulation of Transient Receptor Potential Ion Channels by Cholesterol." Current Topics in Membranes(80): 139-162.

119. Morris, G. M., R. Huey, et al. (2009). "AutoDock4 and AutoDockTools4: Automated docking with selective receptor flexibility." Journal of Computational Chemistry **30**(16): 2785-2791.

120. Muller, M. P., T. Jiang, et al. (2019). "Characterization of lipid-protein interactions and lipid-mediated modulation of membrane protein function through molecular simulation." Chemical Reviews **119**(9): 6086-6161.

121. Murata, M., J. Peränen, et al. (1995). "VIP21/caveolin is a cholesterol-binding protein." Proceedings of the National Academy of Sciences **92**(22): 10339-10343.

122. Murell-Lagnado, R. D. (2017). "Regulation of P2X Purinergic Receptor Signaling by Cholesterol." Current Topics in Membranes(80): 211-232.

123. Nasrabadi, N. M. (2007). "Pattern recognition and machine learning." Journal of Electronic Imaging **16**(4): 049901.

124. Needham, D. and R. S. Nunn (1990). "Elastic deformation and failure of lipid bilayer membranes containing cholesterol." Biophysical journal **58**(4): 997-1009.

125. Noble, D. (1965). "Electrical properties of cardiac muscle attributable to inward going (anomalous) rectification." Journal of Cellular and Comparative Physiology **66**(S2): 127-135.

126. O'Connell, K. M., J. R. Martens, et al. (2004). "Localization of ion channels to lipid Raft domains within the cardiovascular system." Trends in cardiovascular medicine **14**(2): 37-42.

127. Olesen, S.-P., D. E. Clapham, et al. (1988). "Hemodynamic shear stress activates a K+ current in vascular endothelial cells." Nature **331**(January 14): 168-70.

128. Paila, Y. D., E. Jindal, et al. (2011). "Cholesterol depletion enhances adrenergic signaling in cardiac myocytes." Biochimica et Biophysica Acta (BBA)-Biomembranes **1808**(1): 461-465.

129. Pavlopoulos, G. A., M. Secrier, et al. (2011). "Using graph theory to analyze biological networks." BioData mining **4**(1): 10.

130. Periole, X., M. Cavalli, et al. (2009). "Combining an elastic network with a coarse-grained molecular force field: structure, dynamics, and intermolecular recognition." Journal of Chemical Theory and Computation **5**(9): 2531-2543.

131. Piao, L., J. Li, et al. (2007). "Transgenic upregulation of IK1 in the mouse heart is proarrhythmic." Basic Research in Cardiology.

132. Picazo-Juarez, G., S. Romero-Suarez, et al. (2011). "Identification of a binding motif in the S5 helix that confers cholesterol sensitivity to the TRPV1 ion channel." Journal of Biological Chemistry **286**(28): 24966-24976.

133. Piston, D. W. and G.-J. Kremers (2007). "Fluorescent protein FRET: the good, the bad and the ugly." Trends in biochemical sciences **32**(9): 407-414.

134. Pons, C., F. Glaser, et al. (2011). "Prediction of protein-binding areas by small-world residue networks and application to docking." BMC Bioinformatics **12**(1): 378.

135. Prasanna, X., A. Chattopadhyay, et al. (2014). "Cholesterol modulates the dimer interface of the β2-adrenergic receptor via cholesterol occupancy sites." Biophysical journal **106**(6): 1290-1300.

136. Proks, P., C. E. Capener, et al. (2001). "Mutations within the P-loop of Kir6. 2 modulate the intraburst kinetics of the ATP-sensitive potassium channel." The Journal of general physiology **118**(4): 341-353.

137. Pucadyil, T. J. and A. Chattopadhyay (2004). "Cholesterol modulates ligand binding and G-protein coupling to serotonin1A receptors from bovine hippocampus." Biochimica et Biophysica Acta (BBA)-Biomembranes **1663**(1-2): 188-200.

138. Purves, D., R. Cabeza, et al. (2008). Cognitive neuroscience, Sunderland: Sinauer Associates, Inc.

139. Rarey, M., B. Kramer, et al. (1997). "Multiple automatic base selection: Protein-ligand docking based on incremental construction without manual intervention." Journal of computer-aided molecular design **11**(4): 369-384.

140. Romanenko, V. G., Y. Fang, et al. (2004). "Cholesterol sensitivity and lipid raft targeting of Kir2. 1 channels." Biophysical Journal **87**(6): 3850-3861.

141. Romanenko, V. G., G. H. Rothblat, et al. (2002). "Modulation of endothelial inward-rectifier K+ current by optical isomers of cholesterol." Biophysical Journal **83**(6): 3211-3222.

142. Romanenko, V. G., G. H. Rothblat, et al. (2004). "Sensitivity of volume-regulated anion current to cholesterol structural analogues." The Journal of General Physiology **123**(1): 77-88.

143. Rosenhouse-Dantsker, A. (2017). "Insights into the Molecular Requirements for Cholesterol Binding to Ion Channels." Current Topics in Membranes(80): 187-210.

144. Rosenhouse-Dantsker, A., Y. Epshtein, et al. (2014). "Interplay between lipid modulators of Kir2 channels: cholesterol and PIP2." Computational and structural biotechnology journal **11**(19): 131-137.

145. Rosenhouse-Dantsker, A., E. Leal-Pinto, et al. (2010). "Comparative analysis of cholesterol sensitivity of Kir channels: Role of the CD loop." Channels **4**: 63-6.

146. Rosenhouse-Dantsker, A., D. E. Logothetis, et al. (2011). "Cholesterol sensitivity of KIR2. 1 is controlled by a belt of residues around the cytosolic pore." Biophysical Journal **100**(2): 381-389.

147. Rosenhouse-Dantsker, A., D. Mehta, et al. (2012). "Regulation of ion channels by membrane lipids." Comprehensive Physiology.

148. Rosenhouse-Dantsker, A., S. Noskov, et al. (2013). "Identification of novel cholesterol-binding regions in Kir2 channels." Journal of Biological Chemistry **288**(43): 31154-31164.

149. Rosenhouse-Dantsker, A., S. Noskov, et al. (2012). "Distant cytosolic residues mediate a two-way molecular switch that controls the modulation of inwardly rectifying potassium (Kir) channels by cholesterol and phosphatidylinositol 4, 5-bisphosphate (PI (4, 5) P2)." Journal of Biological Chemistry **287**(48): 40266-40278.

150. Rosenhouse-Dantsker, A., S. Noskov, et al. (2013). "Cholesterol sensitivity of KIR2. 1 depends on functional inter-links between the N and C termini." Channels **7**(4): 303-312.

151. Rouviere, E., C. Arnarez, et al. (2017). "Identification of Two New Cholesterol Interaction Sites on the A 2A Adenosine Receptor." Biophysical Journal **113**(11): 2415-2424.

152. Sackmann, E. (1995). "Biological membranes architecture and function." Structure and Dynamics of Membranes **1**: 1-63.

153. Sakmann, B. and G. Trube (1984). "Conductance properties of single inwardly rectifying potassium channels in ventricular cells from guinea-pig heart." The Journal of Physiology **347**(1): 641-657.

154. Saxena, R. and A. Chattopadhyay (2012). "Membrane cholesterol stabilizes the human serotonin1A receptor." Biochimica et Biophysica Acta (BBA)-Biomembranes **1818**(12): 2936-2942.

155. Schmidt, M. R., P. J. Stansfeld, et al. (2012). "Simulation-based prediction of phosphatidylinositol 4, 5-bisphosphate binding to an ion channel." Biochemistry **52**(2): 279-281.

156. Scott, W. R., P. H. Hünenberger, et al. (1999). "The GROMOS biomolecular simulation program package." The Journal of Physical Chemistry A **103**(19): 3596-3607.

157. Segala, E., D. Guo, et al. (2016). "Controlling the dissociation of ligands from the adenosine A2A receptor through modulation of salt bridge strength." Journal of medicinal chemistry **59**(13): 6470-6479.

158. Sengupta, D. and A. Chattopadhyay (2012). "Identification of cholesterol binding sites in the serotonin1A receptor." The Journal of Physical Chemistry B **116**(43): 12991-12996.

159. Sengupta, D. and A. Chattopadhyay (2015). "Molecular dynamics simulations of GPCR-cholesterol interaction: An emerging paradigm." Biochimica et Biophysica Acta (BBA)-Biomembranes **1848**(9): 1775-1782.

160. Sillitoe, I., T. E. Lewis, et al. (2014). "CATH: comprehensive structural and functional annotations for genome sequences." Nucleic Acids Research **43**(D1): D376-D381.

161. Silver, M. R. and T. E. DeCoursey (1990). "Intrinsic gating of inward rectifier in bovine pulmonary artery endothelial cells in the presence or absence of internal Mg2+." The Journal of general physiology **96**(1): 109-133.

162. Singer, S. J. and G. L. Nicolson (1972). "The fluid mosaic model of the structure of cell membranes." Science **175**(4023): 720-731.

163. Singh, A. K., J. McMillan, et al. (2012). "Multiple cholesterol recognition/interaction amino acid consensus (CRAC) motifs in cytosolic C tail of Slo1 subunit determine cholesterol sensitivity of Ca2+-and voltage-gated K+ (BK) channels." Journal of Biological Chemistry **287**(24): 20509-20521.

164. Singh, D. K., A. Rosenhouse-Dantsker, et al. (2009). "Direct regulation of prokaryotic Kir channel by cholesterol." Journal of Biological Chemistry **284**(44): 30727-30736.

165. Singh, D. K., T.-P. Shentu, et al. (2011). "Cholesterol regulates prokaryotic Kir channel by direct binding to channel protein." Biochimica et Biophysica Acta (BBA)-Biomembranes **1808**(10): 2527-2533.

166. Sittel, F. and G. Stock (2018). "Perspective: Identification of collective variables and metastable states of protein dynamics." The Journal of Chemical Physics **149**(15): 150901.

167. Sooksawate, T. and M. Simmonds (2001). "Effects of membrane cholesterol on the sensitivity of the GABAA receptor to GABA in acutely dissociated rat hippocampal neurones." Neuropharmacology **40**(2): 178-184.

168. Sousa, S. F., P. A. Fernandes, et al. (2006). "Protein-ligand docking: current status and future challenges." Proteins: Structure, Function, and Bioinformatics **65**(1): 15-26.

169. Stansfeld, P. J., R. Hopkinson, et al. (2009). "PIP2-binding site in Kir channels: definition by multiscale biomolecular simulations." Biochemistry **48**(46): 10926-10933.

170. Stansfeld, P. J. and M. S. Sansom (2011). "From coarse grained to atomistic: a serial multiscale approach to membrane protein simulations." Journal of chemical theory and computation **7**(4): 1157-1166.

171. Tao, X., J. L. Avalos, et al. (2009). "Crystal structure of the eukaryotic strong inward-rectifier K+ channel Kir2. 2 at 3.1 Å resolution." Science **326**(5960): 1668-1674.

172. Trapp, S., P. Proks, et al. (1998). "Molecular analysis of ATP-sensitive K channel gating and implications for channel inhibition by ATP." The Journal of general physiology **112**(3): 333-349.

173. Trott, O. and A. J. Olson (2010). "AutoDock Vina: improving the speed and accuracy of docking with a new scoring function, efficient optimization, and multithreading." Journal of computational chemistry **31**(2): 455-461.

174. Vaidehi, N. and S. Bhattacharya (2016). "Allosteric communication pipelines in G-protein-coupled receptors." Current opinion in pharmacology **30**: 76-83.

175. Wacker, D., G. Fenalti, et al. (2010). "Conserved binding mode of human β2 adrenergic receptor inverse agonists and antagonist revealed by X-ray crystallography." Journal of the american chemical society **132**(33): 11443-11445.

176. Wacker, D., C. Wang, et al. (2013). "Structural features for functional selectivity at serotonin receptors." Science **340**(6132): 615-619.

177. Wallin, E. and G. V. Heijne (1998). "Genome-wide analysis of integral membrane proteins from eubacterial, archaean, and eukaryotic organisms." Protein Science **7**(4): 1029-1038.

178. Wang, S., S.-J. Lee, et al. (2012). "Structural rearrangements underlying ligand-gating in Kir channels." Nature communications **3**(1): 1-8.

179. Wang, S., R. Vafabakhsh, et al. (2016). "Structural dynamics of potassium-channel gating revealed by single-molecule FRET." Nature structural & molecular biology **23**(1): 31.

180. Wassenaar, T. A., K. Pluhackova, et al. (2014). "Going backward: a flexible geometric approach to reverse transformation from coarse grained to atomistic models." Journal of Chemical Theory and Computation **10**(2): 676-690.

181. Webb, B. and A. Sali (2014). Protein structure modeling with MODELLER. Protein Structure Prediction, Springer**:** 1-15.

182. Weiser, B. P., R. Salari, et al. (2014). "Computational investigation of cholesterol binding sites on mitochondrial VDAC." The Journal of Physical Chemistry B **118**(33): 9852-9860.

183. Whorton, M. R. and R. MacKinnon (2011). "Crystal structure of the mammalian GIRK2 K+ channel and gating regulation by G proteins, PIP2, and sodium." Cell **147**(1): 199-208.

184. Whorton, M. R. and R. MacKinnon (2013). "X-ray structure of the mammalian GIRK2-βγG G-protein complex." Nature **498**(7453): 190-197.

185. Yao, X.-Q., M. Momin, et al. (2018). "Elucidating Allosteric Communications in Proteins with Difference Contact Network Analysis." Journal of chemical information and modeling **58**(7): 1325-1330.

186. Yarbrough, T. L., T. Lu, et al. (2002). "Localization of cardiac sodium channels in caveolin-rich membrane domains: regulation of sodium current amplitude." Circulation Research **90**(4): 443-449.

187. Yeagle, P. (1991). "Modulation of membrane function by cholesterol." Biochimie **73**(10): 1303-1310.

188. Yeagle, P. L. (1985). "Cholesterol and the cell membrane." Biochimica et Biophysica Acta (BBA)-Reviews on Biomembranes **822**(3-4): 267-287.

189. Yi, B. A., Y.-F. Lin, et al. (2001). "Yeast screen for constitutively active mutant G protein-activated potassium channels." Neuron **29**(3): 657-667.

190. Zangerl-Plessl, E.-M., S.-J. Lee, et al. (2019). "Atomistic basis of opening and conduction in mammalian inward rectifier potassium (Kir2. 2) channels." Journal of General Physiology **152**(1): e201912422.

191. Zaritsky, J. J., D. M. Eckman, et al. (2000). "Targeted disruption of Kir2. 1 and Kir2. 2 genes reveals the essential role of the inwardly rectifying K+ current in K+-mediated vasodilation." Circulation Research **87**(2): 160-166.

192. Zidovetzki, R. and I. Levitan (2007). "Use of cyclodextrins to manipulate plasma membrane cholesterol content: Evidence, misconceptions and control strategies." Biochimica et Biophysica Acta (BBA) - Biomembranes **1768**(6): 1311.

193. Zocher, M., C. Zhang, et al. (2012). "Cholesterol increases kinetic, energetic, and mechanical stability of the human β2-adrenergic receptor." Proceedings of the National Academy of Sciences **109**(50): E3463-E3472.

APPENDIX

Elsevier Journal Author Rights

In order for Elsevier to publish and disseminate research articles, we need publishing rights. This is determined by a publishing agreement between the author and Elsevier. This agreement deals with the transfer or license of the copyright to Elsevier and authors retain significant rights to use and share their own published articles. Elsevier supports the need for authors to share, disseminate and maximize the impact of their research and these rights, in Elsevier proprietary journals* are defined below:

Personal Use

Authors can use their articles, in full or in part, for a wide range of scholarly, non-commercial purposes as outlined below:

- Use by an author in the author's classroom teaching (including distribution of copies, paper or electronic)
- Distribution of copies (including through e-mail) to known research colleagues for their personal use (but not for Commercial Use)
- Inclusion in a thesis or dissertation (provided that this is not to be published commercially)
- Use in a subsequent compilation of the author's works
- Extending the Article to book-length form
- Preparation of other derivative works (but not for Commercial Use)
- Otherwise using or re-using portions or excerpts in other works

These rights apply for all Elsevier authors who publish their article as either a subscription article or an open access article. In all cases we require that all Elsevier authors always include a full acknowledgement and, if appropriate, a link to the final published version hosted on Science Direct.

Molecular Dynamics Simulations of Kir2.2 Interactions with an Ensemble of Cholesterol Molecules

Author:
Nicolas Barbera,Manuela A.A. Ayee,Belinda S. Akpa,Irena Levitan
Publication:
Biophysical Journal
Publisher:
Elsevier
Date:
2 October 2018

Taylor and Francis Publishing

Reprints and Permissions

Nicolas A. Barbera, Baruch Minke & Irena Levitan (2019) Comparative docking analysis of cholesterol analogs to ion channels to discriminate between stereospecific binding vs. stereospecific response, Channels, 13:1, 136-146, DOI: 10.1080/19336950.2019.1606670

VITA

NAME: Nicolas Barbera

EDUCATION:

Doctor of Philosophy, Chemical Engineering, University of Illinois at Chicago, Illinois, 2020
Dissertation Title: Uncovering the Functional Effects of Multifaceted Cholesterol-Kir2 Interactions via Molecular Modeling

Master of Science in Engineering, Chemical and Biomolecular Engineering, Johns Hopkins University, Baltimore, Maryland, 2014

Bachelor of Science, Chemical and Biomolecular Engineering, Johns Hopkins University, Baltimore, Maryland, 2013

TEACHING EXPERIENCE:

Undergraduate Mentor, Senior Honors Project, Bioengineering, University of Illinois at Chicago, 2019-2020

Undergraduate Mentor, Senior Design Project, Bioengineering, University of Illinois at Chicago, 2018-2019

Teaching Assistant, Chemical Process Control, Chemical Engineering, University of Illinois at Chicago, 2015

Teaching Assistant, Chemical Engineering Process and Product Design, Chemical and Biomolecular Engineering, Johns Hopkins University, 2014

CONFERENCE PRESENTATIONS:

Barbera, N., Akpa, B.S., Levitan, I. (2019) Kir-Cholesterol Interactions: Molecular Simulations Reveal Cholesterol-Mediated De-Coupling between Functionally Important Domains Essential for Gating. *AIChE 2019 Annual Meeting, Orlando, FL, USA*

Barbera, N., Akpa, B.S., Levitan, I. (2019) Molecular Dynamics Simulations of Kir2.2 and Cholesterol Reveal State- and Concentration-Dependent Binding Sites. Biophysical Society Meeting 2019, Baltimore, MD, USA.

Barbera, N., Akpa, B.S., Levitan, I. (2019) Computational Methods to Investigate the Interactions Between Cholesterol and Ion Channels, UIC Pulmonary, Critical Care, Sleep & Allergy Research Conference Series, Chicago, IL, USA

Barbera, N., Akpa, B.S., Levitan, I. (2018) *Kir-Cholesterol Interactions: Molecular Simulations Reveal a Dynamic Ensemble of Lipid Ligands and a Composite Binding Domain of Asymmetric Concentration Dependence. AIChE 2018 Annual Meeting, Pittsburgh, PA, USA.*

Akpa, B.S.*, **Barbera, N.**, Levitan, I. (2018) Elucidating the action of a regulatory lipid ligand via molecular simulation: Cholesterol swarms and the inwardly rectifying potassium channel. Biology and Medicine Through Mathematics, Richmond, VA, USA.

Barbera, N., Ayee, M.A.A. Akpa, B.S., Levitan, I. (2016) Molecular Dynamics Simulations of Cholesterol-Kir2.2 Interactions. Biophysical Society Meeting 2016, Los Angeles, CA, USA

PUBLICATIONS:

Gutorov, R., Peters, M., Katz, B., Brandwine, T., **Barbera, N. A.**, Levitan, I., & Minke, B. (2019). Modulation of Transient Receptor Potential C Channel Activity by Cholesterol. *Frontiers in Pharmacology*

Barbera, N., Minke, B., Levitan, I. (2019) Comparative docking analysis of cholesterol analogs to ion channels to discriminate between stereospecific binding vs. stereospecific response. *Channels*

Barbera, N., Levitan, I. (2019) Chiral Specificity of Cholesterol Orientation within Cholesterol Binding Sites in Inwardly-Rectifying K+ Channels. *Cholesterol Modulation of Protein Function.*

Barbera, N., Ayee, M.A., Akpa, B.S., Levitan, I. (2018) Molecular Dynamics Simulations of Kir2.2 Interactions with an Ensemble of Cholesterol Molecules*. Biophysical Journal*

Ayee, M.A., LeMaster, E., Shentu, T.P., Singh, D.K., **Barbera, N.**, Soni, D., … & Cho, M. (2017) Molecular-scale biophysical modulation of an endothelial membrane by oxidized phospholipids. *Biophysical Journal.*

Barbera, N., Ayee, M.A., Akpa, B.S., Levitan, I. (2017) Differential effects of sterols on ion channels: binding vs. stereospecific response. *Current Topics in Membranes.*

CONFERENCE POSTERS:

Barbera, N., Akpa, B.S., Levitan, I. (2020) Molecular Simulations of Kir-Cholesterol Interactions Uncover Cholesterol Mediated Decoupling of Functional Domains Important for Gating. Biophysical Society Meeting 2020, San Diego, California

Barbera, N., Akpa, B.S., Levitan, I. (2019) Uncovering Mechanisms of Cholesterol Regulation of K+ Channels through MD Simulations Network Theory. Chicago Center for Cardiovascular Research (CCVR) Research Day 2019

Barbera, N., Akpa, B.S., Levitan, I. (2017) Molecular Dynamics Simulations of Cholesterol Regulation of Kir2.2. UIC College of Medicine Scholarly Activities Day, Chicago, IL, USA.

Barbera, N., Akpa, B.S., Levitan, I. (2017) Coarse-Grained Molecular Dynamics Simulations of Kir2.2 Interactions with an Ensemble of Cholesterol Molecules. South East Lipid Conference, Lexington, KY, USA.